LAS

Jahresbericht / Annual Report 2025

Die Mitarbeiter des Lehrstuhls für Aerodynamik & Strömungslehre
vor dem Anwendungszentrums Fluiddynamik, AZFD"

Prof. Dr.-Ing. Christoph Egbers
Lehrstuhl Aerodynamik und Strömungslehre (LAS)
Institut für Verkehrstechnik
Fakultät 3
Maschinenbau, Elektro- und Energiesysteme
BTU Cottbus-Senftenberg
Siemens-Halske-Ring 15a
03046 Cottbus

Brandenburgische Technische Universität Cottbus - Senftenberg

Vorwort

Der *Lehrstuhl Aerodynamik und Strömungslehre (LAS)* wurde vor 25 Jahren im Juli 2000 mit der Berufung von Dr.-Ing. Christoph Egbers an die Brandenburgische Technische Universität (BTU) Cottbus neu gegründet. Der Lehrstuhl gehört zum *Institut für Verkehrstechnik (IVT)*, welches im Jahr 1999 gegründet wurde. Diesem Institut gehören z. Zt. Folgende Lehrstühle an:

- LS Aerodynamik und Strömungslehre (LAS)
- LS Technische Mechanik und Fahrzeugdynamik
- LS Strukturmechanik und Fahrzeugschwingungen
- LS Verbrennungskraftmaschinen und Flugantriebe
- LS Fahrzeugtechnik- und Antriebe
- LS Triebwerksdesign
- LS Numerische Strömungs- und Gasdynamik
- LS Bildgebende Messverfahren (gemeinsame Berufung DLR-BTU)
- LS Elektrifizierte Luftfahrtantriebe (gemeinsame Berufung DLR-BTU)

Der Lehrstuhl für Aerodynamik und Strömungslehre (LAS) beschäftigt 21 Mitarbeiter/innen und ist in vier Abteilungen gegliedert, in denen z. Zt. Folgende Forschungsthemen bearbeitet werden:

Aerodynamik
- Triebwerks-Flügel-Wechselwirkungen
- Grenzschichtströmungen
- Strömungsbeeinflussung

Strömungsmechanik
- Strukturbildung und Stabilität in hydrodynamischen Systemen
- Rotierende Strömungen
- Turbulente Strömungen
- Geophysikalisch motivierte Strömungen
- Meteorologisch motivierte Strömungen
- Gleitlagerströmungen
- Partikelströmungen
- Thermoelektrohydrodynamik (TEHD)

Raumfahrtanwendungen
- Fluid-Experimente unter Schwerelosigkeit (Raumstation ISS, Parabelflüge, TEXUS)

Messtechnik
- Entwicklung von Strömungsmessverfahren zur Strömungsbeeinflussung
- Partikelmesstechnik
- Zeitreihenanalyse und nichtlineare Datenanalyse
- Koppelung von PIV und Thermographie (simultane Temperatur- und Geschwindigkeitsmessung)

Ich bedanke mich mit diesem Jahresbericht bei meinen Mitarbeiterinnen und Mitarbeitern für die sehr erfolgreich geleistete Arbeit am Lehrstuhl sowie bei unseren Kooperationspartnern und bei allen Förderinstitutionen, von denen der Lehrstuhl Aerodynamik und Strömungslehre (LAS) an der BTU Cottbus-Senftenberg Projektförderung erhalten hat.

Cottbus, im Oktober 2025 Prof. Dr.-Ing. Christoph Egbers

Inhaltsverzeichnis / Index

Mitarbeiter / Staff at the Chair of Aerodynamics and Fluid Mechanics

Prof. Dr.-Ing. Christoph Egbers	Leiter des Lehrstuhls
Silke Kaschwich	Sekretariat
Wissenschaftliche Mitarbeiter	**Aufgabengebiet**
M.Sc. Katharina Biesold	Strömungsmechanik (Doktorandin)
M.Sc. Yann Gaillard-Röpke	Strömungsmechanik (Doktorand)
Dr.-Ing. Mohammed Hamede	Strömungsmechanik (Postdoc)
apl. Prof. Dr. rer. Nat. habil. Uwe Harlander	Strömungsmechanik, Meteorologie
Dr.-Ing. Gazi Hasanuzzaman	Aerodynamik (Postdoc)
Dr. rer. Nat. Andreas Krebs	Rechneradministration CFTMM und HLRN
M.Sc. Simon Kühne	Strömungsmechanik (Doktorand)
M.Sc. Yousuf Mohammed	Strömungsmechanik (Doktorand)
Dr.-Ing Vasyl Motuz	Aerodynamik, (Postdoc)
M.Sc. Kushal Nagaraj	Strömungsmechanik (Doktorand)
M.Sc. Stefan Richter	Aerodynamik (Doktorand)
M.Sc. Yaraslau Sliavin	Strömungsmechanik (Doktorand)
M.Sc. Matthias Strangfeld	Strömungsmechanik (Doktorand)
Dr. Peter Szabo	Strömungsmechanik (Postdoc)
Dr.-Ing. Vadim Travnikov	Strömungsmechanik (Postdoc)
Technische Mitarbeiter	**Aufgabengebiet**
B. Eng. Tark Raj Bista	Parabelflug-/TEXUS-Experimente
Dr. rer.nat. Silvio Misera	Systemadministration, Messtechnik
Techniker Stefan Rohark	Werkstatt-Leitung
M.Sc. Robin Stöbel	Labore, Windkanäle, Messtechnik

Wissenschaftliche Kooperationen und Partner
Scientific contacts and co-operation with industrial partner

Prof. Dr. Detlef Lohse	Physics of Fluids, University of Twente, The Netherlands
Prof. Dr. Vincent Heuveline	URZ, Heidelberg, Universität Heidelberg
Prof. Dr. Peter Read	Dept. of Atmospheric, Oceanic and Planetary Physics University of Oxford, UK
Dr. Wolf-Gerrit Früh	Heriot-Watt University, Edinborough, UK
Prof. Dr. Rainer Hollerbach	Dept. of Mathematics, University of Leeds, UK
Prof. Dr. Daniel Lathrop	Institute for Physical Sciences and Technology, University of Maryland, USA
Prof. Dr. Richard M. Lueptow	Dept. of Mech. Engineering Northwestern University, Chicago, USA
Prof. Dr. Laurette Tuckerman	ESPCI, Paris, France
Prof. Dr. Patrice Le Gal	IRPHE, Université Marseille, France
Prof. Dr. Innocent Mutabazi Dr. Antoine Meyer	LOMC, CNRS Université du Havre, France
Prof. Dr. Pascal Chossat	Directeur Centre International de Rencontres Mathématiques, Luminy (Marseille), France
Prof. Dr. Philippe Cardin	Institut des Sciences de la Terre, Grenoble, France
Prof. Dr. Antony Randriamampianina	CNRS, Université Marseille, France
Prof. Dr. rer. nat. Doris Breuer	DLR-Inst. (Planetary Atmospheres), Berlin
Prof. Dr. Jörg Schumacher	Institut für Thermo- und Fluiddynamik, TU Ilmenau
Prof. Dr. rer. nat. habil. Andre Thess	Institut für Technische Thermodynamik, DLR, Stuttgart
Prof. Dr. Andreas Tilgner	Institut für Geophysik, Universität Göttingen
Prof. Dr. Eberhard Bodenschatz	MPI für Dynamik und Selbstorganisation, Göttingen
Prof. Dr. Uwe Hampel Dr. Frank Stefani	HZDR Rossendorf
Prof. Dr. Jeanette Hussong	FG Strömungslehre und Aerodynamik, TU Darmstadt
Prof. Dr.-Ing. Ulrich Riebel	Lehrstuhl für Mech. Verfahrenstechnik, BTU Cottbus

Fluid-Centrum / Fluid-Center

Das Fluid-Centrum des Lehrstuhls Aerodynamik und Strömungslehre wurde 2004 in Betrieb genommen. Dort sind folgende Labore sowie Prüf- und Versuchsstände des Lehrstuhls untergebracht

Halle I (Aerodynamik- und Aeroakustik-Halle, 400qm):
- Großer Rohrströmungskanal (Cottbus Large Pipe Test Facility, CoLa-Pipe)
- Kleiner Rohrströmungskanal (Cottbus Small Pipe Test Facility, CoSma-Pipe)
- Kleiner Lehr- und Forschungswasserkanal für hochpräzise Strömungskalibration
- Windkanal für Fahrzeugmodell- bzw. Flugzeughalbmodelluntersuchungen
- Aeroakustik-Prüfstand/Freistrahlgebläse

Halle II (Strömungsprüfstands- / Raumfahrt-Halle, 400qm):
- Labore für rotierende Strömungen (150 qm)
- Laserlabor (75 qm)
- Strömungsprüfstandslabore (75 qm)
- 3 Schülerlabore (je 45-50 qm)

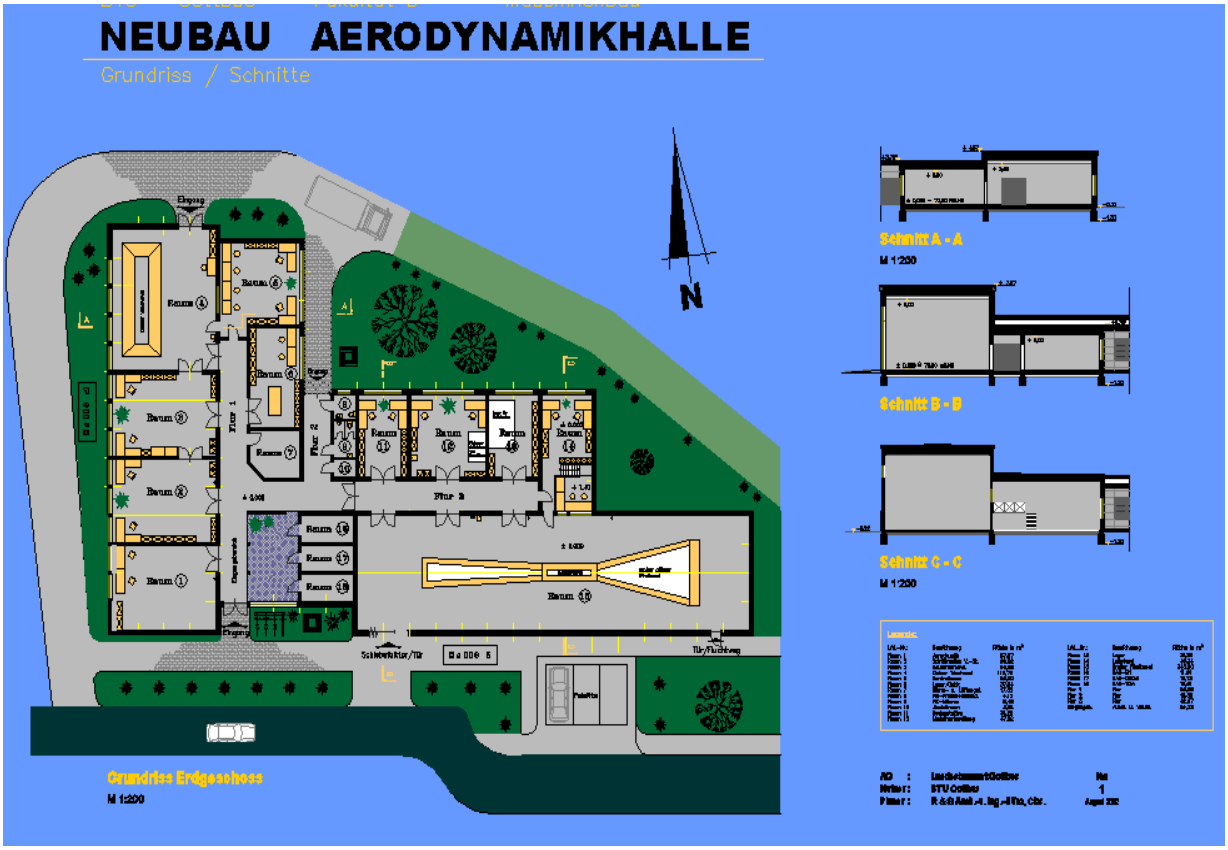

Ansicht des Fluid-Centrums (Aerodynamik- und Strömungsprüfstandshalle)

Neubau des „Anwendungszentrums Fluiddynamik“
New Building „Center of Applied Fluid Dynamics“

EUROPÄISCHE UNION
Europäischer Fonds für regionale Entwicklung

Ch. Egbers (EFRE-Förderung, Antrags-Nr.: 85001205))

Zusammenfassung
Ziel des Ende 2017 genehmigten EFRE-Vorhabens in Höhe von 7.2 Mio. € ist der Neubau des "Anwendungszentrums Fluiddynamik", eines neuen Labor- und Bürogebäudes, neben dem Fluid-Centrum (LH3D) der Brandenburgischen Technischen Universität Cottbus-Senftenberg (BTU) auf dem Zentralcampus in Cottbus. Das neue Gebäude soll die Anzahl der Projekte, insbesondere die Kooperationsvorhaben im Bereich der Energietechnik mit der regionalen Industrie und damit den Technologietransfer maßgeblich erhöhen. Einen vergleichbaren Standort in Brandenburg gibt es nicht. Neben neuen Büros für die bisher in verschiedenen Gebäuden verteilten Mitarbeiter der Lehrstühle LAS, LTA und LNSG sowie dem CFTM² wird auch Platz für 7 weitere Labore geschaffen. Dies sind u. a. ein Labor für Parabelflug-Vorbereitung, ein Labor für akustische Messtechnik und ein Laserlabor. Damit wird das neue Anwendungszentrum zu einem zentralen Forschungspartner für die Energietechnik in der Region und überregional. Baubeginn war Februar 2018, Fertigstellung und Übernahme der BTU fand im März 2020 statt.

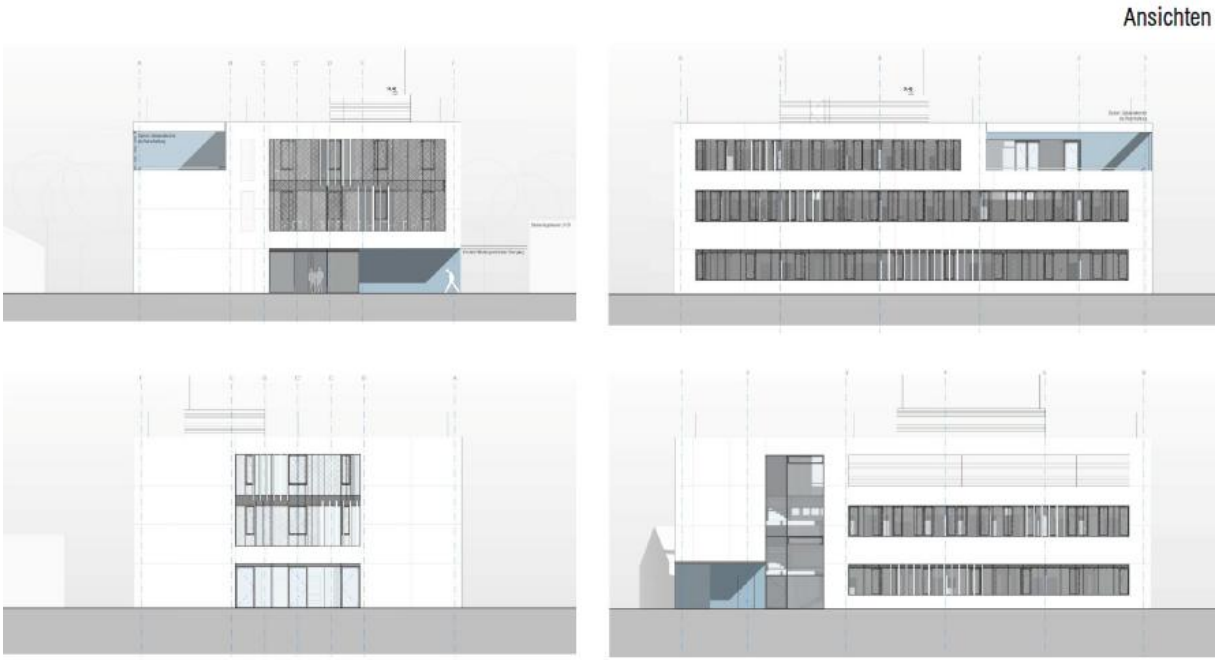

Abb. 1: Ansichten des neuen AZFD-Gebäudes (Quelle: AWB Architekten, Dresden)

Ziele des Bau-Vorhabens
Am Lehrstuhl für Aerodynamik und Strömungslehre (LAS, Institut für Verkehrstechnik, BTU Cottbus-Senftenberg) werden national und international anerkannte grundlagen- und anwendungsorientierte Forschungsarbeiten auf dem Gebiet der experimentellen, theoretischen und numerischen Strömungsmechanik, Aerodynamik sowie Messtechnik durchgeführt.
Der Lehrstuhl gehört ebenso wie die beiden anderen mitbeantragenden Lehrstühle für Technische Akustik (LTA) und Numerische Strömungs- und Gasdynamik, (LNSG), zum BTU-weiten Zentrum für Strömungs- und Transportphänomene, Modellierung und Messtechnik (CFTM2). Das Fluid-Centrum mit seiner Laborhalle steht dabei zentral im Mittelpunkt interdisziplinärer Forschung der beteiligten und weiteren BTU-Lehrstühle.

Das neue Gebäude „Anwendungszentrum Fluiddynamik“
New Building „Center of Applied Fluid Dynamics“

EUROPÄISCHE UNION
Europäischer Fonds für
regionale Entwicklung

Das neue Gebäude "Anwendungszentrum Fluiddynamik (AZFD)", ein kombiniertes Labor- und Bürogebäude, konnte 2020 in Betrieb genommen werden. Es liegt direkt neben dem „Fluid-Centrum“ (LH3D) der Brandenburgischen Technischen Universität Cottbus-Senftenberg (BTU) auf dem Zentralcampus in Cottbus. Das Ende 2017 genehmigte Bauvorhaben mit Baukosten von insgesamt ca. 8.3 Mio. € ist durch das Land Brandenburg und im Rahmen einer EFRE-Förderung finanziert worden. Das AZFD soll die Anzahl der Projekte, insbesondere die Kooperationsvorhaben im Bereich der Energietechnik mit der regionalen Industrie und damit den Technologietransfer maßgeblich erhöhen und steht dabei zentral im Mittelpunkt interdisziplinärer angewandter Forschung der beteiligten und weiteren BTU-Lehrstühle. Das Anwendungszentrum Fluiddynamik war zunächst im benachbarten Fluidcentrum tätig und wurde mit der Fertigstellung des AZFD-Gebäudes deutlich erweitert. Mit den Baumaßnahmen wurde Anfang 2018 begonnen, die Übernahme durch die BTU erfolgte am 28.2.2020. Der Umzug in die neuen Räume erfolgte auf Grund der Pandemie-bedingten Einschränkungen nach und nach in den folgenden Monaten und war im Sommer abgeschlossen. Sowohl die Erarbeitung des Antrages für die EFRE- Förderung (2015), die Beschaffung der Laboreinrichtungen und des Mobiliars als auch die Begleitung der Baumaßnahme über die gesamte Bauzeit hinweg (z.B. mit zeitweise wöchentlichen Bausitzungen) in Vertretung aller (zukünftigen) Gebäudenutzer erfolgte durch die Autoren. Sowohl die Planungs- (ab 7/2016) als auch die Bauphase wurde vom BLB (Brandenburgischer Landesbetrieb für Liegenschaften und Bauen) mit dem verantwortlichen Architekturbüro AWB Werner Bauer, Dresden, koordiniert und BTU-seitig durch die Abteilung „Infrastrukturelles Gebäudemanagement“ sowie bei Bedarf weiteren Abteilungen der BTU (z.B. Technisches Gebäudemanagement, Facility Management, Sicherheitsingenieur) begleitet. Die Zusammenarbeit mit allen Beteiligten – BLB, AWB, BTU, den Systemplanern, der Feuerwehr und nahezu allen Firmen – war konstruktiv, effizient und im Allgemeinen sehr gut.

Das kompakte Gebäude im Passivhaus-Standard wurde nach dem Gebot des kostensparenden Bauens bei gleichzeitig hoher Robustheit, Langlebigkeit und geringen Betriebskosten errichtet. Die Erscheinung des Gebäudes wird durch die vorgehängte Fassade aus Metallpaneelen bestimmt. Im Bereich der großformatigen Fensterbänder und Verglasungen nach Süden hin löst sich mit dem notwendigen Sonnenschutz die Metallfassade in bewegliche Einzelelemente auf. Die Fassadentafeln wurden feuerverzinkt ausgeführt, die fortlaufend variierende Erscheinung soll dem Forschungsansatz des Hauses folgend die ebenso wenig endgültig vorhersagbaren Forschungsergebnisse widerspiegeln und so zum Sinnbild künftiger Entwicklungen einer technisch und technoid geprägten Umgebung werden.

Der Lehrstuhl für Aerodynamik und Strömungslehre (LAS) gehört ebenso wie die anderen im Gebäude ansässigen Fachgebiete für Technische Akustik (TA), Numerische Strömungs- und Gasdynamik (NSG) und Bildgebende Messverfahren zum BTU-weiten Zentrum für Strömungs- und Transportphänomene, Modellierung und Messtechnik (CFTM^2). Neben neuen Büros für die bisher in verschiedenen Gebäuden verteilten Mitarbeiter der Fachgebiete und des CFTM^2 wurde auch Platz für 7 weitere Labore, einen Rechnerpoolraum, 2 Besprechungsräume und einen Seminarraum geschaffen. Damit können verstärkt national und international anerkannte grundlagen- und anwendungsorientierte Forschungsarbeiten auf dem Gebiet der experimentellen, theoretischen und numerischen Strömungsmechanik, Aerodynamik sowie Messtechnik durchgeführt werden. Ergänzt wird das AZFD durch das benachbarte Fluid-Centrum mit seiner großen und kleinen Laborhalle mit verschiedenen Wind- bzw. Strömungskanälen, Laboren für Rotationsexperimente und einer mechanischen Werkstatt. Damit ist das neue Anwendungszentrum ein zentraler Forschungspartner für alle strömungstechnischen Fragestellungen in der Region und überregional.

EUROPÄISCHE UNION
Europäischer Fonds für
regionale Entwicklung

Abb. 2: AZFD-Eingang und Eingang Fluid-Centrum

Abb. 3: AZFD Nordwestseite

EUROPÄISCHE UNION
Europäischer Fonds für
regionale Entwicklung

Abb. 4: Blick in eins der sieben Labore - das Parabelfluglabor

Für die künstlerische Gestaltung des Neubaus hatte das Land Brandenburg einen eingeladenen Wettbewerb mit sieben Teilnehmenden ausgelobt, die aus einer Liste mit 22 in Frage kommenden Künstlern und Künstlerinnen ausgewählt wurden. Ziel war es, das Bauvorhaben durch Kunst am Bau zu bereichern, dem kulturellen Anspruch des Landes Ausdruck zu verleihen und Kunst zugänglich zu machen. Die Installation der Künstlerin polnischen Marlena Kudlicka wurde schließlich ausgewählt und gewann den mit 1.500 Euro dotierten Wettbewerb. Ihr dreidimensionales Werk soll einen Algorithmus abbilden und mit „0 Komma A“ Ungenauigkeiten und Messfehler thematisieren. Das Werk ist nun an einer Wand im Treppenhaus des AZFD angebracht, siehe Abb. 5.

Abb. 5: Installation „0 Komma A“ der polnischen Künstlerin Marlena Kudlicka im 2. Stockwerk.

EUROPÄISCHE UNION
Europäischer Fonds für
regionale Entwicklung

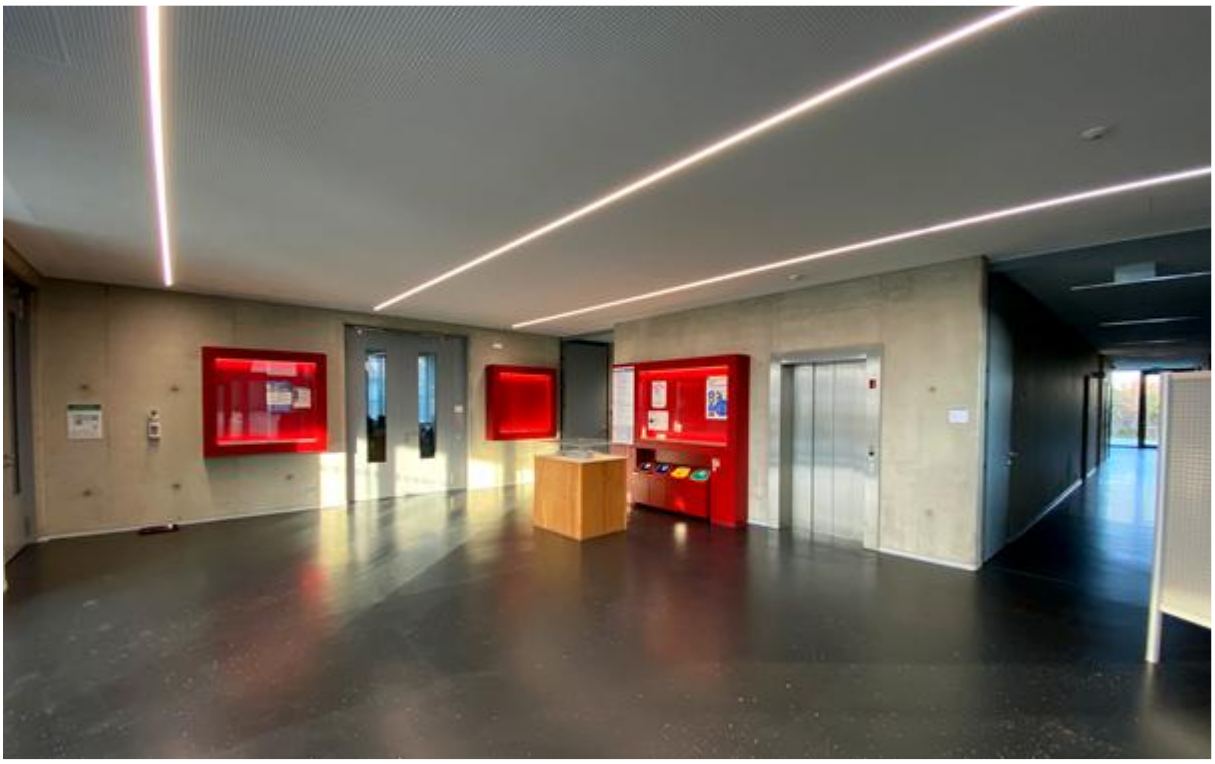

Abb. 6: Eingangsbereich des AZFD

Abb. 7: Foyer im 2. Stockwerk des AZFD

Lehre / Courses offered

Vorlesungen des Lehrstuhls für Aerodynamik und Strömungslehre im SS 2025

Strömungslehre und Strömungslehre für dualen Studiengang (2 SWS VL + 2 SWS UE)
Prof. Egbers / M.Sc. Simon Kühne

- Grundlagen (Stoffgrößen und physikalische Eigenschaften von Fluiden)
- Hydrostatik (Druck, Auftrieb)
- Kinematik der Flüssigkeiten (Kontinuitätsgleichung)
- Kinetik der Fluide (Bernoulli-Gleichung, Massenerhaltung, Impulssatz, Drehimpuls)
- Materialgleichungen (Navier-Stokes Gleichungen, Newtonsche Fluide)
- Schichtenströmungen (Couette-, Poiseuille-Strömung)
- Grenzschichttheorie
- Ausgewählte Strömungsbeispiele

Fahrzeug-Aerodynamik I (2 SWS VL + 2 SWS UE)
Prof. Egbers / Dr. Hasanuzzaman

- Grundlagen der Strömungslehre
- Übertragbarkeitsregeln von Modellmessungen auf Originalausführungen
- Fahrzeugaerodynamik und Design
- Windkanaltechnik
- Messtechnik in der Fahrzeugaerodynamik

Raumfahrtanwendungen (2 SWS VL + 2 SWS UE)
Prof. Egbers / Dr. Vasyl Motuz

- Physikalische Grundlagen der Schwerelosigkeit
- Übersicht zu Forschung unter Schwerelosigkeit
- Verschiedene Experimentierplattformen (Fallturm, Parabelflüge, TEXUS, ISS)

Analyse und Visualisierung von Strömungen mit MATLAB (2 SWS VL + 2 SWS UE)
apl. Prof. Harlander

- MATLAB Tutorial
- Strömungslehre Tutorial
- Statistische Analyse von Strömungsdaten
- Zeitreihenanalyse
- bi- und multivariate Verfahren; nichtlineare Verfahren
- Visualisierung von Strömungen
- Darstellung statistischer Ergebnisse

Convection in Fluids and Gases (2 SWS VL + 2 SWS UE)
apl. Prof. Harlander

- Convection between heated/cooled plates
- The Rayleigh-Bernard experiment
- The differentially heated rotating annulus
- Convection with local sources
- Centrifugal- and Coriolis-effects in rotating convection
- Convection in spheres and spherical shells
- Applications in technical and environmental flows

Lehre / Courses offered

Vorlesungen des Lehrstuhls für Aerodynamik und Strömungslehre im WS 2025

Experiments in Aerodynamics and Fluid Mechanics (2 SWS VL + 2 SWS UE)
Prof. Egbers / Dr. Hasanuzzaman
Einführung in Modellexperimente der Aerodynamik und der Strömungsmechanik: Taylor-Couette Strömungen, Rayleigh-Bénard-Konvektion, Flügelprofil, Windkanalmessmethoden, Reynolds´scher Rohrströmungsversuch, Karman´sche Wirbelstraße, Radhausmodell, Wsserkanal, Particle-Image-Velocimetrie, Laser-Doppler-Anemometrie

Höhere Strömungsmechanik (2 SWS VL + 2 SWS UE)
Prof. Egbers / Dr. Szabo
Einführung, Theoretische Grundlagen; Methoden der Stabilitätsanalyse; Methoden der Zeitreihenanalyse und Chaosdynamik; Modell-Systeme (Strömungsinstabilitäten in Natur und Technik); Experimentelle Methoden; Praktische Beispiele (Rayleigh-Bénard-Konvektion, Taylor-Couette-Strömungen), Turbulente Strömungen

Strömungsmesstechnik (2 SWS VL + 2 SWS UE)
Prof. Egbers / Dr.-Ing. Vasyl Motuz

- Verfahren zur Sichtbarmachung von Strömungen / Übersicht zu optischen Messverfahren
- LDA-, PIV- und PTV-Strömungsmessverfahren
- Flüssigkristall-Messtechnik
- Farbinjektion
- Hitzdraht- und Heißfilm-Technik
- Verfahren zur Messung von Zustandsgrößen (Temperatur, Druck, Feuchte)
- Windkanalmesstechnik (6-Komponentenwaage, Drucksonden, Drucksensitive Farben)

Aerothermodynamik (2 SWS VL + 2 SWS UE)
Prof. Egbers / M.Sc. Simon Kühne
Einführung; Kompressible Strömungen (Gasdynamik), Grenzschichtströmungen, Übersicht über die Tragflügeltheorie; Singularitätenverfahren für Überschallströmungen; Energiesatz für materielles Volumen, Energiesatz für Stromfaden, Gibbsche Gleichung und Entropieungleichung, Ideale Gase, Thermische und kalorische Zustandsgleichung, Schallgeschwindigkeit und Schallausbreitung, Bernoulli Gleichung für ideales Gas, Isentrope stationäre Stromfadentheorie, Flächen-/Geschwindigkeitsbeziehung, Durchflussfunktion, Verdichtungsstoß, Lavaldüse

Wellen in Flüssigkeiten (2 SWS VL + 2 SWS UE)
apl. Prof. Harlander

- Oberflächenwellen
- Reflexion und Refraktion
- WKB Analyse
- Flachwasserwellen, Interne Schwerewellen, Planetare Wellen, Trägheitswellen
- Numerische Verfahren zur Lösung von Wellenphänomenen

Parallel Rechnen (2 SWS VL + 2 SWS UE)
M.Sc. Yann Gaillard

- Die Studierenden lernen grundlegende Konzepte paralleler Rechnerarchitektur (Hardwareaspekt) und der parallelen Programmierung (Softwareaspekt) kennen. Typische Aufgabenstellungen numerischer Simulation aus den Bereichen Computational Physics, CFD und Image Processing können selbständig parallel implementiert werden.

Infrastruktur des Lehrstuhls / Laboratories and research facilities

Laboreinrichtungen	Laboratory facilities
• Labor für exp. Strömungsmechanik	• Fluid laboratory
• Elektronik-/Messtechnik-Labor	• Electronic laboratory
• Mechanik-Labor	• Mechanical workshop
• Laser-Labor	• Laseroptical laboratory
• Labor für Weltraumexperimente	• Space experiments laboratory
• Rechnerraum	• Computation room

Experimenteinrichtungen	Experiment facilities
• Taylor-Couette Apparaturen (DFG)	• Taylor Couette apparatus (DFG)
• Strato-Rotations-Experiment (DFG)	• Strato-Rotational experiment (DFG)
• QBO-Experiment / Rotor-Stator (DFG)	• QBO-experiment, rotor-stator (DFG)
• Kugelspalt-Anlagen (DLR, DFG)	• Spherical gap flow experiment (DLR, DFG)
• Rayleigh-Bénard Experiment (BTU)	• Rotating Rayleigh-Bénard tank (BTU)
• Rotierende Zylinder-Konus-Apparaturen	• Rotating cone facilities
• Barokliner Wellentank (DFG, DLR)	• Baroclinic-wave tank facility (DFG, DLR)
• MS-GWave Tank (DFG)	• MS-GWave tank (DFG)
• Turbulente Rohrströmung (DFG)	• Turbulent pipe flow facility (DFG)
• Lehr-und Forschungswindkanal (BTU)	• Wind tunnel (aerodynamics, BTU)
• Aeroakustik-Freistrahl-Prüfstand	• Aeroacoustic-Test-Facility

Messtechnik	Measuring techniques
• Laserlichtschnitt-Technik	• Laser light sheet technique
• PIV-Technik (2D-Messungen)	• PIV-technique (2D velocity measurements)
• LIF-Technik	• LIF technique
• LDA-Technik (2D-Messung)	• LDA-techniques (2D measurements)
• He-Ne Laser, Ar-Ion Laser	• He-Ne laser, Ar-Ion laser
• Schlieren-/Schattenverfahren und Interferometrie	• Shadowgraph- Schlieren and interferometer optics
• Heissfilm- und Hitzdraht-Technik	• Hotfilm- and hot wire measuring technique
• Ölfilm-Methode	• Oilfilm-technique
• Thermographie	• Thermography

Numerik / Software	Numerics / Software
• 3D zeitabhängige Codes zur Berechnung isothermer und thermisch getriebener Strömungen, FORTRAN	• 3D time dependent computational code (isothermal and thermal flows), FORTRAN
• Zeitreihenanalyse- und nicht-lineare Analysemethoden	• Time series analysis- and non-linear analysis tools
• CREO CAD-tool	• CREO-CAD-tool
• OpenFOAM	• OpenFOAM
• FLUENT, Matlab	• FLUENT, Matlab
• PV wave, Tecplot (Visualisierung)	• PV wave, Tecplot (visualization)

Infrastruktur des Lehrstuhls / Laboratories and research facilities

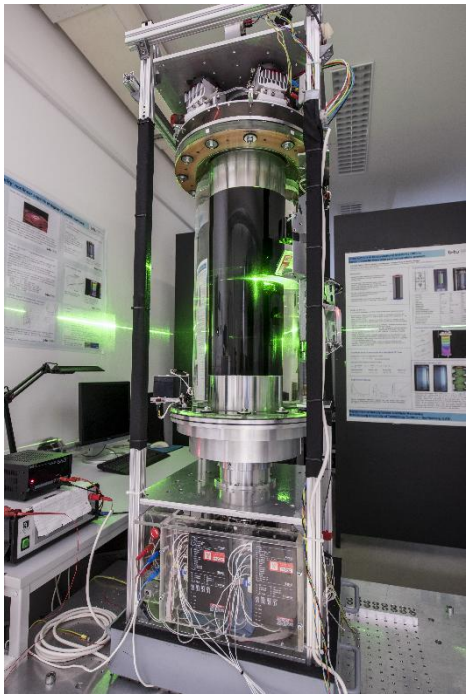

Taylor-Couette-experiment (SRI)

Taylor-Couette experiment (QBO)

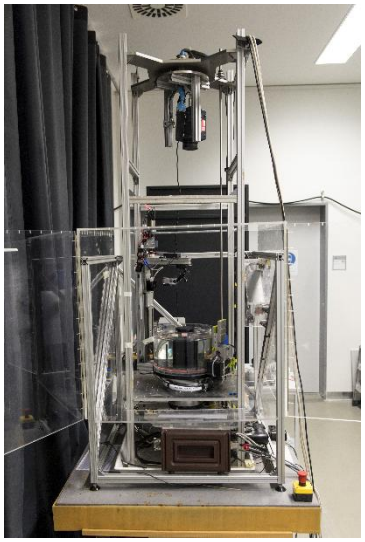

Baroclinic wave tank

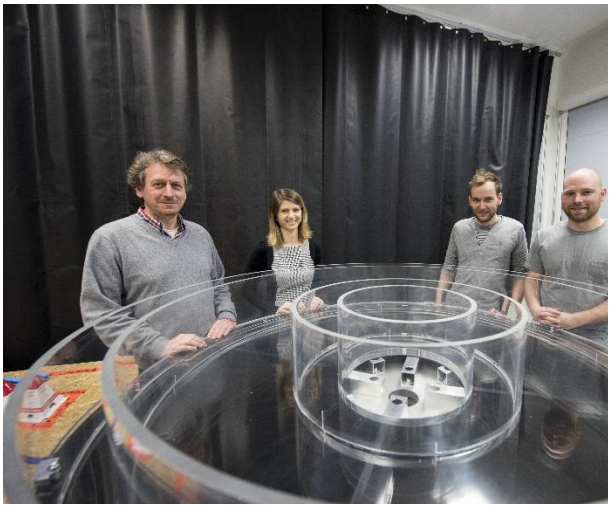

MS-GWaves experiment

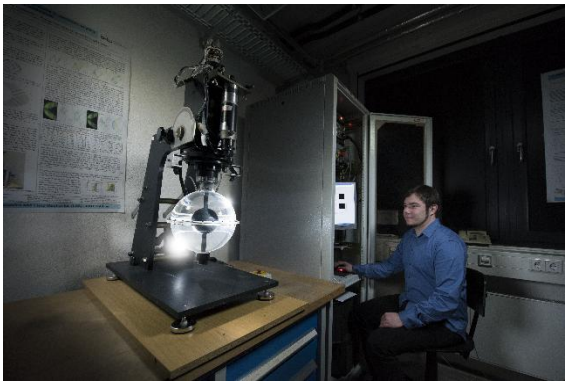

Concentric spherical gap apparatus

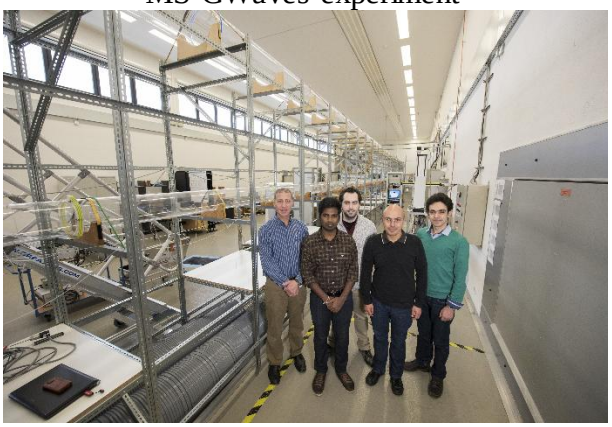

Cottbus Large Pipe Test Facility CoLa-Pipe

Infrastruktur des Lehrstuhls / Laboratories and research facilities

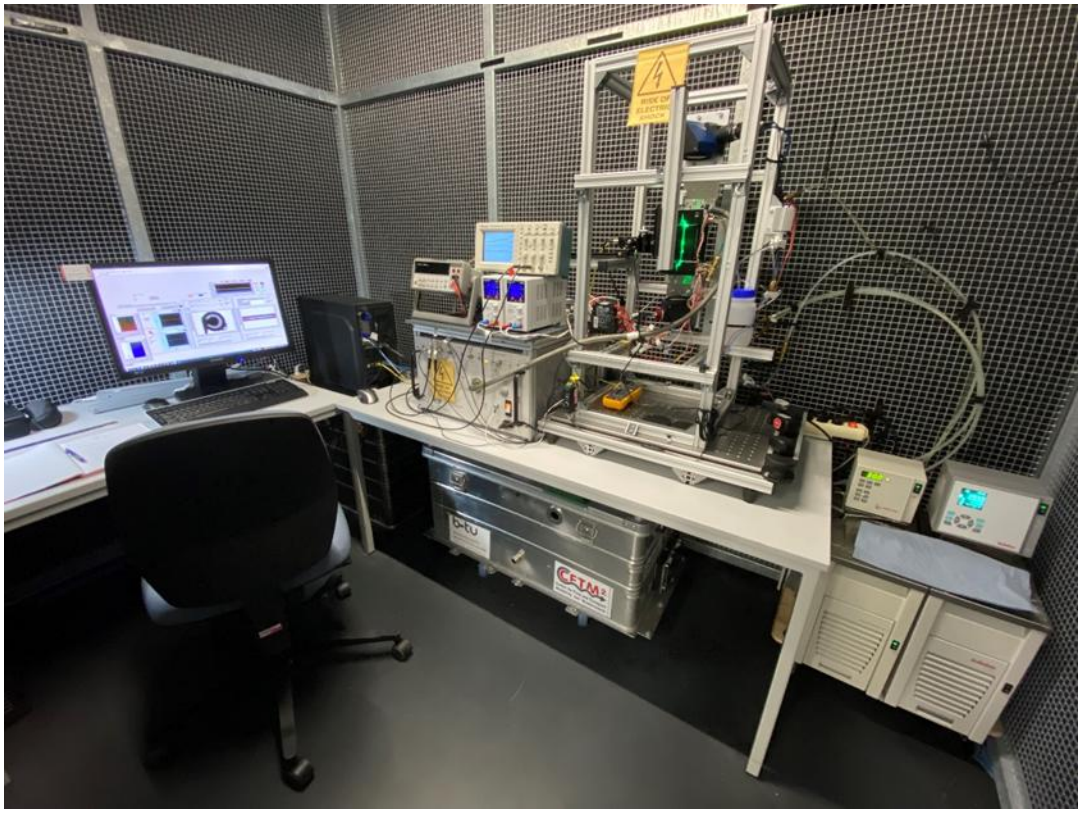

TEHD-Versuchsaufbau mit der Zylinderspaltzelle in vertikaler Ausrichtung im Faraday'schen Käfig des Hochspannungslabors des LAS

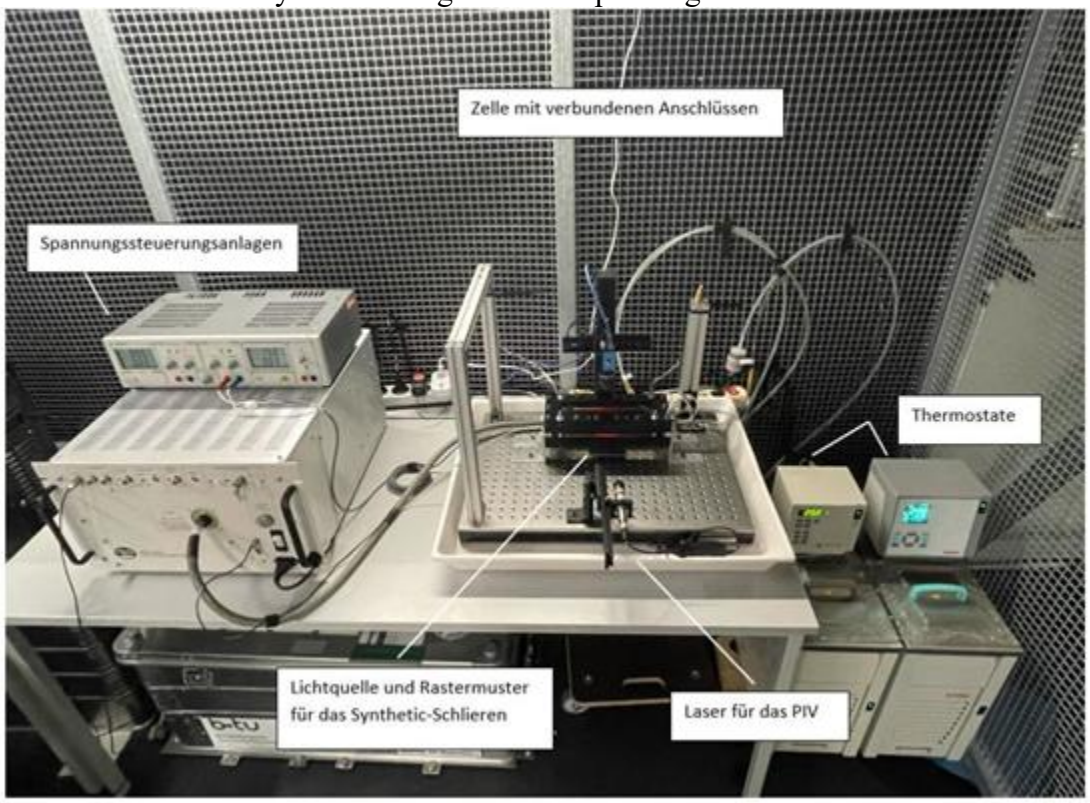

TEHD-Versuchsaufbau mit der Plattenspaltzelle in horizontaler Ausrichtung im Faraday'schen Käfig des Hochspannungslabors des LAS

Infrastruktur des Lehrstuhls / Laboratories and research facilities

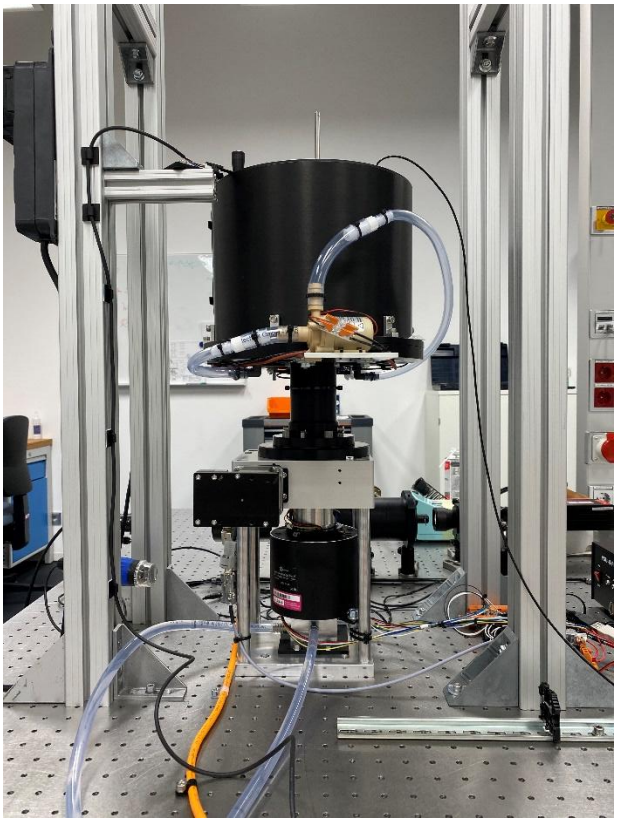

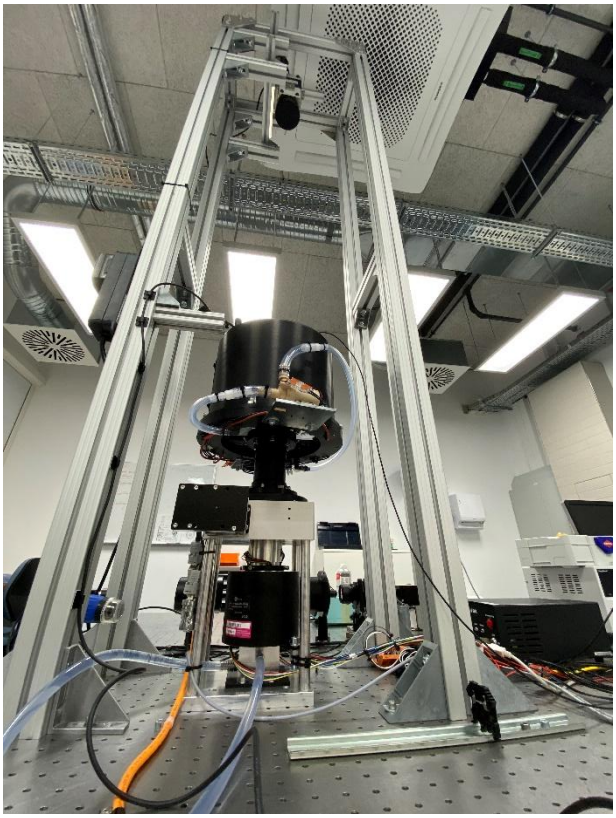

Der Barokline Wellentank für das Atmoflow-Experiment

Aktuelle Forschungsschwerpunkte / Current research topics

A Aerodynamics

A1 The Cottbus Small Pipe (CoSma–Pipe) Test Facility: Relevance of Flow Conditions Along and Downstream of a Heat Exchanger Absorbing Electric Motor Waste Heat in Electric Aviation

Stefan Richter, Sagar Budihal

Introduction

In electric aviation, managing the thermal load from electric motors, power electronics, and batteries is critical for ensuring high efficiency, safety, and longevity of the propulsion system. Heat exchangers that remove waste heat from an electric motor are central components of the thermal management system. The flow conditions along the heat exchanger surface and in the wake (i.e., downstream) of the heat exchanger critically affect both heat transfer performance and aerodynamic penalties.

Flow along the surface of the heat exchanger involves boundary-layer development. Whether laminar or turbulent flow exists strongly influences the convective heat transfer coefficient. Turbulent flow tends to thin the boundary layer and improves heat transfer, but causes higher pressure losses. However, laminar flow reduces drag but limits heat extraction. Design features such as vortex generators or winglets can be introduced to promote turbulence where desired. For example, Sharma (2017) [1] studied the effect of finite-thickness winglet vortex generators in compact heat exchangers and showed that such devices improve heat transfer, albeit with associated pressure drop penalties.

Downstream of a heat exchanger, the flow can separate, vortices can shed, and recirculation regions may form. These wake effects can degrade the performance of the system, increasing drag and disrupting flow to downstream surfaces or components, e.g. a tailplane or further ducting. The shape of the heat exchanger with regard to fin geometry, thickness, orientation, and its interaction with upstream flow (velocity, turbulence, angle of attack) all influence how severe these effects are. One applied example in electric aviation is the work by Anibal et al. (2022) [2], who performed shape optimization of a motor surface heat exchanger in the X-57 Maxwell demonstrator. They found that drag variation across designs was largely driven by flow separation on the aft side of fins, and the optimized shapes shifted fin geometry to reduce adverse pressure gradients and separate flows.

Another domain is system-level trade-offs between heat exchanger pressure drop and fuel or energy consumption. For instance, in the paper on compact heat exchangers for hydrogen-fueled aero engine intercooling and recuperation by Capitao Patrao et al. (2024) [3], the authors show that integrating compact heat exchangers leads to pressure drop penalties that must be modeled alongside aerodynamic losses, and that minimizing air-side pressure losses and ensuring flow uniformity are key to achieving net performance improvements.

In summary, the flow state both along and downstream of a heat exchanger in electric propulsion has multiple, intertwined impacts:

1. It controls the local heat transfer coefficient via boundary layer behavior.
2. It influences pressure drop (hence required fan or ram-air ducting power).
3. Wake flow and separation influence downstream components, potentially degrading aerodynamic efficiency.
4. Geometry optimization (fin shape, placement) can shift the balance to reduce drag while meeting thermal load requirements.

Aktuelle Forschungsschwerpunkte / Current research topics

To address the issues described above, various heat exchanger geometries are being developed and investigated with respect to their flow characteristics. Both purely horizontally aligned heat exchanger fins with varying dimensions and combinations of vertically and horizontally arranged fins are considered. A preview of these geometries is shown in Figure 1. The heat exchanger geometries are installed and tested in the CoSma-Pipe facility, which is operated by the Chair of Aerodynamics and Fluid Mechanics of the BTU. The Cottbuser Small Pipe (CoSma–Pipe) at the Chair of Aerodynamics and Fluid Mechanics (LAS), BTU Cottbus–Senftenberg, is an open-loop, subsonic pipe facility built for high-quality pipe–flow experiments in the range $104 \leq Reb \leq 2 \times 105$. Upstream of the test pipe (inner diameter $D = 60$ mm, total length $L \approx 9.5$ m), the flow is conditioned by a ≈ 1.2 m settling chamber followed by an axisymmetric inlet contraction with a contraction ratio of 12.25. The acceleration homogenizes the stream, suppressing large-scale non-uniformities from the blower and flow-straightening devices, and delivers a nearly plug-like profile with thin boundary layers at the pipe entrance.

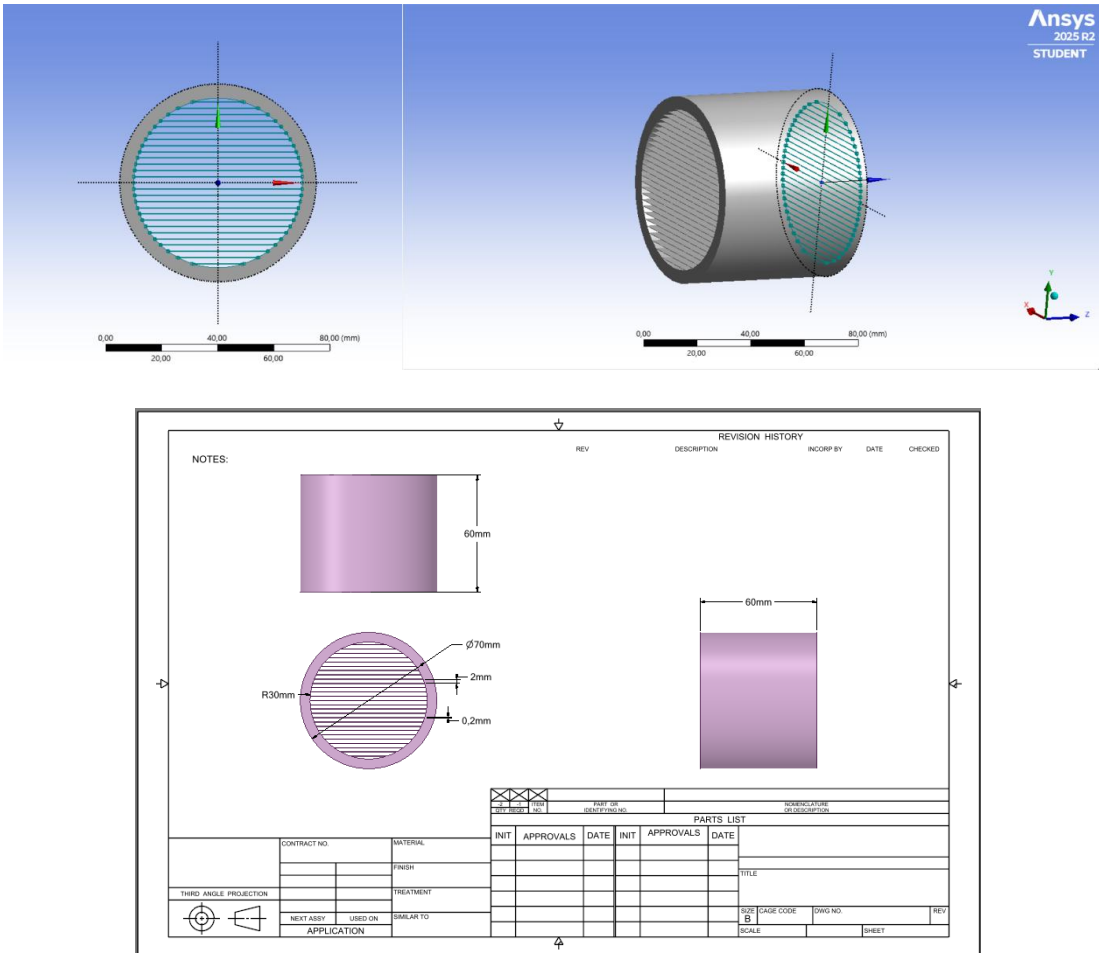

Figure 1: Sketch of an intended heat exchanger geometry

Bibliography

[1] Sharma, B. *Effect of flow structure on heat transfer in compact heat exchanger by using finite thickness winglet at acute angle*. Journal of Thermal Engineering, 3(2), 1149-1162. (2017).
[2] Anibal, J., Mader, C. A., & Martins, J. R. R. A. *Aerodynamic shape optimization of an electric aircraft motor surface heat exchanger with conjugate heat transfer constraint*. International Journal of Heat and Mass Transfer, 198, 123547. (2022).
[3] Capitao Patrao, A., Jonsson, I., Xisto, C. M., Lundbadh, A., & Grönstedt, T. *Compact heat exchangers for hydrogen-fueled aero engine intercooling and recuperation*. Applied Thermal Engineering, 238, 122295. (2024).
Phys. Fluids 11, p. 417422 (1999).

Aktuelle Forschungsschwerpunkte / Current research topics

A Aerodynamics

A2 Flow control and Predictive modelling of shear-driven Flows using Machine-Learning

G. Hasanuzzaman and C. Egbers (DFG - HA 10565/2-1)

Introduction

Boundary layer flows are one of the central topics in aerospace engineering, particularly turbulent boundary layers (TBLs), which characterize the flow field around an aircraft. They are widely studied due to their significant impact on operating costs in the aviation industry, especially in subsonic flight. Wall friction and its associated costs in aviation amount to several billions annually. Therefore, flow control technologies (FCTs) applied to aircraft surfaces play a crucial role in reducing skin friction, but at the same time, they increase measurement complexities. One promising active FCT is uniform blowing through perforated walls, which is well known for its substantial effect in reducing wall friction [1]. However, the measurement complexities and uncertainties associated with FCTs have driven researchers to explore new approaches to analyzing data obtained from TBL flows under such applications. With increasing computational power and advances in data acquisition systems, we now have the opportunity to apply a variety of Machine-Learning (ML) algorithms [2] to large experimental datasets [3].

There are several unresolved aspects that need attention. For instance, the central research questions focus on developing efficient and accurate machine learning models for predicting wall-shear stress in turbulent boundary layers with complex boundary conditions. Key challenges include achieving high accuracy without relying on turbulence modeling assumptions, optimizing model performance while minimizing uncertainty, and identifying low-dimensional parameter spaces to improve training efficiency. Another aim is to design algorithms capable of generalizing beyond the trained flow physics for reliable out-of-the-field predictions. Finally, the role of different input data types, such as velocity or pressure measurements, in influencing prediction accuracy is also requires particular attention. Keeping this in mind DFG project *"Shear-flow Prediction and Drag Estimation using AI-driven Methodology (SPADE-AIM)"* will leverage experimental infrastructure to measure the flow field over a wide range of Reynolds numbers (Re). Figure 1(c) presents a comparison of these parameters between two distinguished wind tunnel facilities: the LAS, BTU wind tunnel [3] and the Laboratoire de Mécanique des Fluides de Lille (LMFL) wind tunnel [4], denoted as BTU and LMFL, respectively. The LMFL wind tunnel, featuring a 21.6 m long flat plate with complete optical access, provides an optimal boundary condition for spatially developing TBL studies using non-intrusive/intrusive optical measurements (see Figure 1(a) and (b)). Further details on the BTU and LMFL wind tunnel test sections and experiments can be found in [1]. Previous studies from [2] has shown that incorporating the physical constraints of the system with the pattern-recognition capability of neural networks (NNs), Physics-Informed Neural Networks (PINNs) can provide more accurate and physically meaningful predictions of velocity data obtained in TBL flows while embedding physical laws into the prediction algorithm. PINN algorithm integrates the

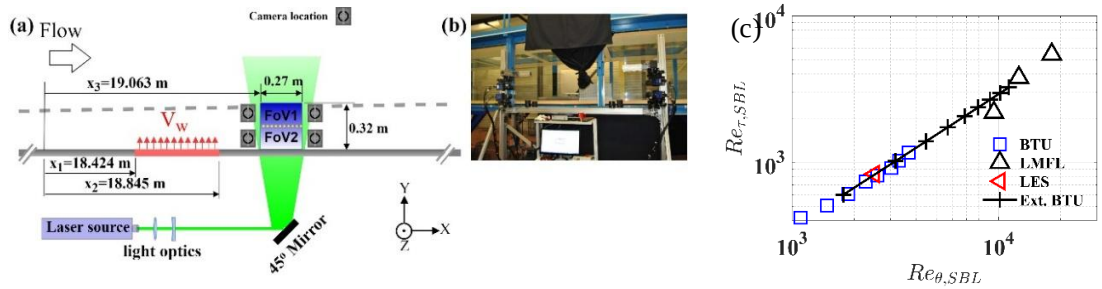

Figure-1: (a) Schematic representation of the flow field and the stereo PIV arrangement (all dimension in meter); (b) photograph of the wind-tunnel test section; (c) Comparison between the facilities with shear and momentum Re.

Aktuelle Forschungsschwerpunkte / Current research topics

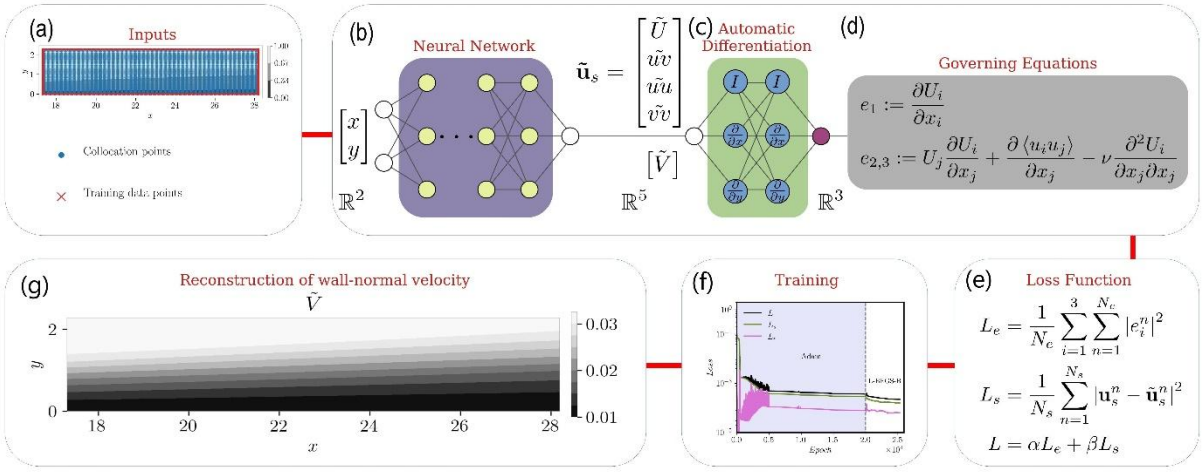

Figure 2: A schematic view of PINNs. Green indicates the neurons with non-linear activation functions, blue represents the implementation of automatic differentiation (AD) for differentiating the outputs u with respect to the inputs x = (x, y) and magenta refers to the calculation of the residual of the RANS equations [2].

governing physics of a system with the learning capabilities of neural networks. This approach enhances the accuracy of Particle Image Velocimetry (PIV) measurements from a TBL shown in Figure 3. The network was trained using PIV velocity data at the boundary together with the physical constraints of fluid flow, such as the Navier–Stokes equations. Through this training, the PINN learns the relationship between the velocity field and physical laws, enabling it to reconstruct higher-resolution velocity fields. The training objective is to minimize the difference between the PINN predictions and the experimental PIV data. Once the predictions converge to within a defined threshold, the algorithm is considered optimized. This process allows for significant improvements in data quality, particularly in cases where the original measurements suffer from limited spatial resolution.

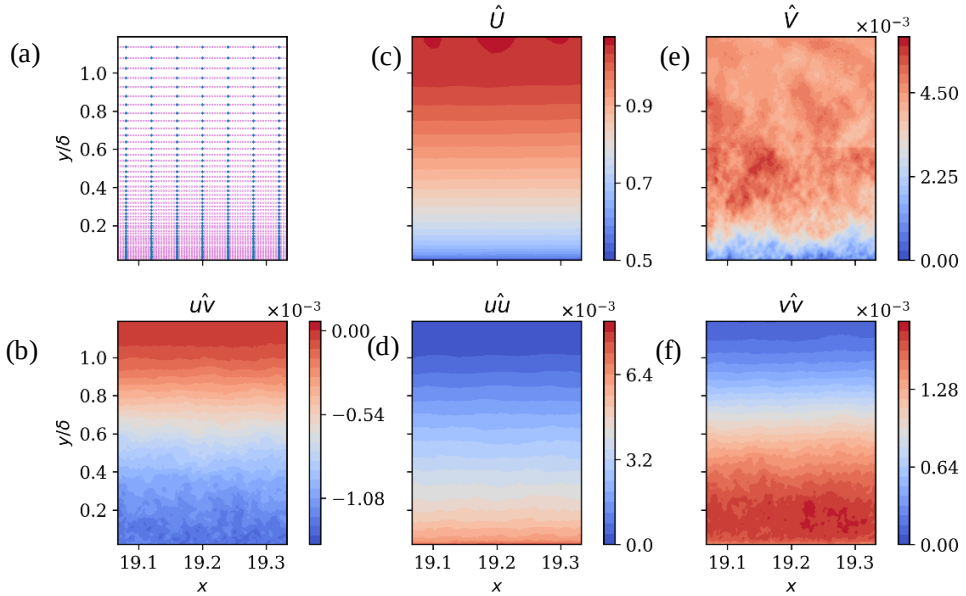

Figure 3: (a) Collocation x_l (pink) and the training-data points x_s (blue) within the computational domain. (b)–(f) Contours of the mean velocities and Reynolds-stress components, for details see reference [2].

Bibliography

[1] G. Hasanuzzaman, Cuvillier Verlag, Göttingen, Germany, ISBN: 978-3-7369-7558-3. (2021).
[2] G. Hasanuzzaman, H. Eivazi,.., C. Egbers, Meas. Sci Tech., **34(4)**, 044002. (2023).
[3] G. Hasanuzzaman, S. Merbold,.., C. Egbers, Jour. Turb., **21(3)**. (2020).
[4] G. Hasanuzzaman, S. Merbold,.., C. Egbers, Jour. Turb., **23(1-2)**. (2022).
[5] G. Hasanuzzaman and C. Egbers, Jour. Turb., **DOI: 10.13140/RG.2.2.31060.92807**. (2024).

Aktuelle Forschungsschwerpunkte / Current research topics

A Aerodynamics

A3 COVID-19 prevention through aerodynamic analysis of dynamic scenarios.

G. Hasanuzzaman, T. Buchwald, S. Merbold, Ch. Egbers, A. Schröder (DFG EG 100/36-1)

The 2019 outbreak of SARS-CoV-2 has emphasized the need to understand how airborne pathogens are transmitted in order to prevent the spread of disease. In particular, it is important to understand the transmission routes of small, pathogen-laden aerosol particles that are light enough to linger in the air in public places such as classrooms for several minutes to hours. Therefore, the following work was funded by the German Research Foundation (DFG) under the project name-Sensors and exposition analyses for aerosol transport in dynamic situations (SENSAERO). A carefully designed experimental facility was developed at BTU C-S, known as Cottbus Aerosol particle Reference Experiment (CARE)[1]. A series of experiments were conducted there using large-field Lagrangian Particle Tracking (LPT) [2] and distributed sensor arrays [3]. The LPT experiment was performed to assess mixed convective flows in a controlled domain of public spaces with different ventilation strategies. Thermal plumes were created using heated dummies, and an approximately 0.4-meter-thick collimated LED light sheet was used to illuminate helium-filled soap bubbles (HFSBs), which acted as passive tracer particles. The particles were then recorded over three minutes using two cameras synchronized with LED illumination. The novel 2D-Shake-The-Box method has been used to track particles in two light sheet planes measuring approximately 4.2 m × 2.8 m each. As shown in Figure 1, a dummy was seated in every other seat in the classroom, as was done during the pandemic to reduce the risk of infection. Large-scale measurements result in time-averaged velocity fields, as shown in Figure 2. These results demonstrate how opening the window influences the thermal plumes, and how operating the air purifier disperses them completely. This indicates strong mixing and therefore more homogeneous pathogen concentrations, which reduce the probability of neighboring students becoming infected. Furthermore, analysis of individual Lagrangian tracks suggests that the risk of infection due to the directed lateral flow of exhaled, virus-laden aerosol particles is relatively low with all ventilation methods examined.

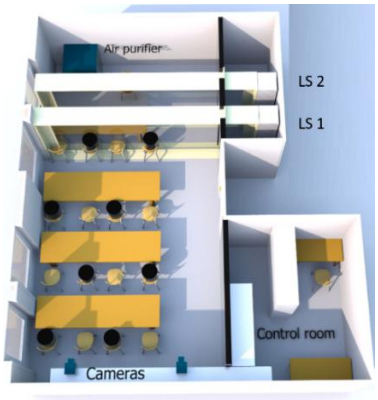

Figure 1: Sketch of the model classroom arrangement.

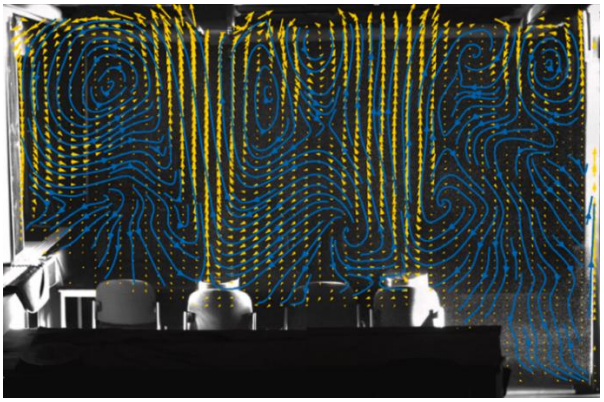

Figure 2: Time-averaged velocity field and corresponding streamlines in a scenario without any ventilation at lightsheet position 1 (LS 1).

Therefore, opening windows or operating an air purifier at the front of a classroom is unlikely to create direct infection pathways in the front row. To obtain information about transport throughout the whole classroom, these measurements are combined with those from another experimental approach conducted in the same classroom. The LPT measurements exhibit the large flow patterns, however, a different approach was necessary for the dynamic situations. A novel measurement system was developed and known as Dynamic Aerosol Transport for Indoor Ventilation (DATIV) [3].

Figure 3 illustrates the DATIV system, a portable and low-cost solution for monitoring air quality in real time. At its core, the setup combines a compact particle sensor (Sensirion SPS30) with a Raspberry Pi Zero 2W single-board computer and a rechargeable lithium-polymer power bank. This combination was chosen for its affordability, making it possible to deploy multiple units simultaneously as an array without significant cost. The system is lightweight, remote, and capable of running for several hours. This allows measurements to be carried out flexibly in different dynamic environments, from classroom to restaurant configurations.

One of the system's major strengths lies in its adaptability. The Raspberry Pi is an open-source platform with broad support from a global community of developers and researchers. This selection ensures that the DATIV system is not only inexpensive but also highly customizable and adaptable. Additional sensors—such as those measuring temperature, humidity, or other air pollutants—can be easily integrated thanks to the Raspberry Pi's versatile input/output connections, which include USB, GPIO, UART, and other standard interfaces. This flexibility makes the platform adaptable, as new sensors or features can be added without redesigning the entire system. Importantly, the reliance on widely available hardware also helps to avoid disruptions caused by shortages of specialized components, a problem that became evident during the COVID-19 pandemic.

The SPS30 particle sensor works on the principle of laser scattering, where, air is drawn into the device and illuminated by a laser beam, with the scattered light detected to estimate particle counts and concentrations. This allows the system to provide real-time measurements of fine particulate matters upto 0.2 micrometers, which is especially relevant for assessing air quality in homes, offices, and urban indoor environments. While compact and inexpensive, the sensor still delivers reliable performance comparable to the commercial particle sensors.

Beyond its technical capabilities, the DATIV system demonstrates how open-source software and electronics can be combined to create sustainable solutions. Because the system is programmable in widely used languages such as Python, it can be easily modified to process data locally, transmit it wirelessly using a UART network protocol, or connect to central servers for large-scale monitoring networks. This makes it an excellent platform for the measurements of indoor aerosol transmission, reduce airborn diseases and examining preventive counter measures. The DFG project SENSAERO ended in the summer 2024.

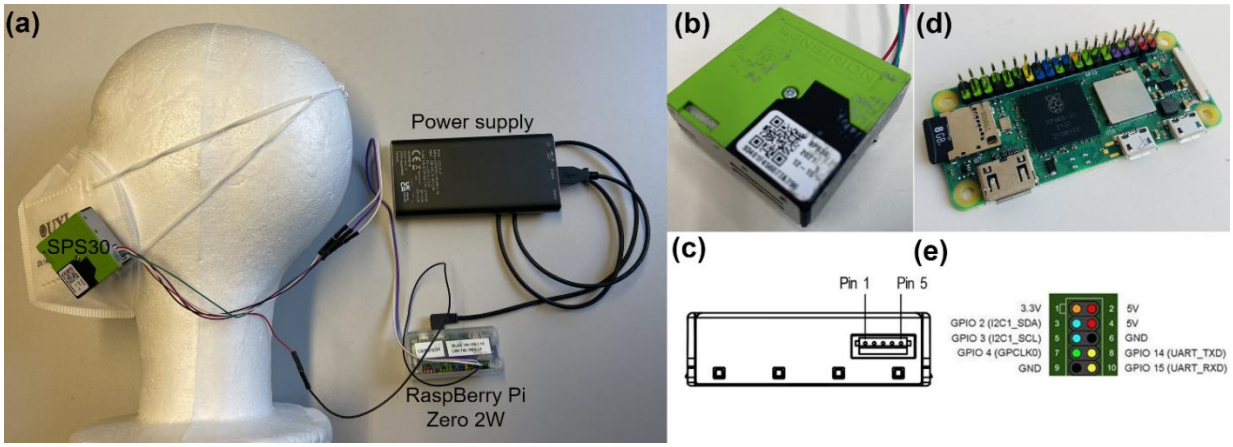

Figure 3: (a) Portable DATIV system where an SBC is powered by a DC power supply; (b) The SPS30 particle sensors; (c) The communication interface connector is located on the side of the sensor opposite to the air outlet; (d) The Raspberry Pi Zero acts as the computer, hosting the measurement software and communicating via an internal antenna within the WiFi domain to transmit the data; (e) The color-coded built-in GPIO of the computer.

Bibliography

[1] S. Merbold, G. Hasanuzzaman,…, C. Egbers and A. Schröder, tm-Technisches Messen **90,** Issue 5 (2023).
[2] T. Buchwald, G. Hasanuzzaman, S. Merbold, D.Schanz, C. Egbers and A. Schröder, Heliyon **9,** Issue 12 (2023).
[3] G. Hasanuzzaman, T. Buchwald, …, U. Hampel and A. Schröder, MDPI (Sensors) **24,** Issue 13 (2024).

B Fluid Mechanics

B1 DFG Core Facility Center "Physics of Rotating Fluids Lab" at BTU

U. Harlander & Ch. Egbers (DFG EG100/23-1, HA 2932/9-1)

The present proposal aims to establish a new international research center in form of a core facility center for "Physics of Rotating Fluids (PRF)" with geo-/astrophysical, meteorological and technical applications located at BTU. The main goal is to integrate cutting-edge rotating and stratified fluid flow experiments across national boundaries in order to foster internationally competitive experimental research in the research field of rotating and stratified fluids by providing an easy access to outstanding experimental facilities (Fig. 1, left) equipped with state-of-the-art instrumentation. The research areas covered by the experimental facilities inside the new center are (Fig. 1, right):

- Planetary and astrophysical flows (with focus on disk formation, instabilities and mixing)
- Geophysical fluid dynamics (with focus on strato-rotational turbulence, mean flow generation and wave interaction)
- Rotating flows with technical applications (centrifuges, turbines, journal bearings and rotor/stator cavities)

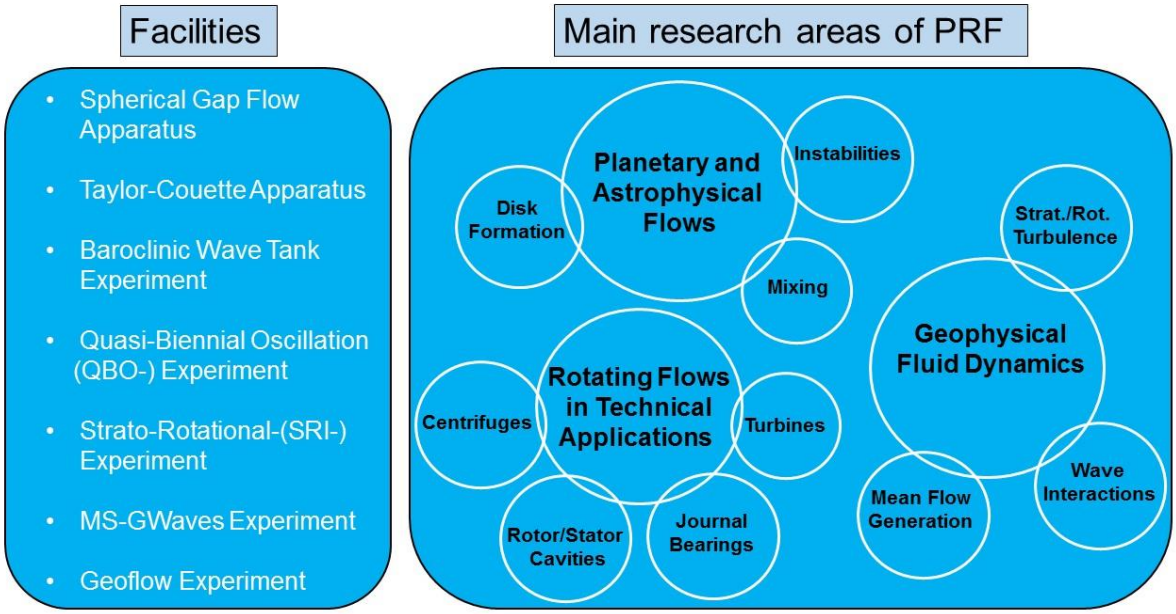

Figure 1: Summary of provided facilities and related and intended research areas of PRF

Thus, the main goals of this proposal are to:

- advertise and enforce the different research activities on rotating and stratified fluid flow experiments at BTU
- provide these outstanding research facilities at BTU to a larger national and international research community

Aktuelle Forschungsschwerpunkte / Current research topics

- bring together the recognized expertise of national and international working groups in the field of rotating and stratified fluids at BTU
- interconnect and help interested users by a networking program and joint research activities
- establish training groups for young researchers (Ph.D. students, Postdocs) in the field of rotating and stratified fluids
- organize exchange of scientific staff between the different research groups
- develop new experiments and models for a better insight into the dynamics and the role of these mean flows in geophysical, astrophysical, meteorological and technical flows at BTU
- deliver experimental data (including the use of modern experimental techniques like Thermography, Laser-Doppler-Anemometry, Particle Image Velocimetry (PIV), Laser Induced Fluorescence (LIF) techniques and Liquid Chrystal Tracer techniques, while the research approach as a whole is experimental, numerical and theoretical for the "PRF"
- organize and prepare collaborative applications to national and international calls for proposals (ANR, DFG, EU_FP8).
- collaborative data analysis of experimental, theoretical and numerical simulations.

<u>These goals will be achieved by</u>

- maintaining a suitable and safe physical environment with access to the required research services
- establishing a transparent and short review process for the external user community
- providing easy application forms for external scientific users, that ensures that proposals fit into the scientific frame of PRF research topics and are also compatible with the experiment facilities available
- sustaining a critical mass of scientific and technical expertise
- training and advising researchers as required
- providing appropriate and timely assistance
- enabling, advising and training on safe working practices
- ongoing research on new developments in instrumentation and responding to changes of experimental research; e.g. by designing, implementing or procuring appropriate mechanical, optical and electronic solutions to meet new experimental and diagnostic requirements
- documentation (user guides, safety-/laboratory manuals, annual reports, publications)
- public relations/ outreach (web-site, flyer, poster, presentations etc.)
- training / education (summer schools, workshops, young researcher meetings)
- continuation of core facility center activities after 3 years DFG funding through succeeding funding by BTU

<u>Organization and interfaces of the core facility center "Physics of Rotating Fluids (PRF)":</u>
The new core facility center for "Physics of Rotating Fluids (PRF)" will cover and focus all previous single research and guest scientist exchange activities like EuHIT, CNRS French/German-co-operation and ESA Topical Team with BTU/CFTM[2] in the field of rotating and stratified fluid flows as illustrated in Fig. 2. After funding from DFG via the present proposal, the core facility center for "Physics of Rotating Fluids (PRF) will be continued and financed sustainably by BTU.

Aktuelle Forschungsschwerpunkte / Current research topics

Services and joint research activities of the core facility center "Physics of Rotating Fluids (PRF)":
The actual status of the core facility center for "Physics of Rotating Fluids (PRF)" comprises all experimental facilities and measurement techniques located in the Fluid-Center-Building in different rooms next to each other.

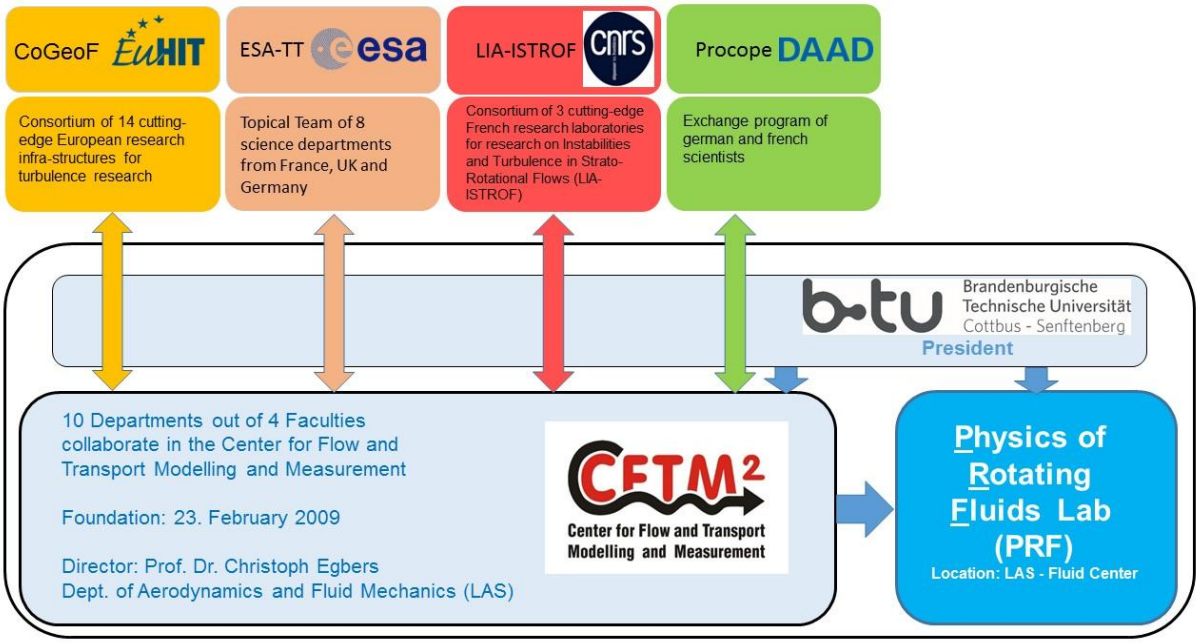

Figure 2: Organization structure and interfaces of core facility "Physics of Rotating Fluids (PRF)" Lab

The PRF is located in the Fluid-Center-building, on the campus of the Brandenburg University of Technology, Siemens-Halske-Ring 14, 03046 Cottbus, Germany. Responsible for the experiments is the Department of Aerodynamics and Fluid Mechanics. In this department about 30 technical & scientific employees work on experimental, theoretical and numerical questions of fluid mechanics. Generally we offer two types of services: i) in situ research with a direct access to the facility, and ii) commissioned research. In the first case i), the user in person will be conducting the research at our facility. To these researchers we offer practical guidance as well as technical assistance on the part of our scientific and/or technical staff, which is necessary due to the high complexity of the experimental installations. In preparation of such joint research project, the user will work with the facility lead scientist and the facility technician. The guesthouse of the BTU will minimize the organizational effort required for arranging the visits to the different facilities. In the second case ii), the commissioned research, the user can demand for certain measurements to be performed at our facility without being actually present in Cottbus. In this case our personnel will carry out the requested measurements and transmit the results to the user. This type of research is particularly appealing to users from the computational fluid dynamics community who are interested in validating their numerical data using experimental data.

Aktuelle Forschungsschwerpunkte / Current research topics

Scientific experimental equipment:

- Spherical gap flow apparatus (DFG EG 100/1-1, 1-2)
- Taylor-Couette apparatus (DFG EG 100/2, EG 100/7; EG 100/15-1, 15-2; FOR1182)
- Baroclinic wave tank experiment (DFG EG 100/3; EG 100/13-1, 13-2, 13-3; SPP 1276 "Metström")
- Quasi-Biennial Oscillation (QBO-) experiment (DFG EG 100/14-1; HA2932/6-1)
- Strato-Rotational-experiment (DFG EG 100/18-1; HA2932/7-1)
- MS-GWaves experiment (HA2932/8-1,2; FOR 1898)
- Geoflow experiments (DLR, ESA)

Measurement equipment

- 2D-Particle Image Velocimetry (PIV) System, 15mJ Nd:YAG LASER, monochromatic CCD camera, resolution 1 megapixel (New Wave Research, TSI)
- Stereo-PIV system, 100mJ Nd:YAG LASER, 2 cameras with 2 MP resolution (Dantec Dynamics)
- Dantec Dyn. Laser Induced Fluorescence (LIF) system to measure concentration and temperature
- Volumetric Velocimetry, 100mJ Nd:YAG LASER, 3 cameras with a resolution of 2 megapixel, telecentric lenses for a measurement volume of 10 x 10 x 10 cm3 (Dantec Dynamics)
- Particle Tracking (2D, 3D) with the dantec system mentioned above
- 2x 1D (He-Ne LASER) and 2D Laser Doppler Anemometry (LDA), Ar-Ion-LASER
- Infrared-Thermography system

Bibliography:

1. Egbers, Ch., Pfister, G., (Eds), 2000, Physics of Rotating Fluids, **Lecture Notes in Physics 549**, Springer
2. Harlander, U., v. Larcher, T., Wang, Y., Egbers, Ch., 2011, PIV- and LDV-measurements of baroclinic wave interactions in a thermally driven rotating annulus, **Exp. Fluids,** 51**,** 37-49, DOI 10.1007/s00348-009-0792-5
3. Feudel, F., Bergemann, K. , Tuckerman, L., Egbers, Ch., Futterer, B., Gellert, M., Hollerbach, R., 2011, Convection patterns in a spherical fluid shell, **Phys. Rev. E**, 83 (2011), 046304
4. Harlander, U., Wenzel, J., Alexandrov, K., Wang, Y., Egbers, C., 2012, Simultaneous PIV- and thermography-measurements of partially blocked flow in a heated rotating annulus, **Exp. Fluids**, 52, 1077-1085
5. Koch, S., Harlander, U., Egbers, Ch., Hollerbach, R., 2013, Inertial waves in a spherical shell induced by librations of the inner sphere: experimental and numerical results, **Fluid Dyn. Res. 45**, Best paper 2013 Jap. Soc. Fluid Mech.
6. Merbold, S., Brauckmann, H.J., Egbers, Ch., 2013, Torque measurements and numerical determination in differentially rotating wide gap Taylor-Couette flow, **Phys. Rev. E** 87, 023014
7. Futterer, B., Krebs, A., Plesa, A.-C., Zaussinger, F., Hollerbach, R., Breuer, D., Egbers, Ch., 2013, Sheet-like and plume-like thermal flow in a spherical convection experiment performed under microgravity, **J. Fluid Mech., vol. 735,** 647-683 , Cambridge University Press 2013, doi:10.1017/jfm.2013.507,
8. Klein, M., Seelig, T., Kurgansky, M. V., Ghasemi V., A., Borcia, I.-D., Will, A., Schaller, E., Egbers, Ch., Harlander, U., 2014, Inertial wave excitation and focusing in a liquid bounded by a frustum and a cylinder, **J. Fluid Mech., vol. 751**, 255-297, doi:10.1017/jfm.2014.304, 2014
9. Vincze, M., Borchert, S., Achatz, U., von Larcher, Th., Baumann, M., Liersch, C., Remmler, S., Beck, T., Alexandrov, K.D., Egbers, Ch., Fröhlich, J., Heuveline, V., Hickel, S., Harlander, U., 2014, Benchmarking in a rotating annulus: a comparative experimental and numerical study of baroclinic wave dynamics, **Meteorolog. Zeitschrift**, 23, 611 - 635
10. Harlander, U., v. Larcher, Th., Wright, G.B., Hoff, M., Egbers, Ch., 2014, Orthogonal decomposition methods to analyze PIV, LDV and thermography data of a thermally driven rotating annulus laboratory experiment. AGU book: **Modelling Atmospheric and Oceanic flows:** insights from laboratory experiments and numerical simulations, Th. v. Larcher and P. Williams (ed.), Wiley

B Fluid Mechanics

B2 The very-wide gap turbulent Taylor-Coette flow.

M. H. Hamede, K. Biesold, and Ch. Egbers (DFG EG100/30-1)

For more than a century, the flow in the gap between two independently rotating coaxial cylinders has been studied. The so-called Taylor–Couette (TC) flow is used as one of the paradigmatic systems of the physics of fluids. It's simple and mathematically well-defined geometry, natural periodicity, and confinement of fluid volume lead to excellent conditions for experimental and numerical studies. The TC flow is a model for general rotating shear flows with technical (turbines or compressors) as well as geo- and astrophysical applications (accretion discs, star formation). Within this geometry a rich variety of flow states can be adjusted by changing the control parameters, namely the ratio of angular velocities $\mu=\omega_2/\omega_1$, the radius ratio $\eta=r_1/r_2$, the aspect ratio $\Gamma=L/d$ with the gap width $d=r_2-r_1$ and the shear rate inside the gap in terms of the shear Reynolds number $Re_s=2r_1r_2d|\omega_2-\omega_1|/((r_1+r_2)\nu)$ with the kinematic viscosity ν of the fluid and the indices 1 for the inner and 2 for the outer cylinder. In the case of purely inner cylinder rotation, the flow is linearly unstable; conversely, when rotation occurs exclusively in the outer cylinder, the flow is linearly stable.

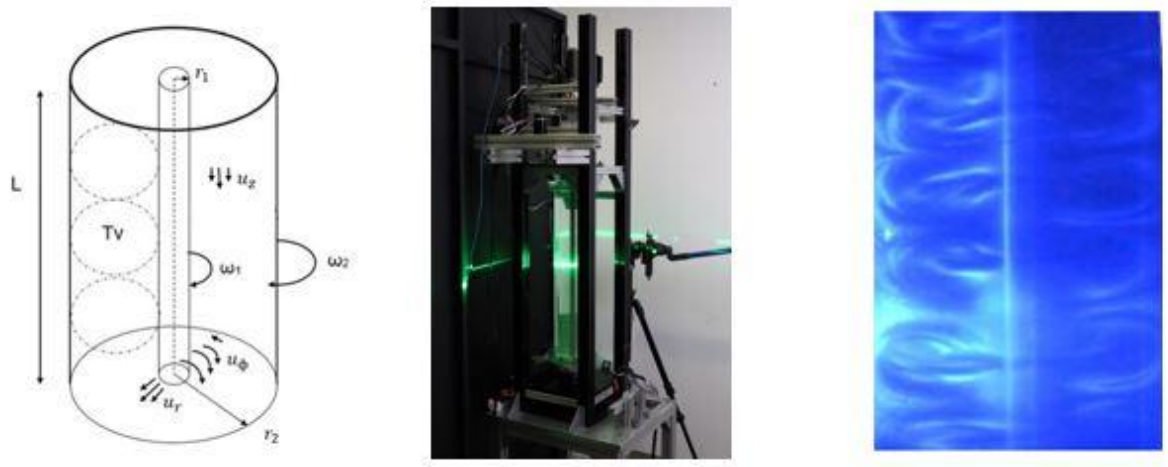

Figure 1: a) Sketch of Taylor-Couette geometry, b) Picture of the TC experiment with the PIV setup, c) the stable Taylor vortices inside the gap

A very important quantity for transport processes in Taylor-Couette flows is the angular momentum current $J_\omega=r^3(\langle u_r\omega\rangle_{t,\varphi,z}-\nu\partial_r\langle\omega\rangle_{t,\varphi,z})$, which can be directly measured by the torque T at the inner or outer cylinder. When J_ω is normalized by its corresponding laminar value $J_{\omega,lam}$, a quasi Nusselt number (Nu_ω) can be defined in analogy to heat transport problems [2].

For investigations of the TC flow, we have two facilities at the Department of Aerodynamics and Fluid Mechanics at the BTU-Cottbus, the Turbulent Taylor-Couette Cottbus (T^2C^2) facility and the Top-view-Taylor-Couette Cottbus (TvTCC) facility. The (T^2C^2) facility has a transparent outer cylinder, a precise torque measurement unit based on strain gauges inside the inner cylinder, and is capable of controlling the angular velocities of the end plate. The (T^2C^2) facility has a radius ratio of (0.5), and it can go up to $Re_s = 10^6$. The TvTCC facility with its transparent top plate and outer cylinder gives the advantage to use visualization and measurement techniques for the three flow component (radial, axial, and azimuthal). Another characteristic of the TvTCC facility is that it has a flexible geometry with a changeable inner cylinder, which allows studying the flow for different radius ratios using one facility. The key geometrical parameters of both facilities are summarized in table 1:

Aktuelle Forschungsschwerpunkte / Current research topics

Table 1: Parameter for T²C² and TvTCC facilities

	Gap width d (mm)	Radius ratio η	Aspect ratio Γ	Re_s
T²C²	35	0.5	20	10^3-10^6
TvTCC	35, 45, 56, 63	0.5, 0.357, 0.2, 0.1	20, 15.5, 12.5 11.1	10^3-$3{\cdot}10^5$

Previous works used these TC facilities to study the flow and the angular momentum transport in the geometry of radius ratios 0.5 [1], 0.357 [3], and 0.1 [4,5,6,7].
In general, the current phase of the project focuses on very wide-gap geometries after our group's long record of studying wide-gap geometries [1, 2, 3]. For the current research phase, the radius ratio of 0.1 is considered.
The question was always raised: do the classical Taylor Vortex flow and the other classical patterns appear in the very wide gap TC flow? We answered yes! For flow with $Re_s \leq 530$ and low counter and surprisingly co-rotating rates, the laminar Taylor vortices (TV) appear. For the same shearing rates and higher counter-rotating rates, the TV turns to be wavy, and for a further increase in the counter-rotating rates, the wavy TV is restabilized again and detaches from the outer cylinder. Due to the stabilizing effect of the outer cylinder, the flow in the gap is mostly laminar for $800 \leq Re_s \leq 5{\times}103$ and relatively high counter-rotating rates of $-0.06 \leq \mu \leq -0.01$. This laminar flow was penetrated by small-scale plumes that formed close to the inner cylinder and destabilized the flow locally, resulting in locally isolated turbulent spots. As the system's driving rates increase, the repetition rate of these spots increases, and they are switched to non-isolated turbulent structures we identify as turbulent bursts, which overlap and interact with each other and destabilize the entire flow. As the driving rates increased, the frequency and size of the bursts also increased, but surprisingly, increasing the Res over a certain limit decreased the frequency of these patterns again. For higher counter-rotating rates $\mu \geq -0.06$ a novel pattern appears, which we assumed just existed in the very wide gap TC flow. The radial inflow and outflow, vertically aligned with the rotation axis, formed a single Axial Columnar Vortex (ACV) between the cylinders as shown in Figure 2, which rotated around the system with a fixed frequency, leading to an azimuthal mode number 1. For further higher counter-rotating rates, the ACV detaches from the outer cylinder, loses its axial alignment, becomes helical, and the Helical Columnar Vortex appears.

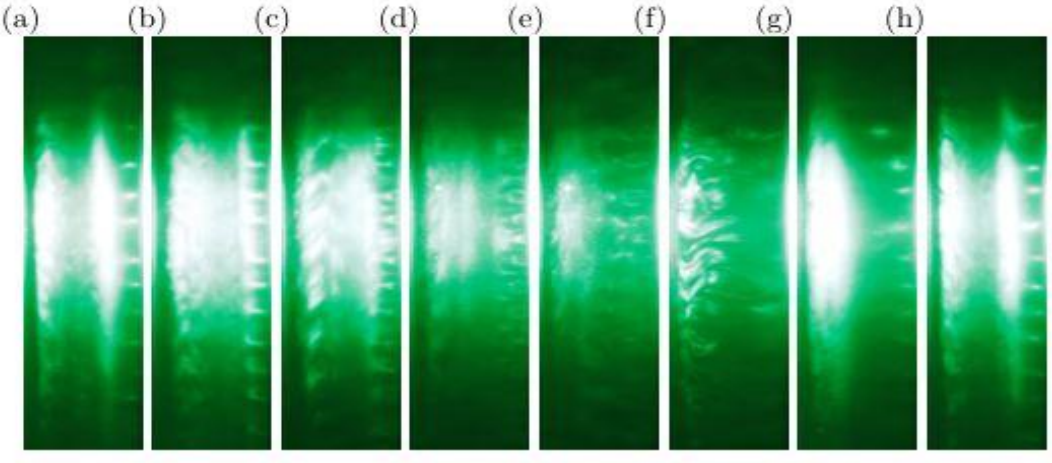

Figure 2: Sequence of meridional plane visualisation of Axial Columnar Vortex flow at $ReS = 1650$, $\mu = -0.111$ for time steps: (a) 0.0 sec, (b) 0.2 sec, (c) 0.4 sec, (d) 0.6 sec, (e) 0.8 sec, (f) 1.0 sec, (g) 1.2 sec, (h) 1.4 sec. The inner cylinder wall is located at the right edge of the images, while the outer cylinder is located at the left edge.

Moreover, the influence of the rotation ratio, specifically in the counter-rotating regime, on the velocity field behavior and the flow global response was studied in the current project for flows with $Re_s = 2{\times}10^4$, $6.1{\times}10^4$ and $13.1{\times}10^4$, and $-0.06 \leq \mu \leq 0$.

This study revealed significant axial dependency in the flow field for the different investigated parameters. The radial velocity component achieved different inflow and outflow regions through the different axial positions, where oval-like vortical patterns with an axial size of approximately 0.43d appeared. These cortical patterns mostly fulfilled the whole gap for $\mu = -0.077$. For higher counter-rotating rates, the radial velocity largely vanishes next to the outer cylinder, and the observed vortical patterns are found to have a smaller axial size and are restricted to the area next to the inner cylinder. Furthermore, the angular momentum transport dependence on the rotation ratio was studied, and presented in terms of the Nu_ω in analogy to the heat transport in the Rayleigh–Bénard flow.

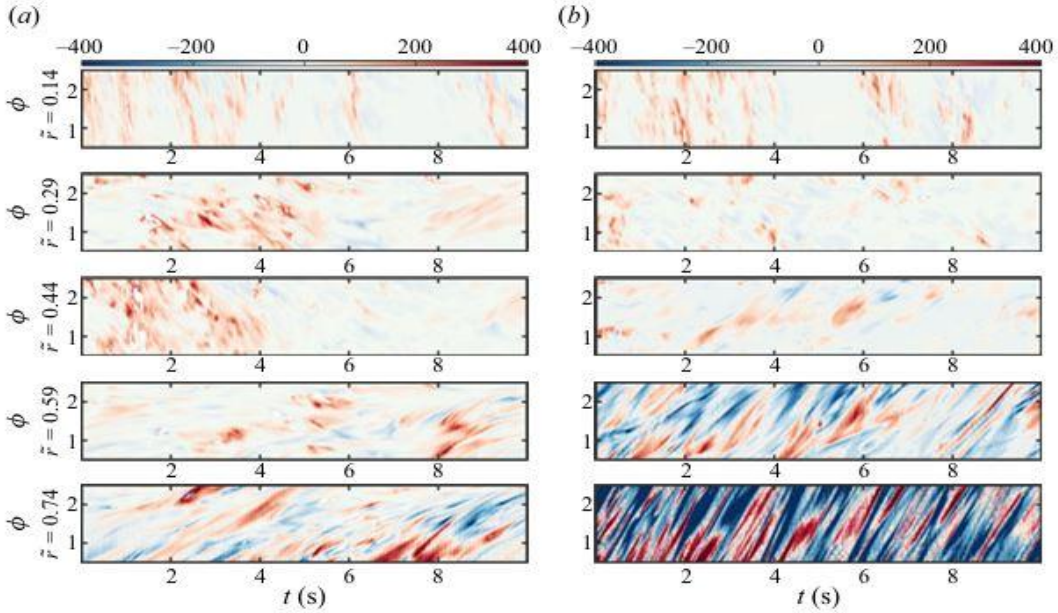

Figure 3: Contour plot showing the space–time diagram of $r^3(\omega u_r)/J_{lam}$ in the azimuthal-time plane for five different radial positions, at (a) z =+4 mm, (b) z =+4 mm from apparatus mid-height, for Re_s= 6.1 ×10^4 for high counter-rotating cases. The top figure is a radial position close to the inner cylinder, and the bottom figure is close to the outer cylinder. Results are shown for (a) μ =−0.04 and (b) μ =−0.06.

For the three investigated Re_s flows, the Nu_ω achieved a maximum value for low counter-rotating rates $-0.011 \leq \mu_{max} \leq -0.0077$, where for this specific rotation rates the large-scale patterns were found to fulfill the whole gap. At μ_{max} a very low radial gradient of $< \omega >_{\phi,z,t}$ profile through the gap was investigated, which reflects the effective mixing of the angular momentum. However, the angular momentum transport decreases from its maximum for higher counter-rotating rates, until it reaches a minimum value μ_{min} and then tends to increase again for higher counter-rotating rates ($\mu_{min} \geq \mu$) where a second maximum is expected. In contrast to μ_{max} observed at the low counter-rotating rates, the position of μ_{min} shows a clear dependence on the shear Reynolds number. The decomposition of the Nu_ω into turbulent and LSC contributions shows a maximum for the first at high rotating ratios and for the second at μ_{max}. It was obvious that the first Nu_ω maximum is a result of the strengthening of the LSC, which fills the whole gap, but the reason behind the second expected maximum was not clear until the space-time behavior of the flow was studied. The flow space-time behavior shows, for high counter-rotating rates $\mu \geq -0.025$, the existence of short-life time patterns in the radial region next to the outer cylinder, propagating inward from the outer cylinder toward the inner one, with increasing intensity as the counter-rotating rates increase, as shown in Figure 3. These newly observed patterns at high counter-rotating rates enhance the angular momentum transport, and a second maximum in the transport mechanism has to be expected.

In addition, the effective scaling of angular momentum transport with the shearing rate for flows with a stationary outer cylinder was also investigated. As expected, the Nu_ω increases with the shear Reynolds number, but a transition in the scaling relation between $Nu\omega$ and Res was observed for a sufficient shearing rate. For $Re_s \geq 2.5 \times 10^4$, the scaling relation $Nu\omega \sim Re_s^{-0.76}$ was found. The transition in the effective scaling reflects a transition in the flow state, as the computed exponent of -0.76 in this study was used to reveal a transition from the classical to the ultimate turbulent regime [1,2,3,8]. The flow velocity field reflects this transition from classical to the ultimate turbulent regime. Another flow feature distinguishing the ultimate regime from the classical turbulent regime is the flow structure's behavior, examined through spatial and temporal azimuthal energy co-spectra profiles. In the classical regime, small-scale structures with high frequencies were observed, in addition to large-scale structures with low frequencies mostly occupying the whole gap, while only a broad variety of large-scale patterns were observed with moderate frequencies in the ultimate regime.

As a second phase of a DFG project studying the very-wide gap TC flow, and based on the results presented above, the study of the topic will continue over the next three years with a special focus on the question that arose from the first phase project. A salient question pertains to the recently identified patterns adjacent to the outer cylinder under conditions of high counter-rotating rates. These patterns have been demonstrated to enhance angular momentum transport, and it has been hypothesized that they are generated due to shear layer instability. However, further investigation is necessary to substantiate this hypothesis. The objective of the present study is to conduct velocity measurements with a focus on the outer cylinder wall. The purpose of this focus is to magnify small-scale flow structures and resolve all flow scales in that area. Furthermore, it is imperative to obtain precise measurements to investigate the flow dynamics in the exceedingly high counter-rotating regime. Current experimental observations suggest the presence of a secondary angular momentum maximum within this flow regime, though its precise position remains to be elucidated. Furthermore, the flow velocity field was measured within the scope of this study for high-shear Reynolds number flows ($Re_s \geq$ 20000). However, the flow visualization reveals the presence of intriguing flow patterns for ($Re_s \leq$ 15000. The analysis of flow regimes revealed the emergence of distinct flow patterns, which we hypothesize to occur exclusively within the confines of the exceedingly broad gap TC flow (e.g., axial, columnar, and helical vortex). However, the underlying mechanism responsible for these instabilities remains an open question. A detailed time-resolved PIV of the radial and azimuthal velocities at the different axial positions for these specific flow parameters is planned for future work. With regard to the flow in the co-rotating regime, particularly the centrifugally stable flow, further investigation, possibly in the form of direct torque measurement, is necessary to provide more conclusive validation of the presence of the hydrodynamics instabilities in this flow regime.

Publication

[1] A. Froitzheim, S. Merbold, C. Egbers, Velocity profiles, Flow structures and scaling in a wide-gap turbulent Taylor-Couette flow, J. Fluid Mech., 831, 330-357, 2017

[2] S. Merbold, H. J. Brauckmann, C. Egbers, Torque measurements and numerical determination in differentially rotating wide gap Taylor-Couette flow, Phys. Rev. E, 87, 023014, 2013

[3] A. Froitzheim, S. Merbold, R. Ostilla-Monico and C. Egbers, Angular momentum transport and flow organization in Taylor-Couette flow at radius ratio of η =0.357, Phys. Rev fluids 4 (2019), 084605.

[4] M. H.Hamede, S. Merbold, and Ch. Egbers. Experimental investigation of turbulent counter-rotating taylor–couette flows for radius ratio η= 0.1. J. Fluid Mech., 964:A36, 2023.

[5] M. H. Hamede, S. Merbold, and Ch. Egbers. Experimental method for investigating the formation of flow patterns in a very wide gap taylor-couette flow (η= 0.1). Technisches Messen, 90(5):332–339, 2023.

[6] M. H. Hamede, S. Merbold, and Ch. Egbers. Transition to the ultimate turbulent regime in a very wide gap taylor-couette flow (η= 0.1) with a stationary outer cylinder. Europhys. lett., 143:23001, 2023.

[7] S. Merbold, M. H. Hamede, A. Froitzheim, and Ch. Egbers. Flow regimes in a very wide-gap Taylor-Couette flow with counter-rotating cylinders. Philosophical transaction A 381(2246):20220113, 2023.

[8] A. Froitzheim, R. Ezeta, S.G. Hisman, S. Merbold, C. Sun, D. Lohse, C. Egbers, Statistics, plume and azimuthally travelling wavs in ultimate Taylor-Couette turbulent vortices, J. Fluid Mech., 876, 733-765, 201

B Fluid Mechanics

B3 Transport in Fluids

Uwe Harlander and Franz-Theo Schön (DFG HA 2932/8-2, DFG HA 2932/17-4)

Introduction

Transport in fluids is of interest in a broad range of fields, from the transport of microplastics in the ocean to the transport of drugs in microchannels. The methods used to describe this transport are equally diverse. For instance, the transport of passive tracers is typically addressed using methods from the theory of dynamical systems [1]. For the transport of fluid in water channels, one focuses on the generation of mean flows due to wave forcing [2]. Transport is an inherent nonlinear phenomenon, either since the particle transport equations are nonlinear, or the excited waves interact nonlinearly with each other or with the background flow. The waves influencing the transport can either be generated by fluid instability or by mechanical forcing. Here, we briefly discuss one example for each of the two categories.

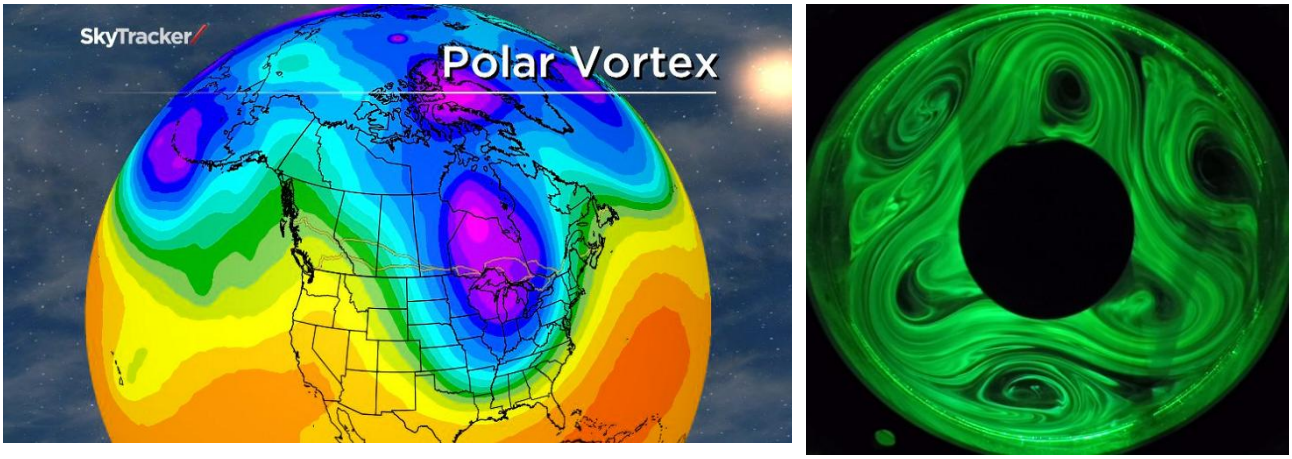

Figure 1: Left: Polar vortex with potential vorticity contours (Image courtesy of Western Carolina University). Right: Experimental analogy in a cylindrical baroclinic wave tank.

Results

Transport in a baroclinic vortex

The polar vortex separates cold polar air from warmer air of the mid-latitudes. The border between these two air masses is not straight but shows large meanders due to Rossby waves generated by baroclinic instability. This instability forms in rotating stratified flows with vertical shear. An example is shown in Fig. 1 (left). In the geosciences, it is important to understand the reasons for the jet's waviness and the possibility of breaking transport barriers so that heat, but also pollutants, can intrude into the vortex. In Fig.1 (right) a laboratory experiment of the polar vortex is shown. Small plastic particles are illuminated with a green laser, allowing the distribution of the particles to be clearly seen. Obviously, there are regions where the particle density is low. The jet stream forms a transport barrier that can be broken by the occurrence of so-called hyperbolic points. We have studied this scenario numerically and experimentally in [3]. We have reproduced the attracting material curves for different models using Lagrangian descriptors, a technique that allows us to successfully reveal the phase space structures. Lagrangian observations indicated that particles and floats can stay a long time inside the eddies. It is argued that strong gradients of potential vorticity act as transport barriers.

Aktuelle Forschungsschwerpunkte / Current research topics

Transport in tidal flows

Tidal flows can be found in the ocean but also in estuaries, where freshwater from rivers mixes with saltwater from the sea, creating a brackish water environment. They are biologically very productive ecosystems. It is an important question whether in such regions and the connected river systems tidal flows over topography can excite a mean transport of nutrients but also of water pollution [4]. In an experiment with an oscillating circular water channel, we tested this using an asymmetric bottom topography. We demonstrated that symmetric oscillations result in asymmetric flow fields, leading to a net transport of water [5]. For topography heights similar to the fluid depth, we find reflective amplification at the hill, similar to the case of a channel with a finite length. Decreasing the height of the topography, we observe transmissive amplification, where at the topography, the surface waves move in the same direction as the topography. Similar effects can be observed using a symmetric topography, but with an asymmetric oscillation [6].

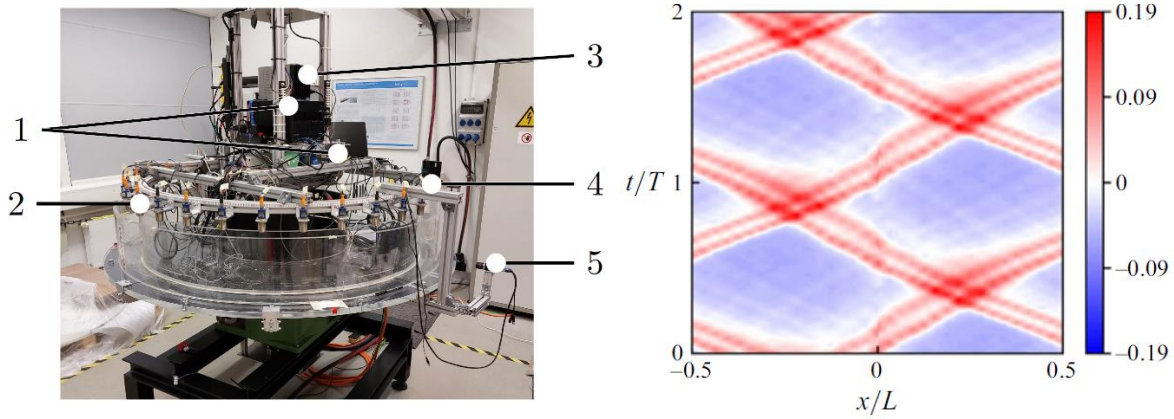

Figure 2: Left: Experimental setup of the oscillating tank. It includes two co-rotating computers (1), 17 ultrasonic sensors (2), a DC power supply (3), a green continuous laser sheet (4), and a 100 FPS global shutter camera (5). Right: Space-time diagram of two solitons traveling in the circular channel with length L=4.76m. The topography is at the center x/L=0 and has a height of 2cm. Fluid depth is 5cm. The oscillation frequency is close to the second eigenfrequency.

Fig.2 (left) shows the experimental setup. In total 17 ultrasound probes have been used to observe the surface height. The flow was measured by using Particle Image Velocimetry (PIV). Fig. 2 (right) shows a space-time plot of two traveling solitons, excited by the oscillating topography in the channel. Obviously, we cannot see reflections at the topography. The solitons can pass the hill that transfers energy to them. This transfer is possible since the hill is moving in the solitons' direction of propagation whenever the soliton comes into contact with the topography. We call this *transmissive amplification* in contrast to *reflective amplification*, which can be found in closed channels [4,5].

Acknowledgement
We thank A. Mancho, M. Bestehorn, R. and I. D. Borcia, and S. Richter for collaboration.

Bibliography

[1] A. Mancho, S. Wiggins, J. Curbelo, and C. Mendoza, Commun. Nonlinear Sci. Numer. Simul., **18**, 3530–3557, (2013).
[2] M.S. Longuet-Higgins, Philosophical Transactions of the Royal Society of London. Series A, **245**, 535-581, (1953).
[3] M. Agaoglou, V. J. García-Garrido, U. Harlander, A. M. Mancho, Phy. Fluids, **36** (1): 016611, (2024).
[4] F.-T. Schön, I.D. Borcia, U. Harlander, R. Borcia, S. Richter, and M. Bestehorn, J. Fluid Mech**., 999**, 69 (2024).
[5] F.-T. Schön, U. Harlander, I.D. Borcia, et al., Water Waves, https://doi.org/10.1007/s42286-025-00121-w, (2025).
[6] I.D. Borcia, M. Bestehorn, R. Borcia, F.-T. Schön, U. Harlander, and S. Richter, Eur. Phys. J. Spec. Top.,**233**, 1665–1672, (2024).

B Fluid Mechanics

B4 TEHD in a cylindrical annulus: laboratory experiments

M. H. Hamede, C. Egbers (DFG EG 100/20-3)

Introduction

The TEHD (Thermo-Electro-Hydro-Dynamics) project is concerned by the effect of the dielectrophoretic (DEP) force on a fluid confined in a cylindrical annulus. A dielectric fluid subjected to a temperature difference and a high frequency non-homogeneous electric field. This, in turn, triggers the DEP force, which originates from the gradient of the electric field's square. This force induced by the differential polarization of fluid particles can be seen as the action of an electric gravity on the density stratification, and is therefore analogous to Archimedean's buoyancy.
In a cylindrical geometry, the electric gravity is directed radially inward, so that one can expect the destabilization of the flow if the inner cylinder is hotter than the outer one. To focus on that thermoelectric instability, many experiments have been performed during the microgravity conditions of parabolic flight campaigns and a TEXUS sounding rocket (see Section C dedicated to space research). As the present project is concerned with laboratory experiments, the Earth's gravity will also act on the fluid density stratification and will modify the stability conditions of the system.

Following the previous phase of the TEHD project, which focused on a vertical cylindrical annulus [1,2], the new phase aims to examine two different systems. First, the DEP force is examined in a horizontal cylindrical annulus with differentially heated cylinders. The base state of this system corresponds to two crescent-shaped convective rolls that are symmetric with respect to the vertical plane containing the cylinder axis, as shown in Figure 1(a) for the case of no applied electric field (Vp = 0). The hot fluid rises along the inner cylinder and falls along the outer cylinder, resulting in an outward hot jet at the top and an inward cold jet at the bottom. As shown in Figure 1, as Vp increases, the strength of the convective rolls increases until a critical Vp value is reached, after which the symmetry of the flow is broken and the flow is destabilized. It is important to note that increasing Vp strengthens the convective rolls, leading to a significant enhancement in heat transfer even before the destabilization of the flow, as shown in [3].

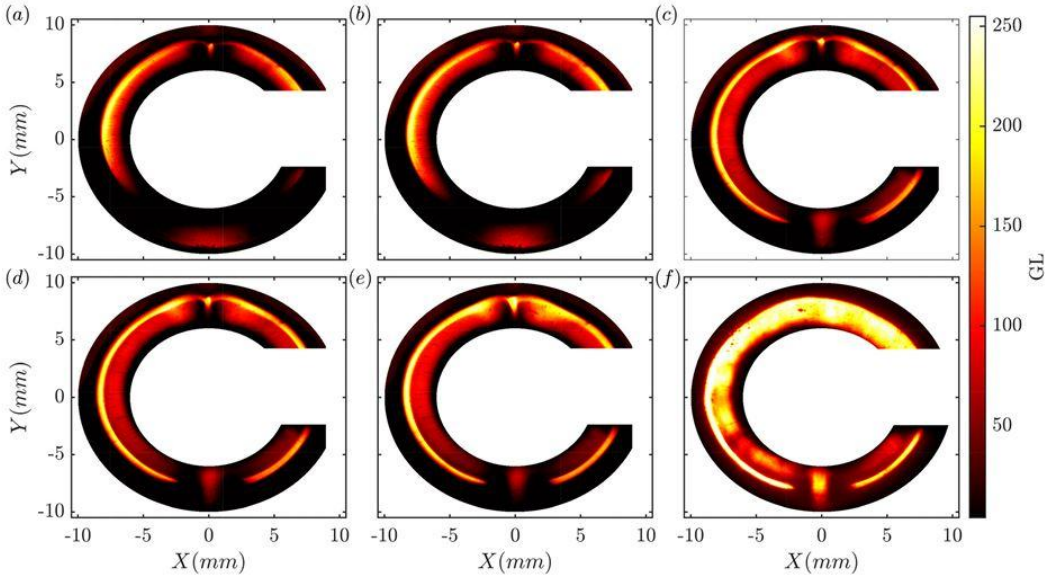

Figure 1 : Shadowgraphs of the flow with ΔT = 7K and different values of the applied voltage:(a) Vp = 0kV, (b) Vp = 6kV, (c) Vp = 14kV, (d) Vp = 15kV, (e) Vp = 16kV, and (f) Vp =18kV.

Aktuelle Forschungsschwerpunkte / Current research topics

The second part of the present project is concerned with the DEP force in a cylindrical annulus in vertical alignment, combined with the rotation of the inner cylinder. In the isothermal case, the resulting stratification of angular momentum can destabilize the flow, leading to the well-known Taylor vortices. When a temperature difference is applied, the Earth's gravitational force, the centrifugal acceleration, and the electric gravitational force act in unison on the density stratification. This experimental investigation, which is applicable to small-sized heat exchangers, should provide information about the transition from the base flow to the first instability, as well as its corresponding flow pattern and heat transfer enhancement. In the present stage of research, the experiment is configured as illustrated in Figure 2. A variety of flow measurement techniques will be employed for the qualitative and quantitative investigation of flow.

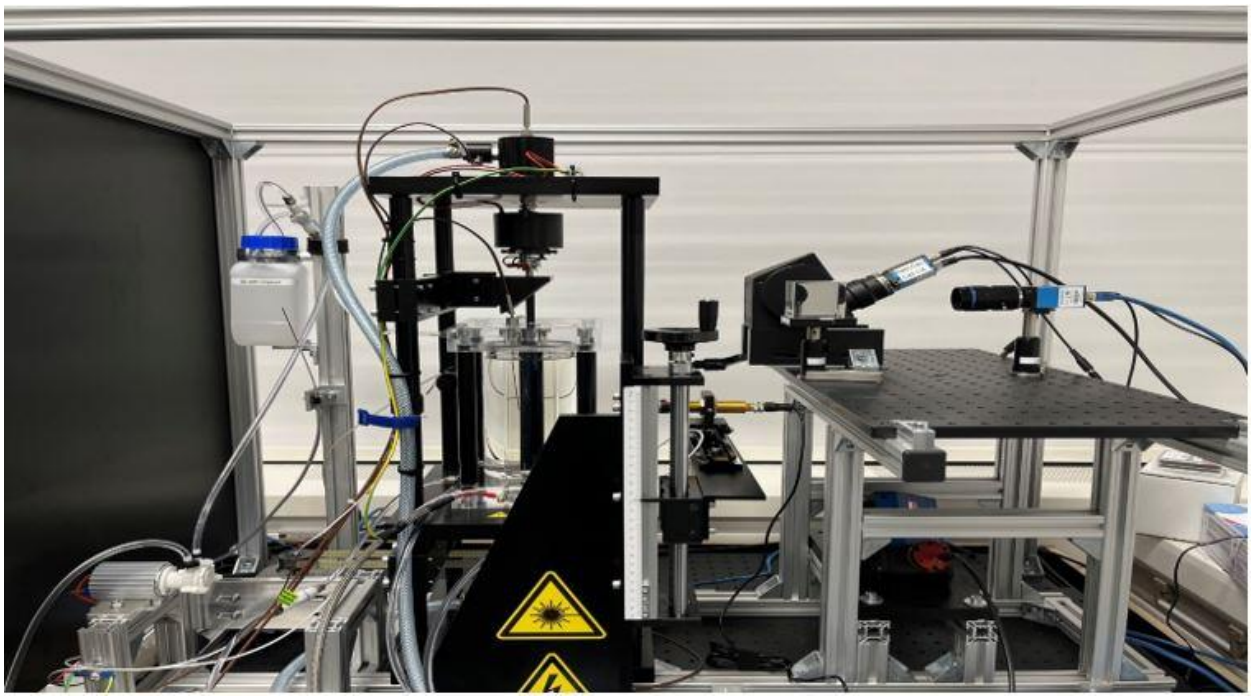

Figure 2: The novel TEHD experiment employs a vertical alignment with a rotating inner cylinder. As illustrated, the configuration of the optical measurement tools is also evident.

Bibliography

[1] Seelig, T., Meyer, A., Gerstner, P., Meier, M., Jongmanns, M., Baumann, M., Heuveline, V., Egbers, C., (2019) Dielectrophoretic force-driven convection in annular geometry under Earth's gravity, International Journal of Heat and Mass Transfer, 139, 386-398.
[2] Szabo, P., Meyer, A., Meier, M., Motuz, V., Sliavin, Y., Egbers, C., (2022). Simultaneous PIV and shadowgraph measurements of thermo-electrohydrodynamic convection in a radial electric force field, Technisches Messen 89(3).
[3] Hamede, M.H., Roller, J., Meyer, A., Heuvelline, V., Egbers, C., (2024). Dielectrophoretic force-enhanced thermal convection within a horizontal cylindrical annulus, Phys. Fluids 36, 124106.

B Fluid mechanics

B 5 Investigating the development of natural convection in a differentially heated annulus using Wollaston shearing interferometry

S. M. Kühne, P.S.B. Szabo, Y. Sliavin and C. Egbers (FKZ: DLR 50WM2441)

The motivation of investigating convective patterns, using *Wollaston Shearing Interferometry* (WSI) arises out of the *AtmoFlow* project. The *AtmoFlow* experiment deals with a spherical shell that mimics a planet at a small scale where terrestrial gravity is artificially induced by an equivalent electric central force field. The measurement system used is a WSI-system that is to be benchmark via ground experiments carried out in a terrestrial, utilizing a cylindrical, differentially heated cell.

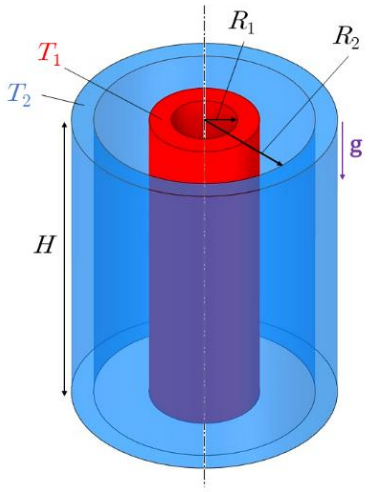

Figure 2: Schematic of the problem geometry

The cell features a cylindrical annulus with the height H and the two radii R_1 and R_2. The cylinder gap is filled with B5 silicone oil. Depending on the measurement campaign, the test cell will be either aligned vertically or horizontally to gravity. To induce the basic flow during an experiment, the temperature difference $\Delta T = T_1 - T_2$ is established in the fluid, utilising two, pump driven fluid loops, connected to two independently heated thermostats with silicone oil baths.

For the experimental procedure, the measured time for each temperature difference amounts to 10 minutes. This value was chosen, to ensure the full development of the basic flow and was derived from the thermal diffusion time scale of silicone oil, being $\tau_\kappa = 323s$. To ensure a proper development of the flow, the measurement time was therefore double this amount. Note, that this time does not include the time of pre-heating needed for the thermostat water baths. After a measurement has concluded, an additional waiting time of 10 minutes, with a temperature difference of 0K is necessary, to restore the initial state of the working fluid.

To capture the convective flow patterns in the annulus, the Wollaston shearing interferometry measurement technique is employed. The basic principle behind this method is the measurement of the fluid's refractive index gradient, caused by density fluctuations, which in return are caused by the temperature gradient ($n \sim \rho \sim T$). If a beam passes through an area with a changed refractive index, it will experience a phase shift $\Delta\varphi$, proportional the refractive index gradient at this point. To make this shift visible, the beam in question must be interfered with a non-disturbed beam, with the subsequent superposition causing wave interference and the resulting constructive and destructive interference leading to a black and white fringe pattern, the so-called *interferogram*. To enable this interference, a Wollaston prism is used, which consists of two birefringent crystal prisms, with different refractive indices but with the same optical axis [1].

An incoming, linearly polarised ray is focused onto the Wollaston prism and subsequently split under the separation angle γ into two separate beams with orthogonal polarisation states. To let these coinciding beams interfere, they must be brought back onto the same polarisation state, which can be achieved by placing a linear polariser behind the prism, which is has been rotated along the beam axis to be at an 45° angle, relative to the Wollaston prism. With that, the Wollaston prism has essentially created two, slightly sheared images, which are now overlapping and interfering.

The resulting interferogram is a 2D image (x-y-plane) representing the 3D information in the test section, which has been integrated along the beam path (z-direction), leading to this technique's description as a *line-of-sight* method. Since one prism can capture only gradients in one direction, a second Wollaston prism, rotated at a 90° angle relative to the other, must be used to capture the other gradient. Additionally, the incoming light must be circularly polarised to capture a phase shift in every direction to capture both gradients simultaneously, which can be achieved by placing a $\lambda/4$-plate in front of the test section [2].

The interferometry setup used for this investigation consists of two separate tabletops, with the test cell placed in between. The upper tabletop contains the laser emitter, equipped with an absorptive filter, reducing its power to safely work with a constant beam. Afterwards it passes through a polarised beam splitter to avoid any back reflections hitting the laser emitter. It then gets circularly polarised by a $\lambda/4$-plate and expanded to 30 times its size by two Galilean beam expanders. After leaving the upper tabletop, it is directed into the test cell by two mirrors. Depending in the measurement campaign, the test cell is either alignment vertically between both tabletops or horizontally, resting on the lower tabletop.
Leaving the test cell, the beam is directed by another set of two mirrors onto the lower tabletop, where its size is decreased 10 time by another Galilean beam expander. It is then split into two beams by a beam splitter, with each individual beam being focused onto a Wollaston prism each, to capture both gradients simultaneously. These prisms, which have been rotated orthogonally in respect to each other, are combined with their respective linear polarisers, to allow an easier adjustment. After passing the Wollaston prisms, both beams are captured by a camera to record the resulting interferograms.

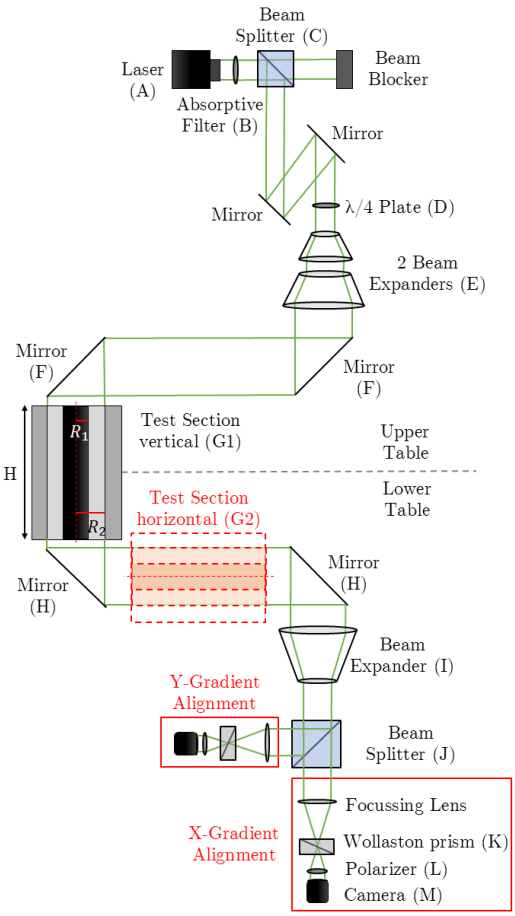

Figure 2: Schematic of the setup used in the experiments

References

[1] Wolgang Merzkirch. Flow visualization. Elsevier, 2012.

[2] Cameron Tropea, Alexander L Yarin, John F Foss, et al., Springer handbook of experimental fluid mechanics, volume 1. Springer, 2007.

B 6 Mean temperature field reconstruction of natural convection by phase demodulation of interferograms

S. M. Kühne, P.S.B. Szabo, Y. Sliavin and C. Egbers (FKZ: DLR 50WM2441)

The image post-processing aims to calculate the temperature profile in the cylinder annulus, using the measured interferograms. Since the temperature gradient is directly related to the refractive index gradient and therefore the phase shift of the passing light, one can acquire the temperature distribution in the test section by demodulating the phase of the fringe pattern. The *Windowed Fourier Transform* (WFT) is a reliable demodulation algorithm, that aims to calculate the phase not globally but rather locally, by subdividing the input pictures into smaller, overlapping windows, where the phase demodulation is then carried out. For this deconstruction, the picture is transformed into Fourier space, where it is multiplied with a window function [1]:

$$Sf(u,v,\zeta,\eta) = \int_{-\infty}^{\infty}\int_{-\infty}^{\infty} f(x,y)\, g^{*}_{u,v,\zeta,\eta}(x,y)\, dxdy$$

with $f(x,y)$ being the input picture, $g^{*}_{u,v,\zeta,\eta}(x,y)$ the WFT-Basis and $Sf(u,v,\zeta,\eta)$ the WFT-Spectrum [2,3]. The WFT-Basis is responsible for the subdivision of the picture and consists of the regular Fourier basis $exp(j\zeta x + j\eta y)$, as well as a window function $g(x-u, y-v)$ [4,5]. Using this function, the spatial extension of the Fourier Transform is limited to the size of one window and can now deliver accurate frequency information for each pixel of the image. To deconstruct the input image and acquire the WFT spectrum, a 2D convolution of the image and the window function is performed by multiplying the two in the spectral domain [6]:

$$Sf(u,v,\zeta,\eta) = |f(u,v) \otimes h_{\zeta,\eta}(u,v)| exp(j\zeta x + j\eta y)$$

with $h_{\zeta,\eta}(u,v) = g_{0,0,\zeta,\eta}(x,y) = g(x,y)exp(j\zeta x + j\eta y)$. Within the individual windows, the phase is demodulated, using the *Windowed Fourier Ridges* (WFR) technique. As the name suggests, this algorithm searches for a ridge, which, in the context of an interferogram, denotes areas of high and low amplitude, which coincide with the interferogram's fringes [2,7,8]. To find them, the image is given a set of sampling frequencies with an interval of $\zeta_l - \zeta_h$ and $\eta_l - \eta_h$ and a step size of ζ_i and η_i. For every frequency pair, a WFT element can now be generated, where the search for a ridge begins by checking the magnitude of all pixels inside this window. By comparing the value with neighbouring windows, the area of the highest amplitude can be determined, and a ridge is found. The frequency pair for this window, containing a ridge, is now set as the spatial frequencies $k_x(u,v)$ and $k_y(u,v)$, while the phase of this window can be derived by calculating the arctangents of its imaginary and the real part:

$$\left| k_x(u,v), k_y(u,v) \right| = \max_{\zeta,\eta} |Sf(u,v,\zeta,\eta)|$$

$$\varphi(x,y) = angle\left(Sf\left[u,v,k_x(u,v),k_y(u,v)\right]\right) + k_x(u,v) + k_y(u,v)$$

By comparing neighbouring windows, the phase is only calculated in areas of amplitude variation, therefore in a path orthogonally to the fringes, while areas alongside the fringes signify no phase variation and are, therefore, kept constant. Continuing this procedure for all windows will lead to an accurate phase calculation but the resulting phase, however, will not be a steady gradient, as expected, rather it oscillates between π and $-\pi$. This so-called *wrapped phase* needs to be subsequently unwrapped, by compensating for every jump higher than π by adding 2π.

To now calculate the temperature values in the annulus, the 2D phase gradient field, derived from the demodulation, must be integrated to obtain the absolute phase values. For this integration, the sign of the phase gradient must match the sign of the phase recorded by the Wollaston prism. Although an interferogram delivers no direct information about the sign of the phase gradient, the curvature of the fringes can provide insight in the gradient direction if the shear direction of the Wollaston prism is known. In the case of a shear in positive x- and y-directions, as present in the experimental results, concave fringes, bending opposite of the shear direction, signify locations where the sheared beam encounters areas of higher temperature and phase values, leading to a positive gradient. If the fringes are convex and therefore bending in the shear direction, the sheared beam hits areas with lower phase values, with the resulting phase gradient being negative [9]. If all gradient directions are correct, the absolute values can be calculated with a simple integration:

$$\varphi_x(x,y) = \varphi_x(x+dx,y) + \delta\varphi_x(x,y)$$
$$\varphi_y(x,y) = \varphi_y(x,y+dy) + \delta\varphi_y(x,y)$$

where $\delta\varphi_x(x,y)$ and $\delta\varphi_y(x,y)$ represent the phase gradient fields in x- and y-direction respectively, dx and dy the chosen step sizes, both set to 1 and $\varphi_x(x,y)$ and $\varphi_y(x,y)$ are the reconstructed absolute phase profiles. Both profiles are equal, which means, that there is only one interferogram necessary to reconstruct the absolute phase profile. Since the phase is linearly related to the temperature, one can now simply rescale the absolute values to the applied temperature difference for each measurement, with the reference temperature $T_{Ref} = 25°C$ set as the minimum value.

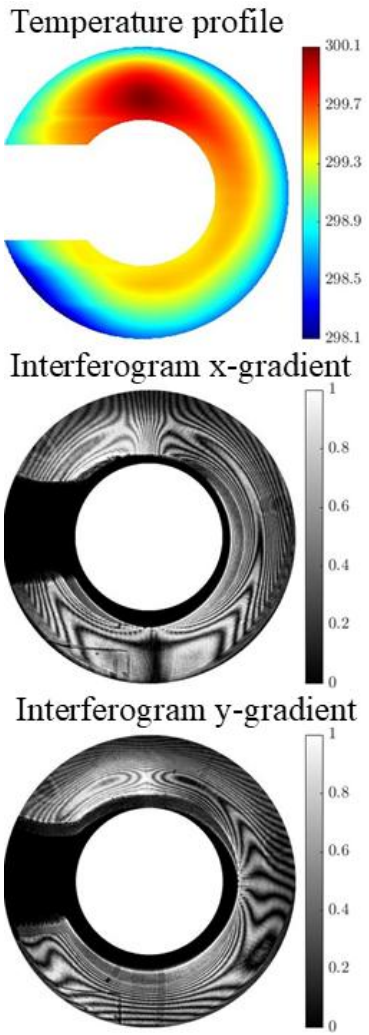

Figure 1: The experimentally derived interferograms for the vertical 2K case and the

References

[1] Qian Kemao. Two-dimensional windowed fourier transform for fringe pattern analysis : principles, applications and implementations. Optics and Lasers in Engineering, 45(2):304–317, 2007
[2] Qian Kemao. Windowed fourier transform for fringe pattern analysis. Applied Optics, 43(13):2695–2702, 2004
[3] Stephane Mallat. A wavelet tour of signal processing. Elsevier, 1999
[4] Rafael C Gonzales, Richard E Woods, and Steven L Eddins. Digital image processing using MATLAB. Pearson Prentice Hall, 2004
[5] AV Oppenheim. Discrete-time signal processing. Prentice-Hall google schola, 2:878–882, 1999
[6] Jonathan B Buckheit and David L Donoho. Wavelab and reproducible research. Springer, 1995
[7] Nathalie Delprat, Bernard Escudié, Philippe Guillemain, Richard Kronland-Martinet, Philippe Tchamitchian, and Bruno Torresani. Asymptotic wavelet and gabor analysis: Extraction of instantaneous frequencies. IEEE transactions on Information Theory, 38(2):644–664, 1992
[8] Philippe Guillemain and Richard Kronland-Martinet. Characterization of acoustic signals through continuous linear time-frequency representations. Proceedings of the IEEE, 84(4):561–585, 1996
[9] Daniel Malacara. Optical shop testing. John Wiley \& Sons, 2007.

B 7 Numerical simulation of temperature profiles and generation of artificial interferograms

S. M. Kühne, P.S.B. Szabo, Y. Sliavin and C. Egbers (FKZ: DLR 50WM2441)

The convective patterns, captured with the Wollaston shearing interferometry system allow for a good qualitative analysis of the flow and act as a benchmark for the *AtmoFlow* experiment. The post-processing of these results helps in gaining insights about the exact temperature distribution in the flow. To now validate both the calculated temperature distribution and the measured interferograms, a series of numerically simulated temperature profiles have been created, which were then modulated into interferograms.

To simulate a temperature profile, a viscous fluid, with the density ρ, is confined in a cylindrical annulus with a gap width of d is assumed. The temperature difference $\Delta T = T_1 - T_2$ between the two cylinders is assumed to be small. Assuming the validity of the Boussinesq approximation for small temperature differences, the temperature dependence of the fluid density ρ is linear and can therefore be described as:

$$\rho(T) = \rho_0(1 - \alpha\theta)$$

with $\theta = T - T_2$ and α being the thermal expansion coefficient [1]. Considering this assumption, the dynamics of the fluid can be described by the conservation equation of the mass, momentum and energy as follows [2]:

$$\nabla \cdot \boldsymbol{u} = 0$$

$$\frac{\partial \boldsymbol{u}}{\partial t} + (\boldsymbol{u} \cdot \nabla)\boldsymbol{u} = -\nabla P + P_r(\nabla^2 \boldsymbol{u} - Ra\, T \boldsymbol{e_z})$$

$$\frac{\partial T}{\partial t} + (\boldsymbol{u} \cdot \nabla)T = \nabla^2 T$$

with the Prandtl number $Pr = \nu/\kappa$ and the Rayleigh number $Ra = \alpha g \Delta T d^3/\nu\kappa$. For a cylindrical surface, the following boundary conditions are applied [2]:

$$\boldsymbol{u} = 0, \quad T = 1 \quad \text{at} \quad r = \frac{\eta}{1-\eta}$$

$$\boldsymbol{u} = 0, \quad T = 0 \quad \text{at} \quad r = \frac{1}{1-\eta}$$

The resulting system of equation with these boundary conditions should now be solved numerically and the resulting temperature values are stored in a *csv* file, containing the temperature values and the corresponding x- and y-coordinates in three separate columns. These values will have to be extracted from the file, brought back into a ring shape, and finally interpolated along the z-direction to obtain a 2D temperature profile. For this purpose, a preliminary O-mesh is created, consisting of 100 circles and 200 angles, which is used to create a set of polar coordinates, which are then transformed into Cartesian coordinates as a base for the upcoming interpolation.

The interpolation of the simulation data is done by fitting the scattered temperature data onto the rectangular 2-D grid, using the Cartesian coordinates as query points. To get the interpolated data in a circular shape, the newly interpolated, rectangular matrix can now be plotted, using the previously calculated polar coordinates. For a more detailed result and to facilitate the upcoming interferogram generation, the now circular data is transferred onto a bigger O-mesh, consisting of 300 circles and 700 angles. The same interpolation procedure is applied for this operation.

To convert the newly acquired temperature profile into an interferogram, the interference process, initiated by the Wollaston prism, must be replicated digitally. First, the temperature values must be converted into phase values, beginning with the calculation of the refractive index n. For this purpose, the known thermal variation of refractive index coefficient $n = T * dn/dT$ is utilized, which corresponds to $dn/dT = 3.8 * 10^{-4}$ for B5 silicone oil. With the refractive index, the phase can be calculated, using the following relation [3]:

$$\varphi(x,y) = \frac{2\pi}{\lambda} n(x,y)$$

To simulate the interference, the image must be overlapped with a shifted version of itself. The magnitude of the shift d can be calculated using the distance of the Wollaston prism to the camera, which is assumed to be equal to the focal length of the focusing length, utilised in the measurements $f = 50mm$ and the dispersion angle of the Wollaston prism $\gamma = 0.26°$:

$$d = f \tan\gamma$$

With the known shift, the overlapping pictures can be implemented. For that, two matrices are created, each containing the image, padded with a number of zeros, equivalent to the magnitude of the shift d, on the left side and on the right side of the picture respectively. Now, the difference of these two matrices is calculated like this:

$$\delta\varphi_x(x,y) = \varphi_x(x,y) - \varphi_x(x-d,y)$$
$$\delta\varphi_y(x,y) = \varphi_y(x,y) - \varphi_y(x,y-d)$$

with $\delta\varphi_x(x,y)$ and $\delta\varphi_y(x,y)$ representing the phase difference in x- and y-direction respectively. This difference can now be used to modulate the interferograms, using the following equation:

$$I_x(x,y) = \cos\left(\frac{\delta\varphi_x}{2}\right)^2$$
$$I_y(x,y) = \cos\left(\frac{\delta\varphi_y}{2}\right)^2$$

The resulting matrices $I_x(x,y)$ and $I_y(x,y)$ contain the interferograms in x- and y-direction. Additionally, to reduce noise and smooth out the fringes, the interferograms are filtered with a Gaussian kernel.

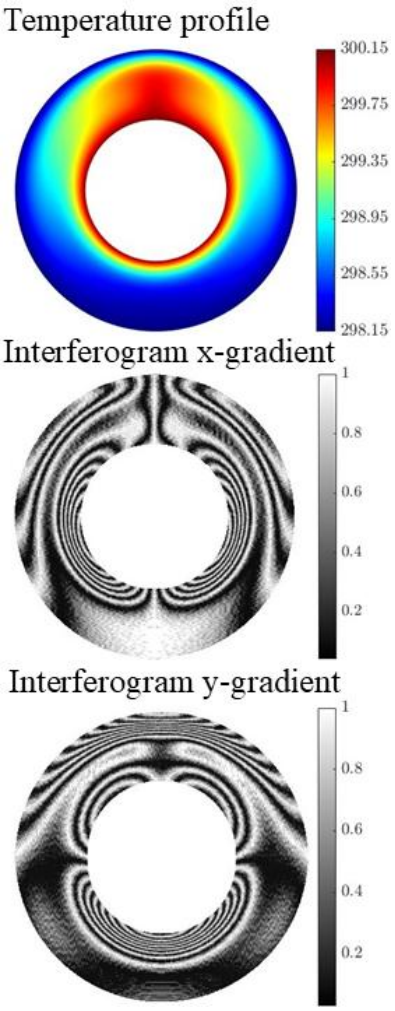

Figure 1: Results of the numerical interferogram generation. Depicted is the

References

[1] Vadim Travnikov, Olivier Crumeyrolle and Innocent Mutabazi. Influence of the thermo-electric coupling on the heat transfer in cylindrical annulus with a dielectric fluid under microgravity. Acta Astronautica, 129:88–94, 2016.

[2] Vadim Travnikov, Olivier Crumeyrolle and Innocent Mutabazi. Numerical investigation of the heat transfer in cylindrical annulus with a dielectric fluid under microgravity. Physics of Fluids, 27(5), 2015.

[3] K Wozniak and J Siekmann. Benard-convection analysis using a new interferometer. Flow measurement and Instrumentation, 6(3):181–186, 1995

C Space Research

C1 Convection in spherical Taylor-Couette flow under the influence of the DEP force

Yann Gaillard, Peter S.B. Szabo and Christoph Egbers (FKZ: DLR 50WM2441)

Introduction

This paper presents a detailed numerical study of thermo-electrohydrodynamic (TEHD) convection in spherical Taylor–Couette (sTC) flow, focusing on the combined effects of differential rotation and dielectrophoretic (DEP) forcing. The work forms part of the AtmoFlow microgravity experiment [1], designed to extend the findings of the earlier GeoFlow [2,3] experiment on the International Space Station (ISS), enabling investigations of atmospheric and planetary-like flows in a rotating spherical geometry.

The study aims to understand how DEP-driven convection interacts with rotation-driven flow in a differentially rotating, non-isothermal spherical shell. The authors examine three principal regimes—DEP-dominated, rotation-dominated, and transitional—to identify scaling relations for heat and momentum transport and to clarify how DEP forces modulate angular momentum exchange in the equatorial region.

A dielectric fluid is confined between independently rotating inner and outer spherical shells, heated at the inner boundary and cooled at the outer. An alternating high-frequency electric field generates a radial DEP force due to the temperature dependence of the fluid's permittivity. The governing equations include the Navier–Stokes, energy, and Gauss's laws, non-dimensionalized using gap width and thermal diffusion timescale.

Simulations are performed using a custom OpenFOAM [4] finite volume solver, employing the SIMPLE algorithm with implicit discretization. The model resolves both rotational and electrohydrodynamic effects through parameters such as the electric Rayleigh number, rotation rate and differential rotation.

Results

The results demonstrate how the interaction between dielectrophoretic (DEP) forcing and differential rotation governs the convective dynamics and heat transfer within the spherical Taylor–Couette system. In the purely DEP-driven thermo-electrohydrodynamic (TEHD) case, convection intensifies with increasing electric Rayleigh number, evolving from steady plume-like structures to irregular, turbulent-like motion. When rotation alone is imposed, the flow transitions from axisymmetric laminar states to more complex patterns featuring equatorial jets and Stewartson-like patterns.

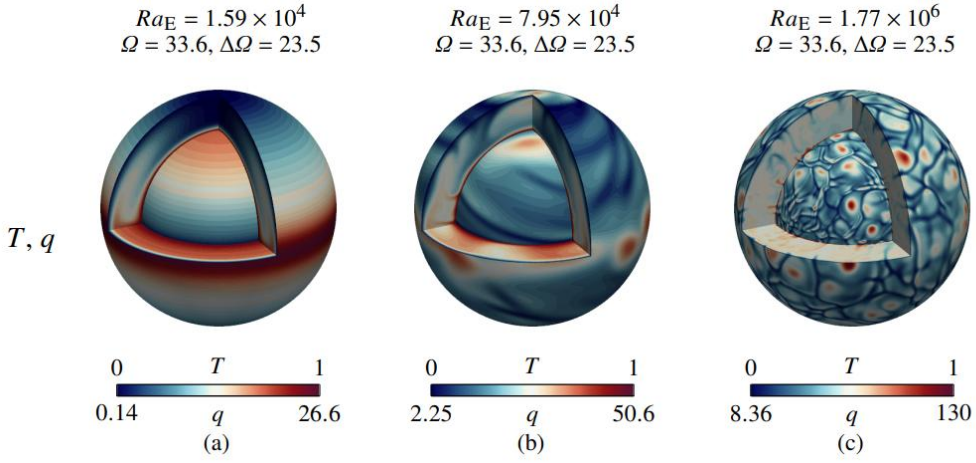

Figure 3: Isosurface plots of temperature are shown respectively, across equatorial,meridional, and radial cross-sections.

Aktuelle Forschungsschwerpunkte / Current research topics

When both forcing mechanisms are active, the combined TEHD–sTC flow exhibits three distinct regimes: a DEP-dominated regime at low differential rotation where radial plumes drive efficient heat transport; a transitional regime where increasing rotation suppresses DEP-induced plumes near the equator, reducing overall heat transfer; and a rotation-dominated regime at high differential rotation where the flow becomes meridional velocity dominant, and heat transfer recovers as the system approaches classical Taylor–Couette behaviour. Across these regimes, the interplay of DEP and rotational effects leads to complex, sometimes chaotic flow states, characterized by temporal oscillations and spatial asymmetries.
The mapping of results in the regime diagram defines clear boundaries between time-invariant, periodic, and irregular convective states, establishing a framework for interpreting the flow transitions observed in the forthcoming AtmoFlow microgravity experiments.

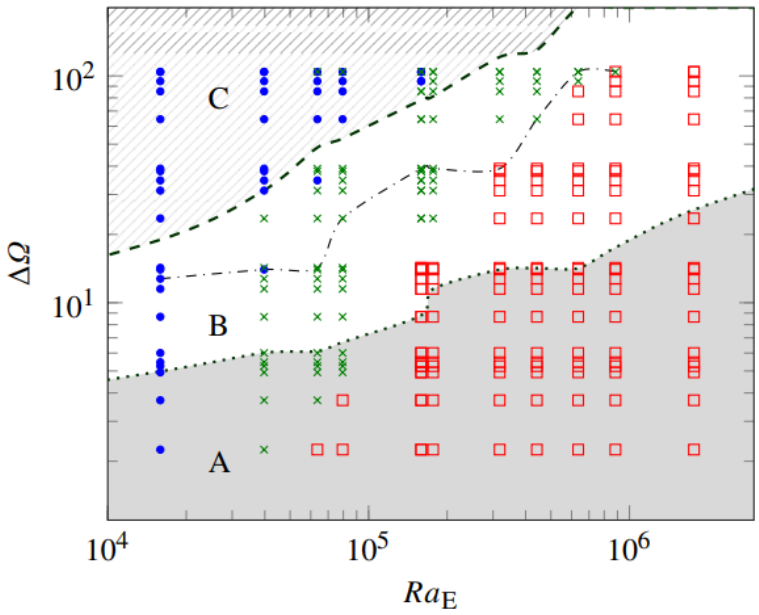

Figure 4: Regime diagram in the ΔΩ–RaE parameter space, where time-invariant,periodic, and irregular flow states are denoted by (•), (×), and (square), respectively. The line(dotted) marks the onset of the transition from the DEP force-dominated regime (A),passing through the transitional regime (B), characterised by a drop in Nusselt number„ to the non-isothermal sTC flow-dominated regime (C) found above line (dashed). The minimum in defines the transition line (dash-dotted)

Conclusion

The study demonstrates that DEP forces significantly influence convection and heat transfer in rotating spherical systems, introducing a transitional regime where electric and rotational mechanisms compete. The scaling relations established here bridge electrohydrodynamic and rotating convection theories, providing valuable insights for future AtmoFlow microgravity experiments.

Bibliography

[1] F. Zaussinger, P. Canfield, A. Froitzheim, V. Travnikov, P. Haun, M. Meier, A. Meyer, P. Heintzmann, T. Driebe, and C. Egbers, *Microgravity Science and Technology* **31**, 569-587 (2019).
[2] V. Travnikov, J. Fütterer & C. Egbers, *Acta Astronautica* **63**, 809–820 (2008).
[3] J. Futterer, V. Travnikov & C. Egbers, *Adv. Space Res.* **52**, 1724–1733 (2013).
[4] Y. Gaillard, P. S. B. Szabo, V. Travnikov, and C. Egbers, *OpenFOAM® Journal* **5**, 1–16 (2025).

C Space Research

C2 Modelling Thermo-Electrohydrodynamic Convection in Rotating Spherical Shell Using OpenFOAM

Y. Gaillard, P. S. B. Szabo, V. Travnikov, Ch. Egbers (FKZ: DLR 50WM2441)

Introduction

This study presents a numerical investigation of thermo-electrohydrodynamic (TEHD) [1,2] convection in a rotating spherical shell, a configuration that serves as a fundamental model for a wide range of geophysical and astrophysical phenomena. Such systems are key to understanding the interaction between thermal, electrical, and rotational forces, as observed in planetary interiors, stellar convection zones, and advanced laboratory experiments.

The work focuses on the development and validation of a custom finite volume solver (FVM) implemented within the OpenFOAM® open-source computational framework. This solver was specifically designed to simulate TEHD convection under rotation and to be directly benchmarked against established finite element (FEM) and pseudo-spectral (PSM) methods. By integrating electrohydrodynamic effects with buoyancy-driven and rotational convection, the model extends the capabilities of OpenFOAM® to a new class of multiphysics problems.

The primary objective is to validate a newly developed OpenFOAM®-based solver capable of accurately reproducing TEHD convection in rotating dielectric fluids, with the long-term goal of applying it to the AtmoFlow experiment [3]—the successor of the GeoFlow experiment conducted on the International Space Station. The solver is designed to handle complex geometries, coupled physical effects, and multi-region domains while remaining fully open-source and accessible to the broader scientific community.

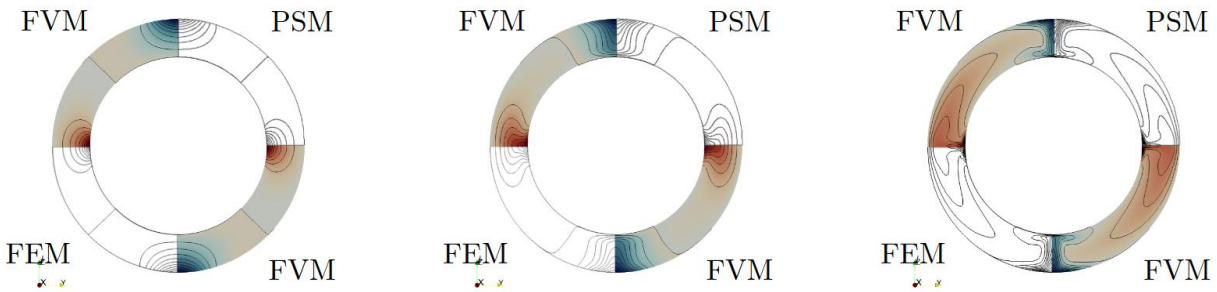

(a) $Ta = 10^3$ $Ra_E = 0$ (b) $Ta = 1.5 \cdot 10^4$ $Ra_E = 19182$ (c) $Ta = 10^3$ $Ra_E = 1 \cdot 10^5$

Figure 5: Temperature contour plot with range (0,0.05,1) of the north-south plane ofthe spherical shell. The panels represent the regimes (I-III) from left to right, respectively.Each panel consists of a quarter of the individual solution method PSM and FEM, whilethe solution of FVM is given twice to compare the contours of each solution.

The model considers a Boussinesq dielectric fluid [4,5] confined between two concentric, differentially heated, and rotating spheres subjected to an alternating electric field. The governing equations include the continuity, momentum, and energy equations, along with Gauss's law for electrostatics, all modified to incorporate dielectrophoretic (DEP), Coriolis, and centrifugal body forces. The simulations explore three characteristic flow regimes determined by combinations of the Taylor number and electric Rayleigh number, representing rotation-dominated, mixed, and electric-dominated convection states.

Aktuelle Forschungsschwerpunkte / Current research topics

Results

The numerical implementation employs the PIMPLE algorithm—a hybrid of the SIMPLE and PISO schemes—for efficient pressure–velocity coupling, ensuring numerical stability and robust convergence. Implicit time integration and high-order spatial discretization are used to accurately capture the coupled thermal and electric effects while maintaining computational stability over long simulations.

Benchmark comparisons were performed against two well-established methods: a finite element model (COMSOL Multiphysics) and a Fortran-based pseudo-spectral solver. Each solver used discretizations optimized for its framework—structured hexahedral meshes in OpenFOAM®, unstructured tetrahedral elements in FEM, and spherical harmonic expansions in PSM.

Across all regimes, the OpenFOAM® solver reproduced the temperature distributions, velocity fields, and heat transfer characteristics with remarkable accuracy, achieving agreement within 1% compared to FEM and PSM results. The simulated flow structures successfully captured transitions between rotationally dominated and electrically driven regimes, including the emergence of multiple meridional circulation cells in mixed cases.

The computed Nusselt numbers confirmed the solver's ability to reproduce correct global heat-transfer behavior, validating both the thermal and hydrodynamic consistency of the model. While the FVM approach required greater computational resources due to mesh resolution and solver overhead, it offered clear advantages in flexibility, scalability, and adaptability to complex boundary conditions and multiphysics coupling. This makes the OpenFOAM® solver particularly valuable for future investigations extending beyond idealized benchmark configurations.

Conclusion

The validated OpenFOAM®-based solver effectively models thermo-electrohydrodynamic convection in rotating spherical shells, achieving benchmark-level accuracy against state-of-the-art FEM and PSM solvers. Despite higher computational demands, the framework provides a versatile and extendable platform for studying electrohydrodynamic and magnetohydrodynamic flows in both terrestrial and space-relevant contexts.

This open-source development significantly enhances the computational toolkit available for the analysis of coupled multiphysics systems, enabling detailed studies of rotating convection, electric field interactions, and thermal instabilities under realistic boundary conditions. Future work will extend this solver to non-Boussinesq conditions, time-dependent AC field dynamics, and three-dimensional transient flows, further advancing its relevance to upcoming experimental missions such as AtmoFlow.

The solver and accompanying documentation are publicly available via GitHub at:
https://github.com/AtmoFlow/TEHDBoussinesqPimpleFoam

Bibliography

[1] M. Mutabazi, H. N. Yoshikawa, M. T. Fogaing, V. Travnikov, O. Crumeyrolle, B. Fütterer & C. Egbers, Fluid Dyn. Res. **48**, 061413 (2016).
[2] H. Senftleben & W. Braun, Z. Phys. **102**, 480–506 (1936).
[3] V. Travnikov & C. Egbers, Phys. Rev. E **104**, 065110 (2021).
[4] H. N. Yoshikawa, C. Kang, I. Mutabazi, F. Zaussinger, P. Haun & C. Egbers, Phys. Rev. Fluids 5, 113503 (2020).
[5] H. N. Yoshikawa, O. Crumeyrolle & I. Mutabazi, Phys. Fluids 25, 024106 (2013).

C Space Research

C3 Numerical Investigation of the Atmosphere-Like Flows in the Spherical Geometry

V. Travnikov, C. Egbers (DFG, TR 986/6-3)

Introduction

Large-scale rotating flows are essential in atmospheric applications. The study of planetary atmospheres is particularly important for weather forecasting, climate analysis, and understanding the greenhouse effect. Atmospheric flows are primarily driven by gravity, the planet's rotation, and heating from solar radiation. This heating is uneven, as the Sun's rays strike the Earth's surface perpendicularly at the equator, resulting in higher temperatures compared to the poles. To better understand the dynamics of these flows, various simplified models have been developed.

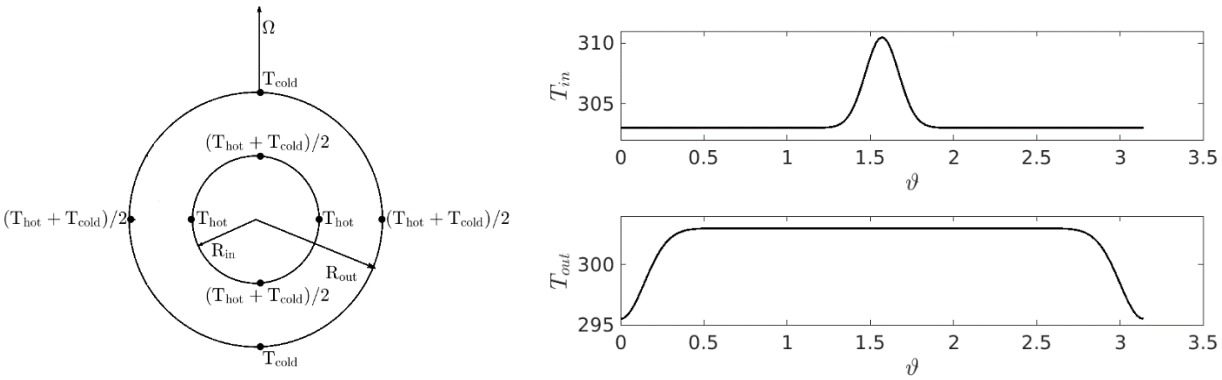

Figure 1: Geometry and boundary conditions for the temperature

Our model [1]-[3] is structured as follows. The spherical gap is filled with a dielectric medium. The rapidly oscillating electric field generates a radially symmetric field with artificial gravity [2]. The most significant milestone is the realisation of the temperature distribution with boundary conditions that depend on the polar angle

$$T_{in}(\vartheta) = \left(\frac{T_{hot}+T_{cold}}{2}\right) + \left(\frac{T_{hot}-T_{cold}}{2}\right) sin^n \vartheta, \;\; n = 100.$$

The temperature on the outer surface should be constant, but on the poles, large gradients should be taken into account in the $\vartheta -$ direction:

$$T_{out}(\vartheta) = T_{cold} + \left(\frac{T_{hot}-T_{cold}}{2}\right) \frac{ch(a_{th} cos\vartheta) - ch(a_{th})}{1 - ch(a_{th})}, \; a_{th} = 50.$$

The problem is solved using a standard algorithm suitable for problems that allow a steady, axisymmetric, two-dimensional basic flow:

- First, we determine the basic flow $\boldsymbol{u_0}$, which is steady axisymmetric, as well as equatorially symmetric.
- Secondly, we solve the linearised system to identify the critical Rayleigh number , Ra_{Ec}. Additionally, the linear analysis reveals a critical azimuthal wavenumber m_c that corresponds to the dominant perturbation and its frequency ω_c. This part of project is solved due to the Hollerbach Code [4].
- Third, after conducting the stability analysis, the three-dimensional flows will be calculated and examined. This part of the project is performed using MagIC Code [5].

Aktuelle Forschungsschwerpunkte / Current research topics

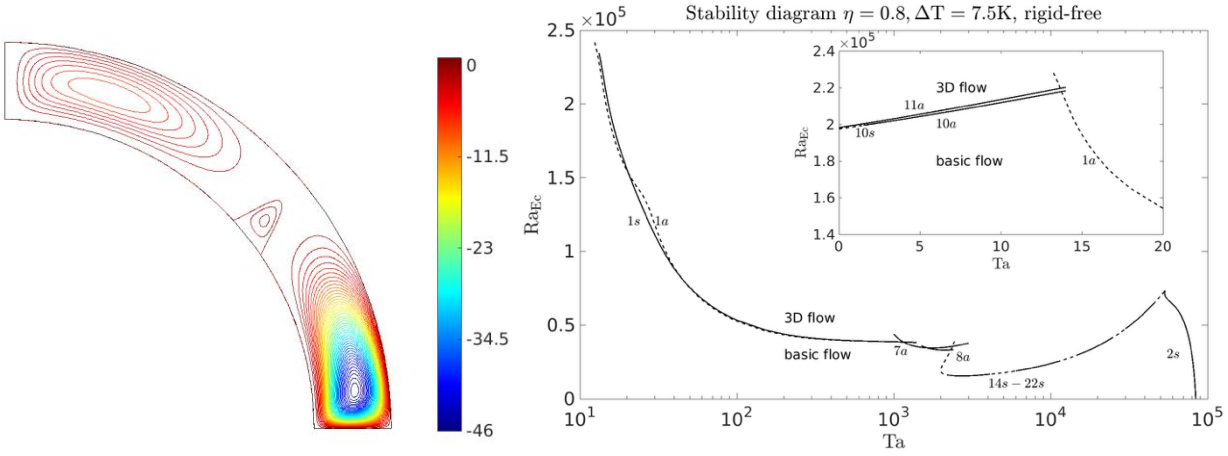

Figure 2: Stream function (left) of the basic flow for $\eta = 0.8$, $\mathrm{Ra_E} = 5 \cdot 10^4$, Ta=100, stability diagram (right) for $\eta = 0.8$ [2].

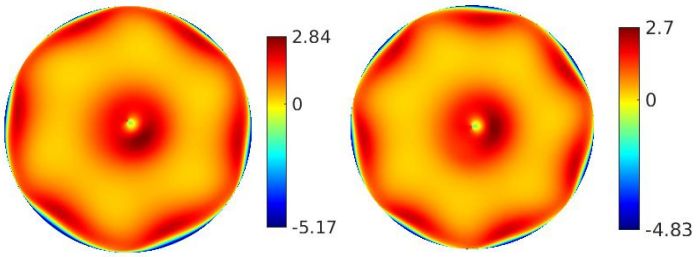

Figure 3: Azimuthal velocity component from the North Pole at $\eta = 0.8$, $\mathrm{Ra_E} = 6 \cdot 10^4$, $\mathrm{Ta} = 1500$ (m=6 left), $\mathrm{Ta} = 1700$ (m=7 right). Rigid-free boundary conditions.

References

[1] V. Travnikov, P. Szabo, Y. Gaillard, and C. Egbers, Centrifugally driven spherical gap convection with polar-angle dependent boundary condition: Can the Nusselt number fall below unity? Physics of Fluids 37, 083618 (2025)

[2] V. Travnikov, C. Egbers, Numerical investigation of atmosphere-like flows in a spherical geometry, Phys. Rev. E 104, 065110 (2021)

[3] F. Zaussinger, P. Haun, P. Szabo, V. Travnikov, M. Kawwas, and C. Egbers, Rotating spherical gap convection in the GeoFlow International Space Station (ISS) experiment, Phys. Rev. Fluids 5, 063502 (2020)

[4] R. Hollerbach, A spectral solution of the magneto-convection equations in spherical geometry, Int. J. Num. Met. Fluids, 32, 773-797 (2000)

[5] Christensen, U.R., Aubert, J., Cardin, P., Dormy, E., Gibbons, S., Glatzmaier, G.A., Grote, E., Honkura, Y., Jones, C., Kono, M., Matsushima, M., Sakuraba, A., Takahashi, F., Tilgner, A., Wicht, J., and J., Zhang, K. 2001 *A numerical dynamo benchmark*, Phys. Earth Planet. Inter., 128, 25-34

C Space Research

C4 Convection in a fluid layer driven by internal dielectric heating

P.S.B. Szabo, K. Nagaraj, Y.A. Mohammed, M. Strangfeld, F. Zaussinger, C. Egbers
(DLR 50WM2244 and 50WM2441; NHR bbi00021)

Internally heated convection plays a central role in many natural and industrial systems, from Earth's mantle dynamics to advanced material processing. Unlike classical Rayleigh–Bénard convection, where heat enters only through boundaries, dielectric fluids can experience internal heating when subjected to alternating electric fields. The control parameter of convection within a heated fluid is given by the Rayleigh–Roberts number, Ra_H.

Our recent direct numerical simulations investigated convection in horizontal layers of dielectric fluids cooled from both top and bottom walls under microgravity conditions, eliminating Archimedean buoyancy. The study focused on two fluids with contrasting Prandtl numbers Novec7200 and 1-Nonanol to explore the role of fluid properties and dielectric losses on flow regimes and energy transport. The simulations were performed with a custom coded solver in OpenFOAM v2012 [1]. The governing equations incorporated electrohydrodynamic forcing terms derived from the temperature-dependent electrical permittivity of the fluids. Both 50 Hz and 10 kHz forcing frequencies were applied, corresponding to experimentally measured dielectric loss factors. Boundary conditions included uniform cooling at the top and bottom walls with no-slip and periodicity in lateral directions. Grid independent tests ensured accuracy, while validation against benchmark cases [2] showed excellent agreement of less than 1% deviation).

A sequence of four distinct convective regimes was observed as the effective electric potential (VE) increased:Regular hexagonal plume patterns for small forcing in Ra_H, for moderate forcing the mixed hexagonal–rectangular structures emerged to rectangular convection rolls. For larger forcing time-dependent flow patterns with irregular structured evolved. All structures are depicted in Figure 1.

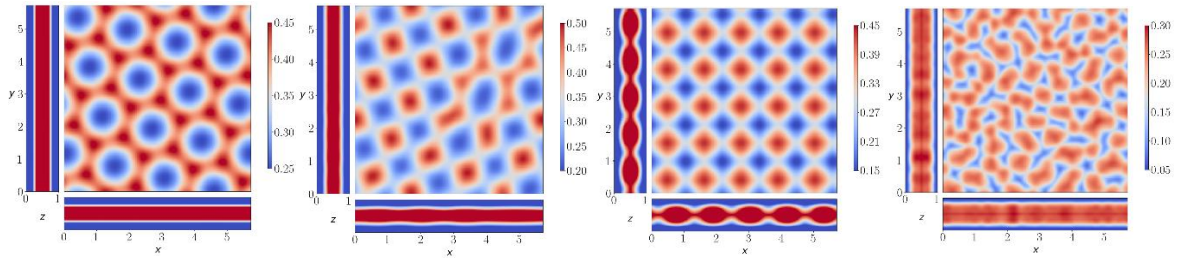

Figure 1:I so-surface of the non-dimensional temperature, T, projected along the x, y and z direction of 1-Nonanol at 50 Hz. (a) Ra_H=1657, (b) Ra_H=2441, (c) Ra_H= 6 846), (d) Ra_H= 106 096).

Cross-sectional averages revealed parabolic temperature profiles at weak forcing, transitioning to steeper boundary gradients and thinner thermal layers at stronger forcing. Interestingly, while thermal boundary layers followed classical scaling laws given by $\delta_T \sim Ra_H^{-0.23}$ to $Ra_H^{-0.25}$, kinetic boundary layers exhibited weaker decay of $\delta_u \sim Ra_H^{-0.13}$ to $Ra_H^{-0.18}$. This contrasts with boundary-heated convection and suggests modified energy dissipation pathways in dielectric heating.

Aktuelle Forschungsschwerpunkte / Current research topics

Energy diagnostics of thermal and kinetic energy dissipation confirmed these deviations: thermal dissipation dominated within the boundary layers, while kinetic dissipation shifted toward the bulk only gradually. Scaling relations for thermal energy density, kinetic energy density, and the Nusselt number were derived, showing consistent power-law behavior across several orders of magnitude in Ra_H.given by

$$Nu_H^{av} \sim Ra_H^{0.245} \quad \text{(1-Nonanol)} \quad (1)$$

$$Nu_H^{av} \sim Ra_H^{0.253} \quad \text{(Novec 7200)} \quad (2)$$

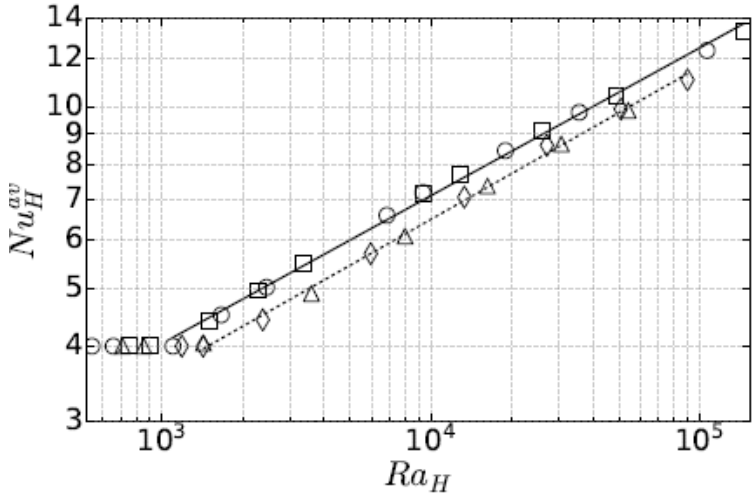

Figure 2: The Average Nusselt number, Nu_H^{av}, is plotted as a function of the electric Rayleigh–Roberts number, Ra_H. The markers ○ and □ represent 1-Nonanol at 50 Hz and 10 kHz, while △ and ◊ denote Novec 7200 at 50 Hz and 10 kHz, respectively. Power-law fits of Nu_H^{av} for 1-Nonanol solid lines (—) and for Novec 7200 dashed lines (– –) are given in equation 1 and 2, respectively.

The study highlights that internal dielectric heating fundamentally alters convection dynamics compared to classical buoyancy-driven systems. Key findings include a rich sequence of pattern formations driven purely by electric forcing, distinct scaling behavior of boundary layers, especially when considering the kinetic energy dissipation and a shift in the critical onset of convection, sensitive to the thermoelectric coupling parameter.

These results are relevant for both geophysical analog experiments (e.g., mantle convection models in microgravity) and engineering applications (thermal management and heat exchangers using dielectric fluids).
Future work will expand simulations to spherical geometries and extend comparisons with upcoming microgravity experiments, such as AtmoFlow, to validate these numerical insights.

References

[1] Y. Gaillard, P.S.B. Szabo, V. Travnikov &C. Egbers, Modelling thermo-electrohydrodynamic convection in rotating spherical shell using Openfoam®, OpenFOAM® Journal 5, 1–16. (2025)

[2] E.B. Barry, C. Kang, H.N. Yoshikawa, I. Mutabazi, Flow patterns and heat transfer in a dielectric liquid inside a planar capacitor under microgravity conditions, Appl. Phys. Lett. 122 (2023).

C Space Research

C5 Dielectrophoretic-driven thermoelectrohydrodynamic convection in a dielectric fluid layer induced by an inhomogeneous external electric field

P.S.B. Szabo, and C. Egbers (DLR 50WM2244 and 50WM2441; NHR bbi00021)

Since the 1930s, it has been known that electric fields can modify thermal flows in dielectric fluids through electrohydrodynamic forces, consisting of electrophoretic (Coulomb), dielectrophoretic (DEP), and electrostrictive components. At high frequencies, Coulomb forces vanish, leaving DEP forces dependent on temperature-varying permittivity as the primary driver of flow. In non-polar fluids like silicone oils, high-frequency fields can trigger Rayleigh-Bénard-like convection when the electric Rayleigh number exceeds a critical value (≈2128.7 for fluid layers). While planar layers rely on temperature-induced field inhomogeneities, curved geometries or specially arranged electrodes can impose external inhomogeneous fields, potentially altering convection and heat transfer in microgravity conditions which is the subject of this study.

The study examines a dielectric fluid layer of height d, infinitely extended in lateral directions, uniformly heated from below and cooled from above, with no-slip velocity at both walls. To create an inhomogeneous electric field, the bottom wall hosts uniformly spaced electrodes (d/4 size, d/2 spacing) separated by insulated gaps, while the top wall is a continuous electrode. An alternating electric tension V(t) is applied between serially connected lower electrodes and the upper electrode. The setup, illustrated in Fig. 1, enables investigation of how the resulting non-uniform electric field influences fluid motion and heat transfer under varying potentials and fluid properties.

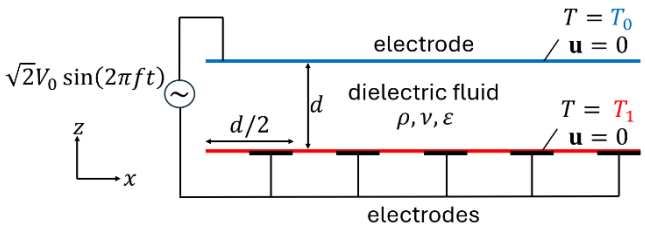

Figure 1: Sketch of the problem geometry.

The study identifies three distinct convection regimes in response to varying forcing intensities given by the electric Rayleigh number

$$L = \frac{\varepsilon_0 \varepsilon_r \gamma_e^2 V_0^2}{\rho \nu \kappa}$$

within an electrode-bounded cavity. First, **regular convective rolls** form after equilibration, producing stationary plumes aligned with the electrode spacing and exhibiting five parallel modes in the y-direction. Second, at L =1600, a **time-invariant bimodal regime** emerges, where symmetry breaks in the yz-plane, producing coexisting plume patterns that remain stationary over time. Third, at L~3200, **skewed variance convection** develops, breaking the bimodal symmetry into irregular, oscillatory plumes with asymmetric thermal and kinetic energy transport, indicating a time-dependent imbalance in convection and heat transfer. All regimes are depicted in Fig. 2.

Aktuelle Forschungsschwerpunkte / Current research topics

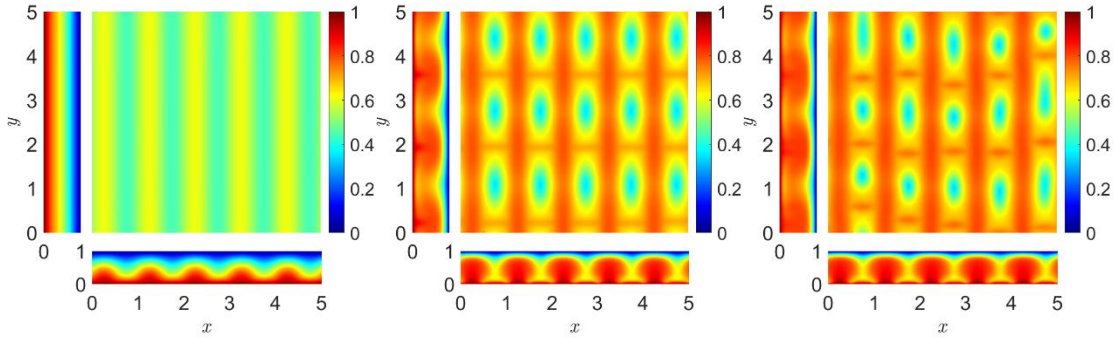

Figure 2: Iso-surface plots of the respective temperature, T, projection in x, y and z-direction, respectively, for Pr=65 and ε_e=0.03$: (a) L=212.82, (b) L=2766.70 and (c) L=4256.40 at t=1.

The study evaluates the relationship between the convective driving force L and heat transfer characterized by the Nusselt number, shown in Fig.3, finding no critical threshold and confirming convection for any $L \neq 0$. Results align with Jawichian et al. [1], showing Nu increases with L, with Prandtl number effects appearing only at larger L due to diffusion time scale influences. A power law scaling $Nu \sim 0.265 L^{0.3047}$ is identified, placing the exponent γ_e at the higher end of Rayleigh–Bénard convection ranges. Differences from some Jawichian studies are attributed to stronger electric field inhomogeneity in their configurations.

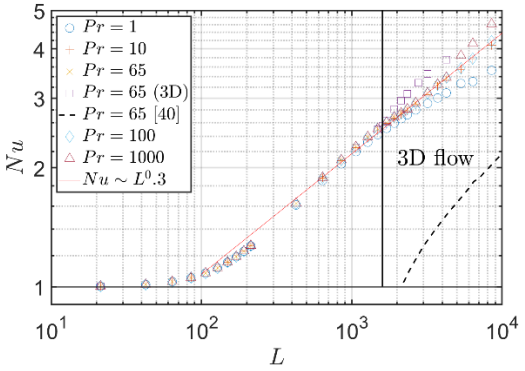

Figure 3: The Nusselt number, Nu, plotted for the equilibrated flow as a function of the electric Rayleigh number, L, for a set of Prandtl number, Pr, with γ_e=0.03. The solid line represents a power law relation of Nu to L which is compared to the benchmark solution of [40] indicated by the dashed line.

The study examined how an inhomogeneous external electric field influences thermoelectro-hydrodynamic convection in a dielectric fluid layer by lower-plate electrode spacing. By using different intensity of the electric tension expressed by the forcing parameter L produces three regimes: regular convective rolls, time-invariant bimodal modes, and time-dependent skewed plume patterns. Unlike systems with supercritical bifurcation, convection occurs for $L \neq 0$, enhancing heat transfer. Scaling analysis shows $Nu \sim 0.265 L^{0.3047}$, a value slightly above the classical Rayleigh–Bénard range (0.2–0.3) and consistent with prior TEHD studies by Jawichian et al. [1] The results highlight electrode spacing as a key control for flow structures and heat transfer in non-uniform electric field-driven convection.

References

[1] A. Jawichian, S. Siedel, and L. Davoust, Dielectrophoretic influence on free convection in a differentially heated cavity, International Journal of Heat and Mass Transfer 200, 123560 (2023).

[40] E. B. Barry, C. Kang, H. N. Yoshikawa, and I. Mutabazi, Flow patterns and heat transfer in a dielectric liquid in side a planar capacitor under microgravity conditions, Applied Physics Letters 122 (2023).

C Space Research

C6 Project TEKUS-DEPIK – Thermo-electric convection in a cylindrical annulus during a sounding rocket flight (TEXUS 57)

V. Motuz, A. Meyer, M. Meier, C. Egbers (DLR FKZ 50WM1944, DLR FKZ 50WM2244)

The dielectrophoretic force includes a non-conservative component, acting as an *electric gravity*, which can induce Rayleigh–Bénard convection between a heated inner and a cooled outer cylinder under a radial electric field.

To investigate the effect of pure dielectrophoretic forces on dielectric fluids and exclude their interaction with the force of earth gravity, this effect was investigated in many experiments conducted on parabolic flights using the Zero-G aeroplane of the Novespace company.

Visualisation of the flow and temperature changes in these experiments allowed the stability of the flow to be determined after 22 seconds of weightlessness (Szabo et al. 2021). Although an increase in turbulence was observed, a steady flow could not be achieved, and it was found that the experimental threshold for flow destabilisation was higher than the value calculated based on linear stability theory (Yoshikawa et al. 2013).

That difference is mostly attributed to the short duration of μg phases provided by the parabolic flight of the ZeroG aeroplane. The result motivated the use of a sounding rocket flight (TEXUS-57). The 6 min of μg conditions would then allow the visualisation of the flow destabilisation at parameters close to the theoretical critical value. The analysis of the growth of convection and of the established flow structure can provide fundamental characteristics of the instability that can serve to validate the previously derived linear stability theory, as well as the numerical models. In addition, the destabilisation of the flow at low control parameters would indicate the possibility to produce an optimised thermal system that would be able to transfer heat at lower energy costs.

Using four independently controlled cells, eight values of the electric Rayleigh number near the instability threshold were investigated during a sounding rocket flight. Flow dynamics and instability growth were analyzed with particle image velocimetry and shadowgraphy. The experimentally determined critical Rayleigh number agrees with linear stability predictions. Compared with parabolic flight results, the study demonstrates the crucial role of long-duration microgravity in enabling thermal convection at low control parameters.

The application of PIV enabled precise measurement of flow velocities within a section co-planar to the cylinder's axis. Complementarily, the shadowgraph technique employed in the sounding rocket experiments provided valuable insight into the breakdown of axisymmetry in fluid density along the azimuthal direction. Across all tested values of the control parameter L, the conductive state of the dielectric fluids became unstable, resulting in the emergence of thermo-electric convection with amplitudes that increased progressively with higher values of L.

By analyzing both the growth rates and amplitudes of the radial velocity, it was possible to experimentally determine the critical electric Rayleigh number, which was found to be in close agreement with the theoretical prediction of Lc=1498*Lc*=1498, see Fig. 1. Notably, the timescale required to reach a stationary convective state was substantial; even after 200 seconds of electric field application, the fluid continued to adapt to the available geometry, with evolving structural patterns in both axial and azimuthal directions (Meyer, A. et. Al., 2023).

In summary, the strong correlation between linear stability analysis (Yoshikawa et al., 2013), numerical simulations (Travnikov et al., 2015; Kang & Mutabazi, 2021), and the current experimental results affirms that extended microgravity experiments are effective in destabilizing dielectric fluids at control parameters near the onset of thermo-electric convection. The experiments substantiate the robustness of theoretical and computational hypotheses and demonstrate that heat transfer can be substantially enhanced at relatively low control parameters, compared to the purely conductive case.

Aktuelle Forschungsschwerpunkte / Current research topics

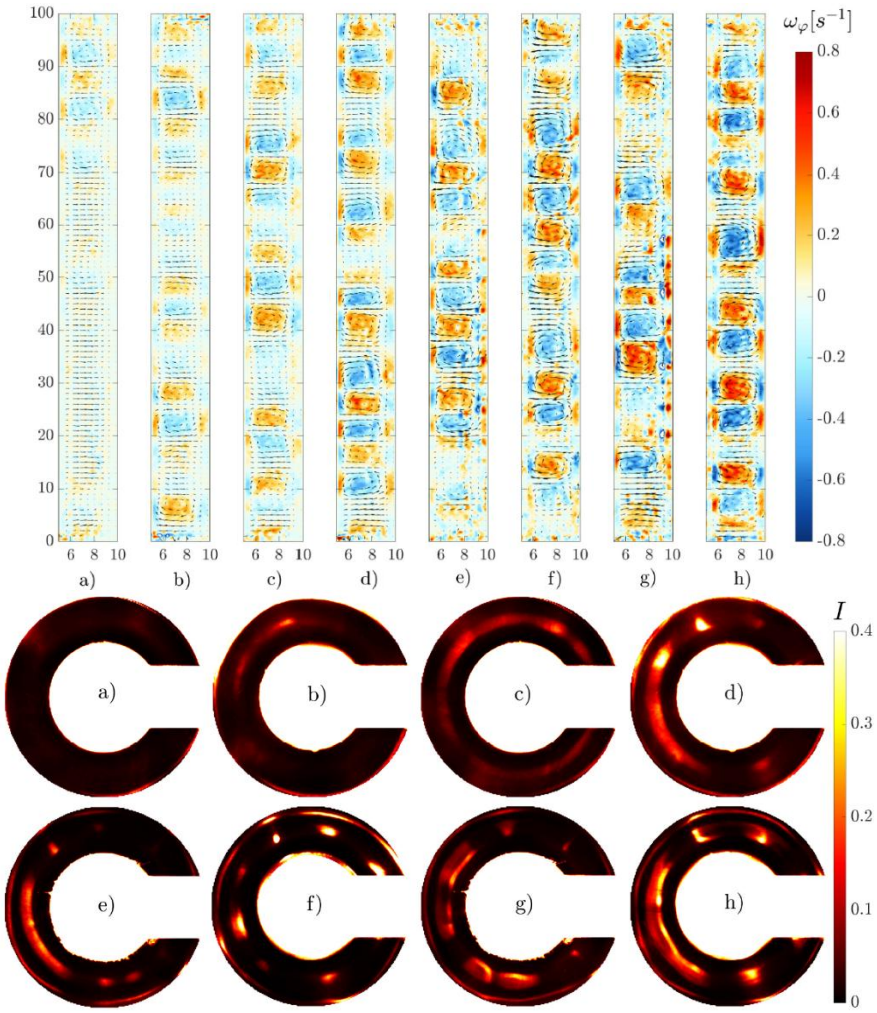

Figure 1. Velocity field and surface of isovalues of the azimuthal component of the vorticity (top) and shadowgraphs (bottom) at the end of the phase of high-voltage application for (a) L = 2774, (b) L = 2933, (c) L = 3995, (d) L = 4583, (e) L = 5586, (f) L = 5905, (g) L = 8044 and (h) L = 9227.

The onset of convective flow is dictated by a critical threshold, determined by the physical properties of the fluid and the geometry of the cylindrical capacitor.
The future experiments, that planned for the next TEXUS mission – could benefit from the use of dielectric fluids with tailored physical properties, potentially reducing the required electric field to further enhance heat transfer efficiency in these systems.

References

- Kang, C., Mutabazi, I. 2021 Columnar vortices induced by dielectrophoretic force in a stationary cylindrical annulus filled with a dielectric liquid. *J. Fluid Mech.* 908, A26.
- Szabo, P.S.B., Meier, M., Meyer, A., Barry, E., Motuz, V., Mutabazi, I., Egbers, C. 2021. PIV and shadowgraph measurements of thermo-electrohydrodynamic convection in a horizontal aligned differentially heated annulus at different gravity conditions. Exp. Therm. Fluid Sci. 129, 110470.
- Travnikov, V., Crumeyrolle, O., Mutabazi, I. 2015 Numerical investigation of the heat transfer in cylindrical annulus with a dielectric fluid under microgravity. *Phys. Fluids* 27 (5), 054103.
- Yoshikawa, H.N., Crumeyrolle, O., Mutabazi, I. 2013 Dielectrophoretic force-driven thermal convection in annular geometry. Phys. Fluids 25 (2), 024106.
- Meyer, A., Meier, M., Motuz, V., and Egbers, Ch.: Thermo-electric convection in a cylindrical annulus during a sounding rocket flight. Journal of Fluid Mechanics (2023), Vol. 972:A26

C Space Research

C 7 Measurement of the heat flux in fluid dynamics experiments

Y.Sliavin, M.H.Hamede, V.Motuz, M.Strangfeld, C.Egbers (DLR 50WM2244)

Introduction

Heat flux sensors enable direct measurement of thermal energy transport in different convection systems, providing precise quantification of heat transfer. A HukseFlux sensor was integrated into the experimental setup. This was done to validate analytical correlations and numerical models for natural convection heat transfer in a horizontal concentric annulus filled with silicone oil. The validated measurement approach provides the foundation for future investigations of electric field-induced heat transfer modifications, where dielectrophoretic forces can significantly alter convective patterns and thermal transport rates. The present results demonstrate excellent agreement between experimental heat flux measurements, Kuehn-Goldstein analytical predictions, and ANSYS numerical simulations across temperature differences of 0-15 K.

Experimental setup and results

Modern heat flux sensors operate on the principle of measuring temperature gradients across a thermally conductive element and converting the resulting temperature difference into an electrical signal proportional to the heat flux [2]. The fundamental operating principle relies on Fourier's law of heat conduction, where the heat flux is directly proportional to the temperature gradient within the sensor material. HukseFlux sensors [3], utilized in the current experiments, employ advanced thermopile technology that provides high sensitivity and rapid response characteristics essential for dynamic heat transfer measurements. The sensors demonstrated high accuracy over a wide operating range with typical uncertainties below 3% under standard conditions.

In the application experiment, the heat flux sensor is mounted in the annular cavity on the outer glass wall and is exposed to forced convection in the cooling chamber (Figure 1 a,b). The annular gap is filled with a dielectric fluid; the inner and outer walls are heated and cooled, respectively. The integration of heat flux measurements with Particle Image Velocimetry (PIV) enables simultaneous velocity and thermal measurements, allowing direct correlation between flow structures and local heat transfer enhancement or reduction [4].

Geometry and fluid

Annular gap thickness d = 5 mm with inner radius R_1 = 5 mm and outer inner radius R_2 = 10 mm. Height L = 100 mm, aspect ratio Γ = 20. The fluid is silicone oil Elbesil B2 with properties at 25 °C: $\nu = 2 \times 10^{-6}$ m^2 s^{-1}, $\alpha = 7.4 \times 10^{-8}$ m^2 s^{-1}, $\rho = 870$ kg m^{-3}, $\varepsilon = 2.04 \times 10^{-11}$ F m^{-1}, k ≈ 0.11 W m^−1 K^{-1}, $\beta = 1.124 \times 10^{-3}$ K^{-1}, Pr = ν/α. The imposed temperature difference ΔT was varied from 0 to 15 K.

Numerical model

A 2D ANSYS Fluent model was used to simulate natural convection in the annulus with conduction through the outer glass wall (thickness d_{out} = 2 mm). Forced convection at the exterior was modeled by a fixed heat transfer coefficient h_{cold} = 80 W m^{-2} K^{-1}.

Analytical model used in MATLAB

The analytical solution follows the Kuehn–Goldstein correlation for natural convection in horizontal concentric annuli [5]. The mean Nusselt number is computed from: $Nu = -2/ln\big((1+A)/(1+B)\big)$, where the coefficients could be found in [5].

Aktuelle Forschungsschwerpunkte / Current research topics

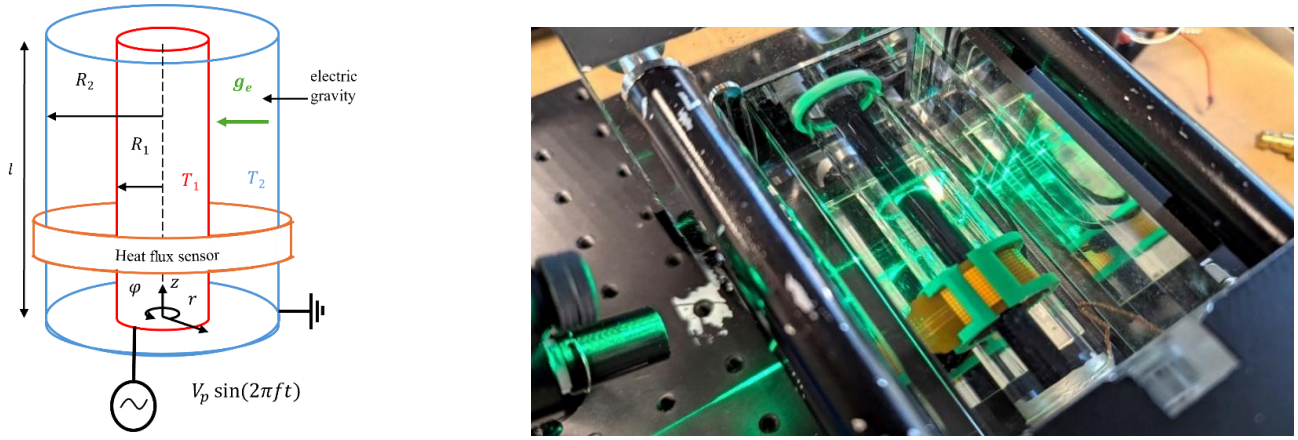

Figure 1: (a) Schematic representation of the setup, (b) Photo of the setup in horizontal configuration.

The analytical heat flux is $q''_{analytical} = h_{overall}\Delta T$, where $h_{overall}$ is obtained from overall resistance model for concentric annular cylinders. Experimental heat transfer coefficients were obtained as $h_{exp} = \frac{q''_{exp}}{\Delta T}$.

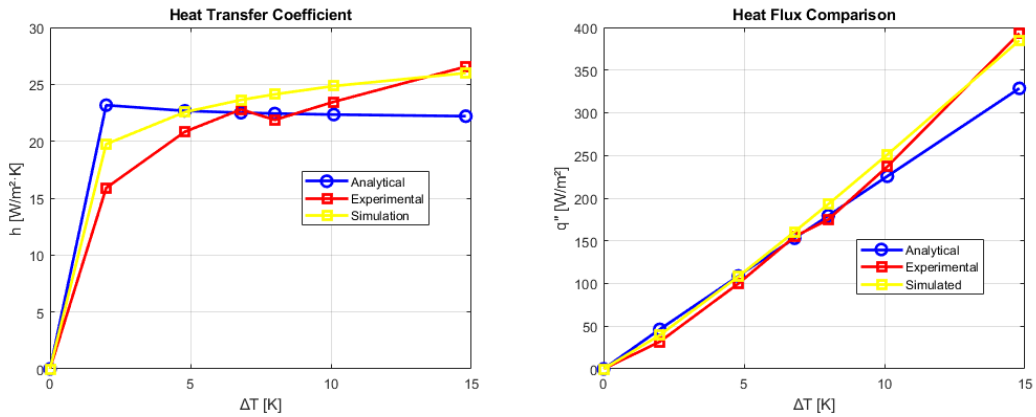

Figure 2: Heat transfer coefficient (a) and heat flux (b) plotted over the ΔT.

Comparison and discussion

Figure 2 presents the comparison between analytical, numerical, and experimental results for both the heat transfer coefficient and heat flux. The three approaches agree closely over the range 0–15 K, with deviations increasing slightly at the highest ΔT where natural convection strengthens and sensitivity to exterior boundary conditions increases. The consistency confirms that the heat flux sensor can reliably capture local heat transfer variations and that the combined PIV and heat-flux approach is a powerful diagnostic for studying heat-transfer modification and enhancement in annular flows. Heat flux sensors will be incorporated into the system in future, with an electric field influencing the flow, allowing building correlation between the applied electric potential and heat flux increase to be established.

Bibliography

[1] Kierkus, W.T. (1987). An analysis of heat flux measurement techniques. Journal of Heat Transfer, **109**(1), 1-6.
[2] Diller, T.E. (1993). Advances in heat flux measurements. Advances in Heat Transfer, **23**, 279-368.
[3] Hukseflux Thermal Sensors. (2023). Industrial heat flux and heat transfer measurement applications. Technical Documentation.
[4] Diller, T.E. (1993). Advances in heat flux measurements. Advances in Heat Transfer, **23**, 279-368.
[5] Kuehn T.H., Goldstein R.J. (1976). Correlating equations for natural convection heat transfer between horizontal circular cylinders. IJHMT, **19**(10), 1127-1134, 10.1016/0017-9310(76)90145-9.

C Space Research

C 8 Experimental investigation of TEHD convection in a rectangular cavity

M. Strangfeld, P.S.B. Szabo, V. Motuz, Y. Sliavin, C. Egbers (DLR FKZ 50WM2244)

Introduction

The parallel-plate configuration is a common model to investigate thermo-electrohydrodynamic (TEHD) convection and extends insights from cylindrical and spherical systems. The focus is directed towards heat exchanger applications, with active control possible without moving parts. Theoretical aspects have been reviewed (Mutabazi et al., 2016) and expanded by stability analyses (Yoshikawa et al., 2013) and simulations (Barry et al., 2024), covering both terrestrial and microgravity. Volumetric heating in this geometry has also been addressed in detail (Yoshikawa et al., 2020; Barry et al., 2023).

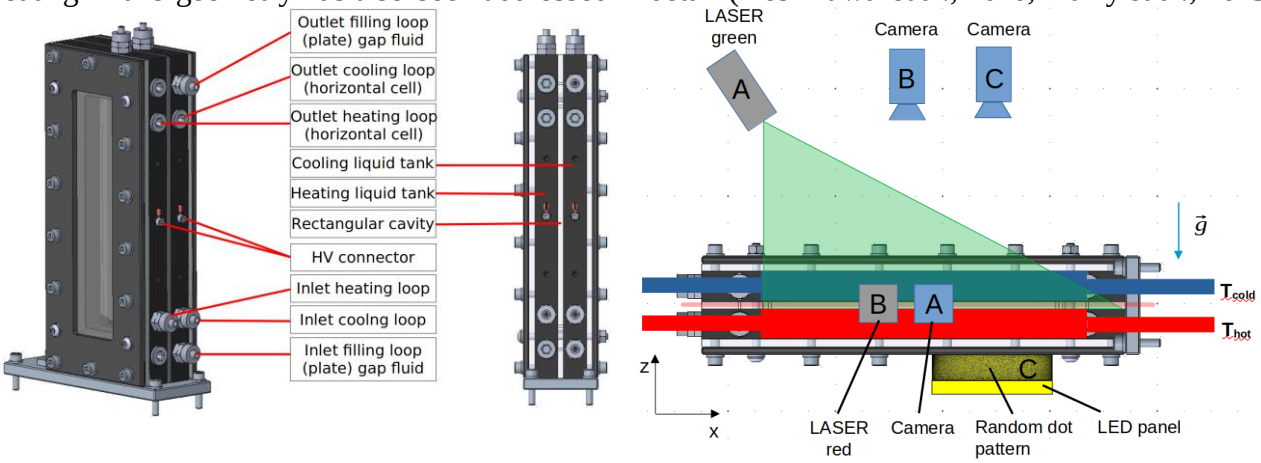

Figure 1: The design of the plate cavity experimental cell (left) and the schematics of the experimental arrangement of the measurement setup (left).

The experimental cell features a 200 mm × 40 mm cavity with adjustable gap heights (5-10 mm); acrylic glass walls and borosilicate plates bound the reservoirs. Polyoxymethylene reservoirs connected to thermostats set the boundary gradient. High voltage is applied to ITO-coated borosilicate plates, providing the electric field. Silicone oils (Elbesil B2,B5) serve as work fluids due to their good dielectric properties and 1-Nonanol and Novec 7200 for internal heating studies.

Measurement techniques

Optical methods are enabled by the cavity's transparent boundaries. Particle Image Velocimetry (PIV) is used for quantitative flow analysis and visualisation, employing two planes: one in the xz-plane for height-resolved flows, with the laser sheet along the xy-midline, and one lasersheet in the xy-plane allowing the quantification of plume side flows.

A Background Oriented Schlieren (BOS) system may be installed,with a camera imaging a random dot pattern through the gap. High-precision Pt100 sensors in the reservoir inlets/outlets measure temperature differences. Additionally, a heat flux sensor (85 mm × 15 mm) on the borosilicate plate enables direct measurement of heat transfer.

Experimental Results

Reference experiments under terrestrial gravity preceded microgravity studies. PIV was used to investigate Rayleigh–Bénard convection patterns (Strangfeld et al., 2024), with Elbesil B5 (Pr = 64.6) as a working fluid enabling observation of regime transitions. Fig. 2 shows steady rolls evolving into zig-zag and bimodal patterns as the Rayleigh number increases, matching Busse (1978).

Aktuelle Forschungsschwerpunkte / Current research topics

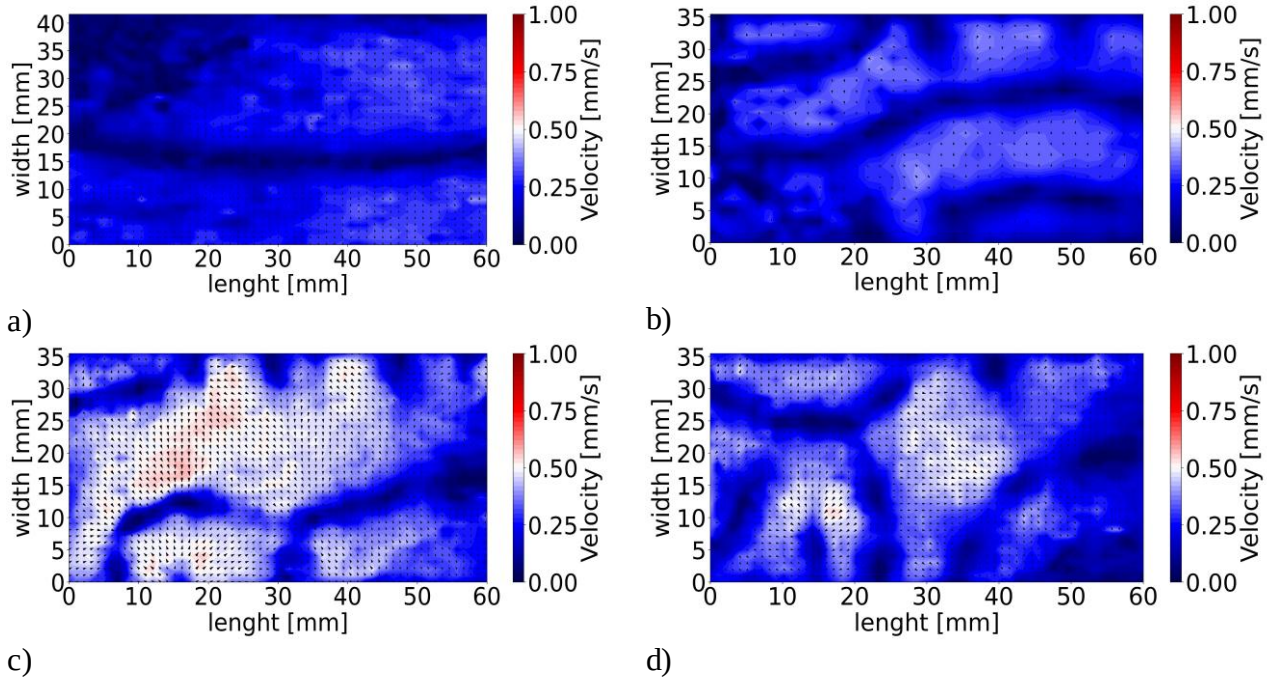

Figure 2: Velocity fields in yx-plane a) Ra = 3.3E4, b) Ra = 5.5E4, c) Ra = 6.43E4, d) Ra = 8.19E4.

Strangfeld et al. (2022) demonstrated internally heated flows under gravity in parallel-plate setups, thus expanding earlier theory (Yoshikawa et al., 2020). Numerical results by Barry et al. (2023) support these findings. BOS revealed the onset of polygonal structures; with rising voltage, structure regularity decreased and refractive index variations became more chaotic.

References

- Mutabazi, I., Yoshikawa, H.N., Tadie Fogaing, M., Travnikov, V., Crumeyrolle, O., Futterer, B., Egbers, C. 2016. Thermo-electro-hydrodynamic convection under microgravity: A review. Fluid Dyn. Res. 48(6), 061413.
- Yoshikawa, H.N., Tadie Fogaing, M., Crumeyrolle, O., Mutabazi, I. 2013. Dielectrophoretic Rayleigh-Bénard convection under microgravity conditions. Phys. Rev. E 87(4), 043003.
- Barry, E.B., Kang, C., Yoshikawa, H.N., Mutabazi, I. 2024. Electric buoyancy-driven convection in stable and unstable thermal stratifications. Phys. Fluids 36(8), 084121.
- Yoshikawa, H.N., Kang, C., Mutabazi, I., Zaussinger, F., Haun, P., Egbers, C. 2020. Thermoelectrohydrodynamic convection in parallel plate capacitors under dielectric heating conditions. Phys. Rev. Fluids 5(11), 113503.
- Barry, E.B., Kang, C., Yoshikawa, H.N., Mutabazi, I. 2023. Flow patterns and heat transfer in a dielectric liquid inside a planar capacitor under microgravity conditions. Appl. Phys. Lett. 122(18), 182903.
- Strangfeld, M., Motuz, V., Szabo, P.S.B., Sliavin, Y. 2024. Simultane Particle Image Velocimetry und Background Oriented Schlieren Messung in einer konvektiven Strömung. Proc. GALA-Fachtagung Experimentelle Strömungsmechanik, Berlin, 3–5 Sept. 2024, 26-1.
- Busse, F.H. 1978. Non-linear properties of thermal convection. Rep. Prog. Phys. 41(12), 1929–1967.
- Strangfeld, M., Bölük, O., Szabo, P.S.B., et al. 2022. Thermo-electrohydrodynamic convection in a dielectric fluid layer with volumetric heating. Proc. GALA-Fachtagung Experimentelle Strömungsmechanik, Illmenau, 6–8 Sept. 2022, 43-1.

D DLR_School_Lab BTU Cottbus-Senftenberg

D1 Overview on DLR-School-Lab activities

Stefan Richter

Introduction

The DLR_School_Lab is an extracurricular learning facility where students can conduct hands-on experiments under the guidance of scientists or specially trained instructors. Its primary goal is to make scientific topics tangible and to spark enthusiasm for research and technology.

Across Germany, 17 DLR_School_Labs are already in operation, each focusing on different themes that reflect the research priorities of the DLR institutes and universities located at their respective sites.

The DLR_School_Lab at BTU is a joint initiative between the Brandenburg University of Technology Cottbus–Senftenberg (BTU) and the German Aerospace Center (DLR). The focus at the Cottbus site lies on the development of sustainable aircraft propulsion systems and thermal energy technologies, as well as research in microgravity and aerodynamics. The latter two areas, in particular, highlight the close cooperation between the Chair of Aerodynamics and Fluid Mechanics and the BTU DLR_School_Lab, which is located within the Chair's facilities—enabling both institutions to benefit mutually from their close collaboration.

The core activity of the BTU DLR_School_Lab is to host school classes on-site, where students conduct experiments in small groups. The selection of experiments and the structure of each experimental day are planned in advance, with special consideration given to the teachers' wishes and learning objectives.

Beyond its in-house activities, the DLR_School_Lab also participates in a variety of public outreach and science events, such as the award ceremony *"MINT – Zukunft schaffen"* in Paderborn, the *"Night of Creative Minds"* in Cottbus, and the regional *"Jugend forscht"* competition. It also visits schools and even offers workshops at music festivals.

In addition, the DLR_School_Lab supports students in preparing seminar papers and runs an extracurricular robotics club, further fostering curiosity, creativity, and scientific engagement among young learners.

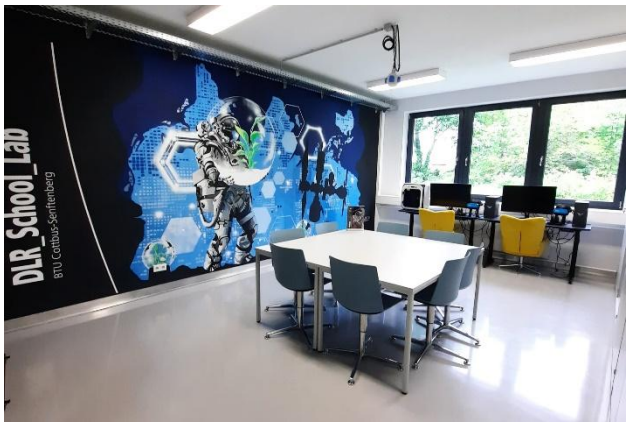

Figure 1: Show Room for Space Related Experiments

Figure 2: Show Room for Experiments for Electrified Aviation

Staff

The DLR_School_Lab is headed by Stefan Richter, a doctoral researcher at the Chair of Aerodynamics and Fluid Mechanics. He is supported by student assistants and one to two participants of the Federal Voluntary Service. Each year, the team provides more than 1,000 students with fascinating insights into the world of science.

Aktuelle Forschungsschwerpunkte / Current research topics

Experimental Offer

Experiment	Cluster / Focus Area	Description
Drop Tower	Spaceflight and Microgravity Research	Understanding the concept of weightlessness and exploring the background of research conducted under microgravity conditions.
Mission ISS		Work and life aboard the International Space Station; using VR headsets to explore the ISS virtually.
Rotating Platform	Aerodynamics, Flight Mechanics, and Flow Visualization	Explanation of flight mechanics; comparison of different wing profiles; discussion of lift and drag coefficients.
Wind Tunnel		Visualization of airflow; studying the aerodynamics of vehicles and buildings; discussion of lift and flow resistance.
Heat Pump	Thermodynamics and Low-Carbon Industrial Processes	Demonstration of how a heat pump works; reconstructing the heat pump principle in a hands-on experiment.
Thermal Energy Storage		Exploring methods of heat storage using sensible and latent heat; building a small thermal storage unit to take home.
Solar Thermal Power		Examining specific heat capacities and comparing different materials while demonstrating the principles of solar thermal power plants.
Electrochemistry	Fundamentals of Electrified Aviation	Explanation of electrolysis, fuel cells, and the Daniell cell as the basis for electric propulsion systems.
Power Electronics		Introduction to semiconductor technology; assembling AC and DC converters.
Electric Motor		Demonstrating the effects of magnetic fields leading up to the operation of electric motors.
Robot Dogs	A.I. & Robotics	Experience cutting-edge technology by remotely controlling a robotic dog through an obstacle course.
Mission Biolab	Drone Flight & Study Program Promotion	Piloting an FPV drone through a simulated biolab with escape-room elements designed to promote the biotechnology degree program.
Paper Airplanes	Primary School Program	Constructing and comparing different types of paper airplanes; introducing the basic principles of aerodynamics.
Spintronics		Illustrating electrical engineering concepts through mechanical analogies.
Water Rocket		Building and launching a water rocket to demonstrate the principles of rocket propulsion.
Ozobot		Introduction to basic programming using small educational robots.

Veröffentlichungen, Konferenzbeiträge und Vorträge/ Publications, contributions to conferences and invited lectures

Veröffentlichungen in reviewten Zeitschriften 2022

Peter Szabo, Antoine Meyer, Martin Meier, Vasyl Motuz, Yaraslau Sliavin, Christoph Egbers, Simultaneous PIV and shadowgraph measurements of thermo-electrohydrodynamic convection in a differentially heated annulus, **Technisches Messen**, Oldenbourg Wissenschaftsverlag, https://doi.org/10.1515/teme-2021-0120, 2022

Zeinab Hallol, Mohamed Yousry, Sebastian Merbold, Christoph Egbers,
Effect of High Reynolds Number on the Behaviour of Large and Very Large Scale Motions in Fully Developed Turbulent Pipe Flow
J. of Fluid Dynamics, DOI: 10.1134/S0015462822040048, 2022
ISSN 0015-4628, Fluid Dynamics, 2022, Vol. 57, No. 4, pp. 524–537. © Pleiades Publishing, Ltd.,

Hasanuzzaman, G, Merbold, S, Motuz, V, Egbers, Ch.,
Enhanced outer peaks in turbulent boundary layer using uniform blowing at moderate Reynolds number, **J. of Turbulence**, 23, 68–95, 2022
URL: https://doi.org/10.1080/14685248.2021.2014058
DOI: 10.1080/14685248.2021.2014058

Hallol, Z., Yousry, M., Merbold, S., Egbers, C.
Experimental investigation to study energetic structures in pipe flow at high Reynolds numbers using POD analysis, **J. Phys. Soc. Japan**, Vol. 91, 094401, 2022

Harlander, U.; Borcia, I.D.; Vincze, M.; Rodda, C.
Probability Distribution of Extreme Events in a Baroclinic Wave Laboratory Experiment. **Fluids**, 7, 274, 2022
https://doi.org/10.3390/fluids7080274

Rodda, C., Harlander, U., Vincze, M.
Jet stream variability in a polar warming scenario – a laboratory perspective, **Weather Climate Dynamics**, 3, 937-950, 10.5194/wcd-3-937-2022
https://wcd.copernicus.org/articles/3/937/2022/

Hasanuzzaman, G., Eivazi, H., Merbold, S., Egbers, Ch., Vinuesa, R.
Enhancement of PIV measurements via physics-informed neural networks,
Measurement Science and Technology, DOI 10.1088/1361-6501/aca9eb, 2022,
https://iopscience.iop.org/article/10.1088/1361-6501/aca9eb

Veröffentlichungen, Konferenzbeiträge und Vorträge/ Publications, contributions to conferences and invited lectures

Veröffentlichungen in Tagungsbänden und Vorträge / Poster 2022

P.S.B. Szabo, Y. Gaillard, P. Haun, R. Carter, A. Adrian, Y. Sliavin, F. Zaussinger, Ch. Egbers, AtmoFlow–Investigating large scale convection in planetary atmospheres, 27th ELGRA Symposium and General Assembly, 2022

M. Meier, A. Meyer, V. Motuz, Y. Sliavin, T.R. Bista, M. Strangfeld, P. Szabo, Ch. Egbers, Dielectrophoretic induced convection in a sounding rocket flight, 27th ELGRA Symposium and General Assembly, 2022

A. Meyer, H.N. Yoshikawa, P.S.B. Szabo, M. Meier, Ch. Egbers, I. Mutabazi, Stability of a dielectric liquid confined in a differentially heated vertical Taylor-Couette system with applied radial electric field, Int. Symp on Bifurcations and Instabilities in Fluid Dynamics, 2022

Hamede, M.H., Merbold, S.,Egbers, Ch., 2022 Angular momentum transport in counter-rotating Taylor-Couette flows for radius ratio $\eta = 0.1$, European Fluid Mechanics Conference (EFMC14), 12 September 2022 – 16 September 2022, Athens, Greece. (Vortrag)

P. S. B. Szabo, Y. Gaillard, Ch. Egbers, Thermo-electrohydrodynamic (TEHD) convection in rotating spherical gap: A 2D-numerical simulation of the AtmoFlow sphere, European Fluid Mechanics Conference EFMC14, Athens, Greece, 2022

P. S. B. Szabo, W.-G. Früh, Effect of intrinsic thermomagnetic convective timescales on the response to periodic modulation of external forcing parameters, European Fluid Mechanics Conference EFMC14, Athens, Greece, 2022

A. Meyer, M. Meier, P. Szabo, Y. Sliavin, V. Motuz, P. Gerstner, J. Roller, V. Heuveline, Ch. Egbers, Thermoelectric instability of a dielectric fluid in a cylindrical annulus with vertical or horizontal orientation, European Fluid Mechanics Conference EFMC14, Athens, Greece, 2022

P. S. B. Szabo, Y. Gaillard, Ch. Egbers, Titel: Thermo-electrohydrodynamic (TEHD) convection in a differentially heated shell of aspect ratio 0.7 with central electric force field, GAMM Annual Meeting 92nd, 2022

P. S. B. Szabo, M. Meier, A. Meyer, Y. Gaillard, P. Haun, Ch. Egbers, Thermo-electrohydrodynamic (TEHD) convection experiments in weightlessness Schottish Fluid Mechnics Meeting 35th, 2022

Gaillard, Y., Haun, P., Szabo, P.S.B., Egbers, C. (2022) Numerical Investigation of Cell Formation on in 2D Cylinder Annulus using Thermo-Electric-Hydrodynamics. European Geophysical Union. Vienna. 2022. Poster

Szabo, P.S.B., Gaillard, Y., Egbers, C. (2022). Thermo-electrohydrodynamic convection in a differentially heated cylindrical shell with electric central force field at. Gesellschaft für Angewandte Mathematik und Mechanik. Aachen. Vortrag

Veröffentlichungen, Konferenzbeiträge und Vorträge/ Publications, contributions to conferences and invited lectures

Veröffentlichungen in Tagungsbänden und Vorträge / Poster 2022

Travnikov, V., Egbers, C. (2022). Stability of atmosphere like flows in a spherical geometry. 14th European Fluid Mechanics Conference, Athens, Greece.Vortrag

C. Rodda and U. Harlander: Gravity wave emission from jet systems in the differentially heated annulus experiment. SPARC GW Symposium 2022 –Frankfurt am Main, 28.3.–1.4 2022, https://www.goethe-university-Frankfurt.de/116594409/SPARC_GW_Symposium_2022_Agenda_2903.pdf

U. Harlander and M. Kurgansky: Two-dimensional internal gravity wave beam instability. Linear theory and subcritical instability. SPARC GW Symposium 2022 –Frankfurt am Main, 28.3.–1.4. 2022, https://www.goethe-university-frankfurt.de/116594409/SPARC_GW_Symposium_2022_Agenda_2903.pdf

U. Harlander, C., Rodda, and M. Vincze: A laboratory perspective of extreme events in a global warming scenario, EGU General Assembly 2022, Vienna, Austria, 23–27 May 2022, EGU22-5050, https://doi.org/10.5194/egusphere-egu22-5050, 2022.

I.D. Borcia and U. Harlander: Surface wave focusing in an oscillating circular channel – part I: general aspects. Workshop "Singularities and attractors in rotating and stratified fluids", 8-9 December 2022 IRPHE, Marseille (France), https://attractors.sciencesconf.org/data/pages/Program_Attractors_1_2.pdf

U. Harlander and I.D. Borcia: Surface wave focusing in an oscillating circular channel – part II: wave attractors. Workshop "Singularities and attractors in rotating and stratified fluids", 8-9 December 2022 IRPHE, Marseille (France), https://attractors.sciencesconf.org/data/pages/Program_Attractors_1_2.pdf

U. Harlander, I.D. Borcia, C. Rodda, and M. Vincze: Probability Distribution of Extreme Events in a Baroclinic Wave Laboratory Experiment. 2022 SIAM Conference on Nonlinear Waves and Coherent Structures (NWCS22), August 30–September 2, Bremen, 2022, https://meetings.siam.org/sess/dsp_talk.cfm?p=122650

Uwe Harlander, I.D. Borcia, and C. Rodda: Small-scale wave emission from weather systems: a review of laboratory studies: Conference of the International Marangoni Association, IMA 10, June 12-16, 2022, Iasi, Romania https://www.physik.tu-cottbus.de/users/iborcia/Book_of_abstracts.pdf

I.D. Borcia, U. Harlander, F.-T. Schön, R. Borcia, and M. Bestehorn: Wave collision in a circular channel - sloshing and resonance: Conference of the International Marangoni Association, IMA 10, June 12-16, 2022, Iasi, Romania https://www.physik.tu-cottbus.de/users/iborcia/Book_of_abstracts.pdf

I. D. Borcia, R. Borcia, W. Xu, M. Bestehorn, S. Richter, U. Harlander, L.R.M. Maas: Resonance on surface waves in a circular channel, 9th Int. Symp. On Bifurcations and Instabilities in Fluid Dynamics, 16-19 August 2022, University of Groningen, The Netherlands, 2022, https://bifd.net.technion.ac.il/files/2023/01/Abstracts-BIFD2022.pdf

Veröffentlichungen, Konferenzbeiträge und Vorträge/ Publications, contributions to conferences and invited lectures

Veröffentlichungen in reviewten Zeitschriften 2023

A. Meyer, H. N. Yoshikawa, P. S. B. Szabo, M. Meier, Ch. Egbers, I. Mutabazi,
Thermoelectric instabilities in a circular Couette flow, **Phil. Trans. R. Soc**., 2023, A 381: 20220139 https://doi.org/10.1098/rsta.2022.0139

Ion-Dan Borcia, Sebastian Richter, Rodica Borcia, Franz-Theo Schön, Uwe Harlander, Michael Bestehorn,
Wave propagation in a circular channel: sloshing and resonance, **The European Physical Journal, Special Topics**, DOI:10.1140/epjs/s11734-023-00790-z, 2023
https://link.springer.com/article/10.1140/epjs/s11734-023-00790-z

Franz-Theo Schön, Michael Bestehorn
Instabilities and pattern formation in viscoelastic fluids, **The European Physical Journal, Special Topics,** DOI: 10.1140/epjs/s11734-023-00792-x
https://link.springer.com/article/10.1140/epjs/s11734-023-00792-x

S. Merbold, M. H. Hamede, A. Froitzheim, Ch. Egbers
Flow regimes in a very wide-gap Taylo-Couette flow with counter rotating cylinders
Phil. Trans. R. Soc. A., Vol. 381 20220113 DOI: 10.1098/rsta.2022.0113, 2023

M. H. Hamede, S. Merbold, Ch. Egbers,
Experimental methods for investigating the formation of flow patterns in a very wide gap Taylor-Couette flow (eta=0.1)
Technisches Messen, vol. 90, no. 5, 2023, pp. 332-339. https://doi.org/10.1515/teme-2022-0107, 2023

S. Merbold, G. Hasanuzzaman, T. Buchwald, Ch. Schunk, D. Schmeling, A. Volkmann, R. Brinkema, U. Hampel, A. Schröder, Ch. Egbers
Reference experiment on aerosol particle transport for dynamic situations
Technisches Messen, vol. 90, no. 5, 2023, pp. 340-352. https://doi.org/10.1515/teme-2022-0118, 2023

M. H. Hamede, S. Merbold, C. Egbers
Experimental investigation of turbulent counter-rotating Taylor–Couette flows for radius ratio η = 0.1, **J. of Fluid Mech.,** Vol. 964, https://doi.org/10.1017/jfm.2023.392

Labarbe, Joris, Le Gal, Patrice, Harlander, Uwe, Le Dizès, Stéphane, Favier, Benjamin Localized layers of turbulence in stratified horizontally sheared Poiseuille flow, **J. of Fluid Mech.,** 2023, https://arxiv.org/abs/2207.09131

Veröffentlichungen, Konferenzbeiträge und Vorträge/ Publications, contributions to conferences and invited lectures

Veröffentlichungen in reviewten Zeitschriften 2023

Harlander, U., Sukhanovskii, A., Abide, S., Borcia, I.D., Popova, E., Rodda, C., Vasiliev, A., Vincze, M. (2023).
New Laboratory Experiments to Study the Large-Scale Circulation and Climate Dynamics.
Atmosphere, 14, 836, https://doi.org/10.3390/atmos14050836

Meletti G., Abide S., Viazzo S. and Harlander U. (2023).
A parameter study of strato-rotational low-frequency modulations: impacts on momentum transfer and energy distribution. **Phil. Trans. R. Soc.** A.3812022029720220297,
http://doi.org/10.1098/rsta.2022.0297

Szabo, Peter S.B.; Gaillard, Yann; Zaussinger, Florian; Egbers, Christoph,
Thermo-electrohydrodynamic convection in a differentially heated shell with electric central force field; **Proc. Appl. Math. Mech**. 23(1); 1-3
https://onlinelibrary.wiley.com/doi/10.1002/pamm.202200121

M. H. Hamede, S. Merbold, Ch. Egbers
Transition to the ultimate turbulent regime in a very wide gap Taylor-Couette flow ($\eta = 0.1$) with a stationary outer cylinder
EPL, **Europhysics Letters**, DOI 10.1209/0295-5075/acdea1, 2023

S. Richter, E.-S. Zanoun, J. Peixinho, C. Egbers
Pipe Flow Development and Transition in CoSmaPipe Facility
Proc. Appl. Math. Mech., PAMM 23, https://doi.org/10.1002/pamm.202300001, 2023

Elhadj B. Barry, Harunori N. Yoshikawa, Changwoo Kang, Antoine Meyer, Martin Meier, Olivier Crumeyrolle, Christoph Egbers, Innocent Mutabazi,
Thermoelectric convection in a planar capacitor: theoretical studies and experiments in parabolic flights
Comptes Rendus. Mécanique, (2023), pp. 1-15
https://comptes-rendus.academie-sciences.fr/mecanique/articles/10.5802/crmeca.143/

Zanoun, E.-S., Dewidar, Y., Egbers, Ch.
Reynolds number dependence of azimuthal and streamwise pipe flow structures
J. Fluid Mechanics, Vol. 973, 25 October 2023 , A1
DOI: https://doi.org/10.1017/jfm.2023.700

Gaillard, Y., Szabo, P., Travnikov, V., Egbers, Ch.
Thermo-electrohydrodynamic convection in a rotating shell with central force field,
Int. J. Heat & Mass Transfer, Volume 218, January 2024, 124760
https://doi.org/10.1016/j.ijheatmasstransfer.2023.124760

Veröffentlichungen, Konferenzbeiträge und Vorträge/ Publications, contributions to conferences and invited lectures

Veröffentlichungen in reviewten Zeitschriften 2023

Tom Buchwald, Gazi Hasanuzzaman, Sebastian Merbold, Daniel Schanz, Christoph Egbers, Andreas Schröder
Large-scale flow field and aerosol particle transport investigations in a classroom using 2D-Shake-The-Box Lagrangian Particle Tracking
HELIYON, HLY 22826
https://www.sciencedirect.com/science/article/pii/S240584402310034X?via%3Dihub

Antoine Meyer, Martin Meier, Vasyl Motuz, Christoph Egbers
Thermo-electric convection in a cylindrical annulus during a sounding rocket flight
J. Fluid Mech. (2023), vol. 972, A26
doi:10.1017/jfm.2023.677

Vincze, M., Hancock, C., Harlander, Rodda, C., Speer, K.
Extreme temperature fluctuations in laboratory models of the mid-latitude atmospheric circulation. **Sci Rep 13**, 20904 (2023). https://doi.org/10.1038/s41598-023-47724-2

Gaillard, Y., Szabo, P. S. B., & Egbers, C. (2023). Thermo-electrohydrodynamic convection in the thermally driven spherical shell with differential rotation. **Proceedings in Applied Mathematics and Mechanics**.

Veröffentlichungen, Konferenzbeiträge und Vorträge/ Publications, contributions to conferences and invited lectures

Veröffentlichungen in Tagungsbänden und Vorträge / Poster 2023

Gaillard, Yann, Szabo, Peter, Egbers, Christoph; (2023), AtmoFlow: Thermo-electrohydrodynamic convection in the thermally driven spherical shell with differential rotation, EGU General Assembly 2023, Vortrag, https://doi.org/10.5194/egusphere-egu23-1841

Haun, P., Egbers, C. (2023) Thermo-electro hydrodynamic convection at moderate Rayleigh numbers in rectangular cavity. ETC18 Valencia. Vortrag

Gaillard, Y., Szabo, P.S.B., and Egbers, C. (2023): Thermo-electrohydrodynamic (TEHD) convection in the thermally driven spherical shell with differential rotation. SFMM36 Glasgow. Vortrag

Gaillard, Y., Szabo, P.S.B., and Egbers, C. (2023): AtmoFlow: Convection in spherical shell with atmospheric boundary conditions. ICTW22 Barcelona. Vortrag

Travnikov, V., and Egbers, C. (2023): GeoFlow vs. AtmoFlow: Numerical results. ICTW22 Barcelona. Vortrag

A Adrian, P Heintzmann, P.S.B. Szabo, P. Haun, C. Egbers and U.M.Kuebler (2023). AtmoFlow - Atmospheric Fluid Flow Experiment in Space, American Society for Gravitational and Space Research Annual Conference, Washington. Vortrag

Hamede, M.H., Merbold, S.,Egbers, Ch., 2023 Transition to the ultimate Turbulent regime in a very wide gap Taylor-Couette flow (η =0.1) with a stationary outer cylinder. 93th Annual Meeting of the International Association of Applied Mathematics and Mechanics GAMM, May 30-June 2, 2023, Dresden, Germany, Book of abstracts. (Vortrag)

Hamede, M.H., Merbold, S.,Egbers, Ch., 2023 Angular momentum transport in a very wide gap TC geometry η = 0.1. 22 International Couette-Taylor Workshop ICTW, 28-30. July, Barcelona, Spain. (Vortrag)

Harlander, U., Schön, F.-T., Borcia, I. D., Richter, S., Borcia, R., and Bestehorn, M.: Resonant water-waves in a circular channel: forced KdV solutions, EGU General Assembly 2023, Vienna, Austria, 23–28 Apr 2023, EGU23-15036, https://doi.org/10.5194/egusphere-egu23-15036, 2023.

G. Meletti, U. Harlander, S. Viazzo and S. Abide: A parameter study of strato-rotational low-frequency modulations, 22nd International Couette-Taylor Workshop, Barcelona, Spain | 28 - 30 June 2023, https://congressarchive.cimne.com/ictw23/assets/book_of_abstracts_ictw_2023.pdf, 2023.

S. Abide, I. Raspo, U. Harlander, A. Randriamampianina, S. Viazzo and G. Meletti: Influence of heat transfers at the free surface of a thermally-driven rotating annulus, 22nd International Couette-Taylor Workshop, Barcelona, Spain | 28 - 30 June 2023, https://congressarchive.cimne.com/ictw23/assets/book_of_abstracts_ictw_2023.pdf, 2023.

Veröffentlichungen, Konferenzbeiträge und Vorträge/ Publications, contributions to conferences and invited lectures

Veröffentlichungen in Tagungsbänden und Vorträge / Poster 2023

P. Le Gal, J. Labarbe, U. Harlander, S. Le Dizes and B. Favier: Localized layers of turbulence in stratified horizontally sheared Poiseuille flow, 22nd International Couette-Taylor Workshop, Barcelona, Spain | 28 - 30 June 2023, https://congressarchive.cimne.com/ictw23/assets/book_of_abstracts_ictw_2023.pdf, 2023.

U. Harlander and A. Sukhanovskii : New laboratory experiments to study the large-scale circulation and climate dynamics, 22nd International Couette-Taylor Workshop, Barcelona, Spain | 28 - 30 June 2023, https://congressarchive.cimne.com/ictw23/assets/book_of_abstracts_ictw_2023.pdf, 2023.

Franz-Theo Schön, Uwe Harlander, Ion Dan Borcia, Rodica Borcia, Sebastian Richter, and Michael Bestehorn: Resonant surface waves in an oscillating periodic tank with a submerged hill: Conference of the International Marangoni Association, IMA 11, 19-22 June 2023, Bordeaux, France, https://ima11.sciencesconf.org/data/pages/abstract_book_11.pdf

I.D. Borcia, F.-T. Schön, U. Harlander, S. Richter, R. Borcia, and M. Bestehorn: Temporal and spatial ratchet for surface waves in a circular channel: Conference of the International Marangoni Association, IMA 11, 19-22 June 2023, Bordeaux, France, https://ima11.sciencesconf.org/data/pages/abstract_book_11.pdf

M. Bestehorn, I. D. Borcia, R. Borcia, S. Richter, F.-T. Schön, U. Harlander: Mass transport in a horizontally vibrated thin fluid layer with a ratchet ground: Conference of the International Marangoni Association, IMA 11, 19-22 June 2023, Bordeaux, France, https://ima11.sciencesconf.org/data/pages/abstract_book_11.pdf

S. Richter, I. D. Borcia, R. Borcia, M. Bestehorn, F.-T. Schön and U. Harlander: Formation of Faraday waves on a liquid in a librating annular channel: Conference of the International Marangoni Association, IMA 11, 19-22 June 2023, Bordeaux, France, https://ima11.sciencesconf.org/data/pages/abstract_book_11.pdf

F.-T. Schön, I.D. Borcia, U. Harlander, R. Borcia, S. Richter, and M.: Water sloshing experiments in a circular tank with submerged topography. European Turbulence Conference, Valencia 4-6 September 2023, https://etc18.webs.upv.es/wp-content/uploads/2023/08/Program_final_impresion.pdf

U. Harlander and A. Mancho: Building transport models from baroclinic wave experimental data, Workshop at Instituto de Ciencias Matemáticas (ICMAT – Institute of Mathematical Sciences), Madrid June 25-26, 2023.

U. Harlander, P. LeGal, S. Viazzo, and S. Abide: Rotating stratified Fluids, DAAD Meeting at Institut de Recherche sur les Phénomènes Hors Equilibre (IRPHE), Marseille, December 7-14, 2023.

Veröffentlichungen, Konferenzbeiträge und Vorträge/ Publications, contributions to conferences and invited lectures

Veröffentlichungen in reviewten Zeitschriften 2024

Gazi Hasanuzzaman, Tom Buchwald, Christoph Schunk, Christoph Egbers, Andreas Schröder, Uwe Hampel, Dynamics of Aerosol Transport for Indoor Ventilation–Remote Enhancement of Smart Aerosol Measurement System Using Raspberry Pi-Based Distributed Sensors, **Sensors** (MDPI), https://doi.org/10.3390/s24134314 https://www.mdpi.com/1424-8220/24/13/4314

Gazi Hasanuzzaman, Christoph Egbers, Flow Control of a Turbulent Boundary Layer Using Uniform Blowing, **Progress in Turbulence X**., Springer Proceedings in Physics (Springer),Volume: 404 Doi: https://doi.org/10.1007/978-3-031-55924-2_36 URL: https://link.springer.com/chapter/10.1007/978-3-031-55924-2_36 ISBN: 978-3-031-55923-5

Mohammed Hussein Hamede, Jonas Roller, Antoine Meyer, Vincent Heauveline, Christoph Egbers. Dielectrophoretic force-enhanced thermal convection within a horizontal cylindrical annulus. **Phys. Fluids** 36, 124106 (2024); doi: 10.1063/5.0234772

Gazi Hasanuzzaman, Tom Buchwald, Christoph Schunk, Christoph Egbers, Andreas Schröder, Uwe Hampel, DATIV—Remote Enhancement of Smart Aerosol Measurement System Using Raspberry Pi-Based Distributed Sensors, **Sensors** (MDPI), https://doi.org/10.3390/24134314

M. Agaoglou, V. J. García-Garrido, U. Harlander, A. M. Mancho, Building transport models from baroclinic wave experimental data. **Physics of Fluids**, 1 January 2024, 36 (1): 016611. https://doi.org/10.1063/5.0179875

U. Harlander, F.-T. Schön, I.D. Borcia, S. Richter, R. Borcia, M. Bestehorn Resonant water-waves in ducts with different geometries: Forced KdV solutions **European Journal of Mechanics - B/Fluids**, Volume 106, 2024, Pages 107-115, ISSN 0997-7546, https://doi.org/10.1016/j.euromechflu.2024.03.008

Borcia, I.D., Bestehorn, M., Borcia, R. *et al.* Mean flow generated by asymmetric periodic excitation in an annular channel. **Eur. Phys. J. Spec. Top**. 233, 1665–1672 (2024) https://doi.org/10.1140/epjs/s11734-024-01181-8

Schön F-T, Borcia ID, Harlander U, Borcia R, Richter S, Bestehorn M. Resonant surface waves in an oscillating periodic tank with a submerged hill. **J. of Fluid Mechanics**. 2024; 999, A69. doi:10.1017/jfm.2024.885, https://www.cambridge.org/core/journals/journal-of-fluid-mechanics/article/resonant-surface-waves-in-an-oscillating-periodic-tank-with-a-submerged-hill/DA9C6F0B47EAC939A4375591FAF6E867

Uwe Harlander; Michael V. Kurgansky; Kevin Speer; Miklos Vincze, Baroclinic instability from an experimental perspective, **Comptes Rendus Physique**, Online first (2024), pp. 1-48. doi : 10.5802/crphys.198, https://comptes-rendus.academie-sciences.fr/physique/articles/10.5802/crphys.198/

Veröffentlichungen, Konferenzbeiträge und Vorträge/ Publications, contributions to conferences and invited lectures

Veröffentlichungen in reviewten Zeitschriften 2024

Gaillard, Y., Szabo, P.S.B, Travnikov, V., & Egbers, C. (2024). Modelling thermo-electro-hydrodynamic convection in rotating spherical shell using OpenFOAM **OpenFoam Journal, 4.**

Gaillard, Y., Szabo, P.S.B, Travnikov, V., & Egbers, C. (2024). Thermo-electrohydrodynamic convection in a rotating shell with central force field. **Int. Journal of Heat and Mass Transfer**, 218, 124760.

Gaillard, Y., Szabo, P.S.B., & Egbers, C. (2024). Thermo-electrohydrodynamic convection in the thermally driven spherical shell with differential rotation. **Proceedings in Applied Mathematics and Mechanics,** 24(1), e202300036.

Veröffentlichungen, Konferenzbeiträge und Vorträge/ Publications, contributions to conferences and invited lectures

Veröffentlichungen in Tagungsbänden und Vorträge / Poster 2024

Gazi Hasanuzzaman & Christoph Egbers
Application of Machine Learning for sustainable aviation: the role of friction drag and flow control in turbulent boundary layer flows, The 2nd International Conference on Advancing Sustainable Futures (ICASF 2024), DOI: 10.13140/RG.2.2.31060.92807

Gaillard, Y., Szabo, P.S.B., & Egbers, C. (2024). Convective regimes in differential spherical shell rotation with electric central force field. American Geophysical Union Annual meeting, Washington.

Gaillard, Y., Szabo, P.S.B., & Egbers, C. (2024). Convective regimes in differential spherical shell rotation with electric central force field. IUTAM Symposium on Laminar-Turbulent Transition, Nagano.-18 50WM2441- Jahresbericht 2024

Gaillard, Y., Szabo, P.S.B., & Egbers, C. (2024). AtmoFlow: Convective regimes in differential spherical shell rotation with electric central force field. 1st European Fluid Dynamics Conference, Aachen.

Travnikov, V. & Egbers, C., (2024): Numerical simulation for the AtmoFlow-Project. 1st European Fluid Dynamics Conference, Aachen.

Gaillard, Y., Haun, P., Szabo, P.S.B., Egbers, C., (2024): Convective regimes of planetary atmospheres in the AtmoFlow spherical shell experiment: Solid body and differential rotation. 28th EL GRA Biennial Symposium & General Assembly, Liverpool.

Gaillard, Y., Szabo, P.S.B., and Egbers, C. (2024): Exploring Thermo-Electrohydrodynamic Flows with Differential Rotation in AtmoFlow. EGU General Assembly, Vienna

Hamede, M.H., Merbold, S.,Egbers, Ch., 2024 Boundary layer dynamics in a Very wide gap Taylor-Couette flow $\eta = 0.1$. IUTAM Symposium on Laminar-Turbulent Transition 2-6th September 2024. Nagano, Japan. (Poster)

Hamede, M.H., Roller, J., Meyer, A., Heuveline, V, Egbers, Ch., 2024. Thermoelectric instability of a dielectric fluid in a Taylor-Couette system with different configurations. European Fluid Dynamics Conference (EFDC1) 16-20 September 2024, Aachen, Germany. (Vortrag)

Harlander, U. and Mancho, A. M.: Transport and fluxes of atmospheric models deduced from laboratory data , EGU General Assembly 2024, Vienna, Austria, 14–19 Apr 2024, EGU24-16445, https://doi.org/10.5194/egusphere-egu24-16445 , 2024.

A. M. Mancho, M. Agaoglou, V. J. García Garrido, Uwe Harlander: From experimental data on baroclinic waves to transport models, Applied Nonlinear Dynamical Systems and Chaos, Celebrating Stephen Wiggins' 65th birthday, Royal Academy of Sciences, Madrid, Spain, 1-3 July 2024, https://events.andsc2024.rac.es/wp-content/uploads/2024/11/AbstractBook2.pdf.

Veröffentlichungen, Konferenzbeiträge und Vorträge/ Publications, contributions to conferences and invited lectures

Veröffentlichungen in Tagungsbänden und Vorträge / Poster 2024

U. Harlander and M. Vincze: Extreme values in geostrophic turbulence: laboratory data from baroclinic wave experiments, 1st European Fluid Dynamics Conference (EFDC1), 16-20 September 2024, Aachen, Germany, https://www.aia.rwth-aachen.de/fileadmin/user_upload/Daily_Scientific_Program.pdf

Franz-Theo Schön, Uwe Harlander, Ion Dan Borcia, Rodica Borcia, Sebastian Richter, and Michael Bestehorn: Resonant shallow water waves in circular channels, 1st European Fluid Dynamics Conference (EFDC1), 16-20 September 2024, Aachen, Germany, https://www.aia.rwth-aachen.de/fileadmin/user_upload/Daily_Scientific_Program.pdf

F.-T. Schön, I. D. Borcia, R. Borcia, S. Richter, U. Harlander, M. Bestehorn: :Measurements of water waves and mean flux in a periodic channel with resonant forcing, GALA-Tagung Experimentelle Strömungsmechanik, 3. bis 5. September 2024, Technische Universität Berlin, https://gala-ev.org/images/Programme/Tagungsprogramm_2024.pdf

U. Harlander: The weather in the water tank: laboratory experiments on geophysical flows and climate. Invited speaker, Fysica 2024, 12 April, TU Eindhoven, Physics of the Human Scale, 2024, https://www.fysica.nl/previous-editions/

M Bestehorn, ID Borcia, R Borcia, S Richter, F-T. Schoen, U. Harlander: Mass transport in a horizontally vibrated fluid layer, 10th International Symposium on Bifurcations and Instabilities in Fluid Dynamics, 24-28 June 2024, The University of Edinburgh, 2024, https://bifd2024.eng.ed.ac.uk/sites/bifd2024.eng.ed.ac.uk/files/FullBook_Abstracts.pdf

ID Borcia, F-T Schön, U. Harlander, R Borcia, M Bestehorn, S. Richter: Periodic excitation of waves in a water filled annular channel with a submerged hill, 10th International Symposium on Bifurcations and Instabilities in Fluid Dynamics, 24-28 June 2024, The University of Edinburgh, 2024, https://bifd2024.eng.ed.ac.uk/sites/bifd2024.eng.ed.ac.uk/files/FullBook_Abstracts.pdf

ID Borcia, F-T Schön, U. Harlander, R Borcia, M Bestehorn, S. Richter: Periodic excitation of waves in a water filled annular channel with a submerged hill, 10th International Symposium on Bifurcations and Instabilities in Fluid Dynamics, 24-28 June 2024, The University of Edinburgh, 2024, https://bifd2024.eng.ed.ac.uk/sites/bifd2024.eng.ed.ac.uk/files/FullBook_Abstracts.pdf

Veröffentlichungen, Konferenzbeiträge und Vorträge/ Publications, contributions to conferences and invited lectures

Veröffentlichungen in reviewten Zeitschriften 2025

Yann Gaillard, Peter Szabo, Vadim Travnikov, Christoph Egbers
Modelling Thermo-Electrohydrodynamic Convection in Rotating Spherical Shell Using OpenFOAM ®, **OpenFOAM® Journal 5:1**-16, 2025
DOI: 10.51560/ofj.v5.136, https://journal.openfoam.com/index.php/ofj/article/view/136

Amir Shahirpour, Christoph Egbers, Jörn Sesterhenn,
Detection of Energetic Low Dimensional Subspaces in Spatio-Temporal Space in Turbulent Pipe Flow, **Flow, Turbulence and Combustion**, Springer Nature, Volume 114, pages 1017–1041, (2025) https://link.springer.com/article/10.1007/s10494-024-00600-z

Peter Szabo & Christoph Egbers
Dielectrophoretic-driven thermoelectrohydrodynamic convection in a dielectric fluid layer induced by an inhomogeneous external electric field
Phys. Rev. E 111, 045105, DOI: https://doi.org/10.1103/PhysRevE.111.045105

Gabriel Meletti, Stéphane Abide, Uwe Harlander, Isabelle Raspo, Stéphane Viazzo
On the influence of the heat transfer at the free surface of a thermally driven rotating annulus
Physics of Fluids 37, 034101 (2025), https://doi.org/10.1063/5.0248712

Franz-Theo Schön, Uwe Harlander, Ion Dan Borcia, Rodica Borcia, Michael Bestehorn
Mean Fluid Transport in an Oscillating Circular Channel with Asymmetric Forcing
Water Waves (2025), https://doi.org/10.1007/s42286-025-00121-w

Marcel Barzantny, Mohammed Hussein Hamede, Michał Majchrzyk, Sebastian Merbold, Christoph Egbers, Wojciech Kostowski, Experimental investigation of the flow characteristics driving the Ranque–Hilsch phenomenon, **Int. J. Heat & Mass Transfer**, Volume 253, 15 December 2025, 127543, https://doi.org/10.1016/j.ijheatmasstransfer.2025.127543

Vadim Travnikov, Peter Szabo, Yann Gaillard, Christoph Egbers,
Centrifugally-driven spherical gap convection with polar angle-dependent boundary condition: Can the Nusselt number fall below unity? **Physics of Fluids,** (Vol.37, Issue 8), 2025
https://doi.org/10.1063/5.0281082

Mohammed Hussein Hamede, Yaraslau Sliavin, Vasyl Motuz, Christoph Egbers
The effect of flow initial conditions and geometry on the saturation of the thermo-electro hydrodynamic instability within microgravity conditions
Physics of Fluids, in press, 2025

Franz Durst & El-Sayed Zanoun
Laminar Pipe FlowInstability: ATheoretical-Experimental Perspective, **Fluids** 2025, 10, 216. https://doi.org/10.3390/fluids10080216

El-Sayed Zanoun, Christian Bauer, Claus Wagner, Franz Durst, Christoph Egbers, Gabriele Bellani, & Alessandro Talamelli, Cross-validation of numerical and experimental data in turbulent pipe flow with new scaling correlations, **J. Turbulence** (2025), accepted

Veröffentlichungen, Konferenzbeiträge und Vorträge/ Publications, contributions to conferences and invited lectures

Veröffentlichungen in Tagungsbänden und Vorträge / Poster 2025

Hamede, M.H., Merbold, S.,Egbers, Ch., 2024 Angular momentum transport scaling in Very wide gap turbulent Taylor-Couette flow ($\eta = 0.1$). ITI interdisciplinary Turbulence initiative conference 27-30 July. Bertinoro, Italy. (Vortrag)

Hamede, M.H., Roller, J., Meyer, A., Heuveline, V, Egbers, Ch., 2025. Dielectrophoretic force induced convection within a cylindrical annulus in various configurations . 23rd International Couette-Taylor workshop (ICTW), 14-16 July, Durham, UK. (Vortrag)

Gaillard, Y., Szabo, P.S.B., and Egbers, C., (2025). Dielectrophoretic-driven convection in spherical Taylor-Couette flow. ICTW2025 Durham. (Vortrag)

Gaillard, Y., Szabo, P.S.B., and Egbers, C. (2025): Thermo-electrohydrodynamic convection in a cylindrical annulus during TEXUS57th sounding rocket flight: Numerical simulation. SFMM36 Glasgow. (Vortrag)

Kühne, S. M., Szabo, P. S. B., Carter, R. M., Krebs, A., Sliavin, Y. & Egbers, C. (2025). Investigation of the development of natural convection in a differentially heated annulus using Wollaston shearing interferometry. In Exp. Strömungsmechanik, 9.-11. Sept. 2025, Darmstadt (pp. 7.1-8).

P.S.B. Szabo, Y. Gaillard, A. Adrian, M. Stauber, P. Heintzmann & Egbers, C. (2025). AtmoFlow: A Space-Based Laboratory for Investigating Large-Scale Planetary Atmospheres. American Society for Gravitational and Space Research Annual Conference, Phoenix. (Vortrag)

Gaillard, Y., Szabo, P.S.B., & Egbers, C. (2025). Dielectrophoretic-driven convection in the spherical shell experiment AtmoFlow. 2nd European Fluid Dynamics Conference, Dublin. Ireland,

Hamede, M.H., Sliavin, M., Motuz, V., Meyer, A., Egbers, Ch., 2025. Thermo-electro hydrodynamic convection in microgravity conditions. 2nd European Fluid Dynamics Conference (EFDC2) 26-29 August 2025, Dublin, Ireland. (Vortrag)

I.D. Borcia, F.-T. Schön, U. Harlander, R. Borcia, and M. Bestehorn: Free-surface flows in a water filled parametrically excited circular channel with a submerged hill, 12th Conference of the International Marangoni Association (IMA12), Interfacial Fluid Dynamics and Processes 9 - 12 June 2024, Madrid, Spain, https://www.nebrija.com/nebrija-IMA12/abstracts-book-IMA12.pdf

G. Meletti, S. Abide, U. Harlander, I. Raspo, and S. Viazzo: On the influence of the heat transfer at the free surface of a thermally-driven rotating annulus, 12th Conference of the International Marangoni Association (IMA12), Interfacial Fluid Dynamics and Processes 9 - 12 June 2024, Madrid, Spain, https://www.nebrija.com/nebrija-IMA12/abstracts-book-IMA12.pdf

U. Harlander, A. M. Mancho, G. Meletti: Meridional heat flux derived from the Eady model and a rotating annulus experiment: a comparison, 23rd International Couette-Taylor Workshop (ICTW 2025), Durham, 14 to 16 July 2025, https://maths.dur.ac.uk/ICTW2025/programme.html

Veröffentlichungen, Konferenzbeiträge und Vorträge/ Publications, contributions to conferences and invited lectures

Veröffentlichungen in Büchern 2022/2023/2024/2025

Yaraslau Sliavin, Peter S B Szabo, Wolf-Gerrit Früh, Björn Schulze, Christoph Egbers
Utilizing infrared thermography to investigate baroclinic instability in the differentially heated rotating annulus, GALA-Fachtagung "Experimentelle Strömungsmechanik", 6.- 8. September 2022, Ilmenau, Hrsg.: C. Cierpka, J. König, B. Ruck, A. Leder, ISBN 978-3-9816764-8-8

M. Strangfeld, O. Bölük, P.S.B. Szabo, M. Meier, A. Meyer, Y. Sliavin, V. Motuz, C. Egbers
Thermo-electrohydrodynamic convection in a dielectric fluid layer with volumetric heating GALA-Fachtagung "Experimentelle Strömungsmechanik", 6.- 8. September 2022, Ilmenau, Hrsg.: C. Cierpka, J. König, B. Ruck, A. Leder, ISBN 978-3-9816764-8-8

S. Merbold, G. Hasanuzzaman, T. Buchwald, Ch. Schunk, D. Schmeling, A. Volkmann, R. Brinkema, U. Hampel, A. Schröder, Ch. Egbers
Reference experiment for aerosol particle transport for dynamic situations,
Experimentelle Strömungsmechanik, 29. GALA-Fachtagung (ISBN 978-3-9816764-8-8), Kap. 9}, 2022

M.H. Hamede, S. Merbold, Ch. Egbers
Formation of flow patterns in a counter-rotating very wide gap Taylor-Couette flow, Experimentelle Strömungsmechanik, 29. GALA-Fachtagung (ISBN 978-3-9816764-8-8), Kap. 48}, 2022

S. Merbold, C.B.V. Kumar, Ch. Egbers
Transparent water tunnel for educational purpose of fundamental flow phenomena and Laser-optical measurement techniques, Experimentelle Strömungsmechanik, 29. GALA-Fachtagung (ISBN 978-3-9816764-8-8), Kap. 53}, 2022

Kühne, S. M., Sliavin, Y., Szabo, P. S. B., Carter, R. M., Krebs, A., & Egbers, C. (2024). Phase demodulation of interferograms of thermo-electrohydrodynamic convection in a differentially heated cylindrical annulus. In Experimentelle Strömungsmechanik, 3.-5. September 2024, Berlin (pp. 7.1-8).

Strangfeld, M., Motuz, V., Szabo, P.S.B., Sliavin, Y.,& Egbers, C. (2024). Simultaneous Particle Image Velocimetry and Background Oriented Schlieren measurements of convective flows. In Experimentelle Strömungsmechanik, 3.-5. September 2024, Berlin (pp. 43-1).

Marcel Barzantny, Mohammed Hussein Hamede, Michał Majchrzyk, Sebastian Merbold, Christoph Egbers, Wojciech Kostowski
The Ranque Hilsch phenomenon. Experimental visualization of the flow structure
German Association for Laser Anemometry, GALA e.V., Berlin, Germany,
ISBN 978-3-9816764-4-0

Veröffentlichungen, Konferenzbeiträge und Vorträge/ Publications, contributions to conferences and invited lectures

Veröffentlichungen in Büchern 2022/2023/2024/2025

Matthias Strangfeld, Vasyl Motuz, Peter S. B. Szabo, Yaraslau Sliavin, Christoph Egbers
Simultaneous Particle Image Velocimetry and Background Oriented Schlieren measurements of convective flows
German Association for Laser Anemometry, GALA e.V., Karlsruhe, Germany,
ISBN 978-3-9816764-4-0

Simon, Kühne, Yaraslau, Sliavin, Szabo, Peter, Carter, R., Krebs, Andreas, Egbers, Christoph
Simultaneous Particle Image Velocimetry and Background Oriented Schlieren measurements of convective flows
German Association for Laser Anemometry, GALA e.V., Karlsruhe, Germany,
ISBN 978-3-9816764-4-0

Master-, Bachelorarbeiten, Dissertationen, Habilitationen
Examinations, theses and habilitations

Dissertationen, Prof. Egbers (seit 2022)

- Mohammed Hussein Haytham Hamede
  The Turbulent Very Wide-Gap Taylor-Couette Flow: Experimental Investigation
  https://doi.org/10.26127/BTUOpen-6445

- Raphael Keßler
  Entwicklung eines raumflugfähigen Moduls zur optischen Untersuchung weicher Materie unter Schwerelosigkeit, https://doi.org/10.26127/BTUOpen-6696

- Amir Shahirpour
  A Characteristic Dynamic Mode Decomposition to Detect Transport-dominated Large-scale Coherent Structures in Turbulent Wall-bounded Flows, https://doi.org/10.26127/BTUOpen-6958

- Hassan Chahi
  Dichtgetriebene vertikale Austauschbewegungen von Gasen in Stabbündelgeometrien während der Lagerung von Brennelementen in Nasslagern-Analytische und experimentelle Untersuchung

- Mohammed Liaket Ali
  Detailed numerical modeling of the iron ore direct reduction process
  https://doi.org/10.26127/BTUOpen-6969

- Peter Haun
  Modelling of Thermo-Electro Hydrodynamic (TEHD) convection,
  https://cuvillier.de/en/shop/publications/9258-modelling-of-thermo-electro-hydrodynamic-tehd-convection

- Yann Ingo Philippe Gaillard,
  Numerical Investigation of thermo-electrohydrodynamic driven convection in spherical Taylor-Couette.

- 2. Gutachten: Christian Bacher
  On the influence of electrohydrodynamically induced turbulence on momentum, heat and mass transport in electrostatic precipitators, https://doi.org/10.26127/BTUOpen-5994

- 2. Gutachten: Elhadj Boubacar Barry
  Modélisation de la convection thermoélectrique dans une cavité rectangulaire
  https://theses.fr/2022NORMLH07

- Kommissionsvorsitz: Federico Pizzi
  Numerical studies of a fluid-filled precessing cylinder: a framework for the DRESDYN precession experiment, https://doi.org/10.26127/BTUOpen-6421

- Kommissionsvorsitz: Franz-Theo Schön, Transport and Waves in parametrically excited Fluid Layers, https://doi.org/10.26127/BTUOpen-6995

Master-, Bachelorarbeiten, Dissertationen, Habilitationen
Examinations, theses and habilitations

Dissertationen, apl. Prof. Harlander (seit 2022)

1. Gutachter: Federico Pizzi
Numerical studies of a fluid-filled precessing cylinder: a framework for the DRESDYN precession experiment
https://doi.org/10.26127/BTUOpen-6421

1. Gutachter: Franz-Theo Schön
Transport and Waves in parametrically excited Fluid Layers
https://doi.org/10.26127/BTUOpen-6995

Kommisionsvorsitz: Yann Ingo Philippe Gaillard
Numerical Investigation of thermos-electrohydrodynamic driven convection in spherical Taylor-Couette

Kommissionsvorsitz: Rakhi
Stochastic modeling of the turbulent boundary layer
Stochastische Modellierung der turbulenten Grenzschicht
https://doi.org/10.26127/BTUOpen-6416

Gutachter: Guillermo Garcia Sanchez
"Universidad Complutense de Madrid" and "Universidad Politecnica de Madrid"
A mathematical and computational approach to the study of transport in ocean flows
https://oa.upm.es/80351/

Gutachter: Denis Martinand (Habilitation)
Hydrodynamique et parois permeables: instabilites, filtration, methodes numeriques
https://federation-peiresc.univ-amu.fr/fr/actualites/soutenance-hdr-denis-martinand

Master-, Bachelorarbeiten, Dissertationen, Habilitationen
Examinations, theses and habilitations

Masterarbeiten (seit 2022)

- M.Sc. Matthias Strangfeld, 2022
  Numerische Voruntersuchung und Vorbereitung des Atmoflow Breadboard Experimentes

- M.Sc. Pranav Hegde, 2022
  Numerical Investigation of Boundary Cooling Effects in AtmoFlow Microgravity Experiment

- M.Sc. Juan Felipe Patino Zuleta, 2022
  Large scale stereoscopic PIV investigation of the flow at a high lift wing configuration with an active Krueger device

- M.Sc. Kasun Sachindra Weerasekara, 2023
  Numerical Investigation of Baroclinic Waves in the Thermally Driven Rotation Annulus

- M.Sc. Hesham Mahfouz, 2023
  Two-Point Streamwise Velocity Correlation for Pipe Flow

- M.Sc. Björn Schulze, 2023
  Natural Convection for High Rayleigh-numbers in Taylor Couette System with large aspect ratio

- M.Sc. Ahmed Oguzhan Erdogdu, 2023
  Investigation of the influence of different tire geometries on vehicle aerodynamics via particle image Velocimetry

- M.Sc. Juan Andres Calderon Valdiviezo, 2023
  Numerical Evaluation of the computed results of the 57 th TEKUS rocket TEKUS experiment

- M.Sc. Aritro Ghosh, 2023
  Experimental Investigation of a wide-gab counter-rotating Turbulent Taylor-Couette Flow

- M.Sc. Kunal Kamleshbhai Jani, 2023
  A thesis submitted in fulfilment of the requirements for the degree of Master of Science in Transfers-Fluids-Materials in Aeronautical and Space Applications

Master-, Bachelorarbeiten, Dissertationen, Habilitationen
Examinations, theses and habilitations

Masterarbeiten (Fortsetzung)

- M.Sc. Juan Andres Calderon Valdiviezo, 2024
  Numerical investigation of Thermo-Electrohydrodynamic convection in a cylindrical annulus under microgravity conditions

- M.Sc. Simon Kühne, 2024
  Investigating thermoelectro-hydrodynamic convective pattern formation in a differentially heated cylindrical annulus

- M. Sc. Marcel Barzantny, 2024
  Vortex tube flow analysis and visualization

- M.Sc. Kushal Nagaray, 2024
  Electrohydrodynamic convection of a dielectric fluid confined in planar cavity under dielectric heating condition

- M.Sc. Gauri Parashar, 2024
  Experimental investigation of controlling the secondary flow in a wide-gap Taylor-Couette flow by the application of an electric field

- M.Sc. Kunal K Jani, 2024
  Experimental Analysis of Bubbles Generated by a Confined Plunging Jet

- M.Sc. Mahek Atul Sanghvi, 2024
  Numerical Investigation of Particle Mixing

- M.Sc. Pedro Aguilera Vassalo, 2024
  Efficiency of models for numerical simulation of propeller-driven flow around nacelles of fuel-cell driven engines

- M.Sc. Lucas Kowal, 2025
  Experimental Investigation of Heat Transfer in a Plate Gap under the Influence of an Alternating Electric Field Using Heat Flux Sensors

Anfahrt / How to get there?

Sie erreichen uns per — You can reach us by

Flugzeug:	über	Flughafen BER Berlin Flughafen Dresden	**Airplane:**	via	Airports BER Berlin Airport Dresden
Bahn:	über	Berlin Dresden Leipzig	**Train:**	via	Berlin Dresden Leipzig
Auto:	über	Berlin A10 Schönefelder Kreuz, A13 Richtung Dresden A15 Richtung Cottbus Abfahrt Cottbus-West über Dresden A4 Kreuz Dresden Nord A13 Richtung Berlin A15 Richtung Cottbus Abfahrt Cottbus-West	**Car:**	via	Berlin A10 Schönefelder Kreuz, A13 direction Dresden A15 direction Cottbus Exit Cottbus-West via Dresden A4 Cross Dresden North A13 direction Berlin A15 direction Cottbus Exit Cottbus-West